Control of lipid droplets biogenesis by the seipin complex in budding yeast

Alexandra Grippa

TESI DOCTORAL UPF - 2015

DIRECTOR DE LA TESIS:

Dr. Pedro Carvalho

ORGANELLES BIOGENESIS AND HOMEOSTASIS GROUP
CELL AND DEVELOPMENTAL BIOLOGY PROGRAM
CENTER FOR GENOMIC REGULATION (CRG)

To my (extended) family

Whose love is colors, nest and lighthouse of my life.

Acknowledgements

This work would have never been possible without the following people:

Dr. Pedro Carvalho for giving me the opportunity to (mostly) enjoy science in his Lab. As first student, I was really excited to join your “little raft” on the science sea. Despite a bit wavy relationship (what doesn’t kill you makes you stronger) and some (reciprocal) misunderstanding, I am proud to have followed you and really grateful for the inspiring mentoring, the useful conversations work and life related, for your help, your time, your lead, and for your different perspectives and insights, during all these nearly five years of PhD.

The members of my thesis committee Dr. Maribel Geli, Dr. Vivek Malhotra and Dr. Timo Zimmermann for their essential support, the constructive critiques and for helping me to keep the project on tracks.

Dr. Maribel Geli, Dr. Robin Klemm, Dr. Albert Pol, Dr. Vivek Malhotra, Dr. Oriol Gallego for the critical reading of this thesis work.

Dr. Ombretta Foresti for mentoring, teaching, advising, supervising, helping, pushing and encouraging me in all scientific and extra-scientific aspects of my PhD. Also thank you for always standing by my side as friend, sister and family, for all the hugs and the slaps, for all the care and the patience and the time and the sharing of whatsoever could possibly happen in the great moments as in the rough ones. You have been the everyday sunshine through these years.

Laura, who shared with me successes and disappointments in and outside the lab, and helped me a lot to produce these data and to take things easier.

Gabi, who joined this metabolic adventure bringing his lipid expertise and discussed with me about data so many times (mostly disagreeing). Thanks for your friendship and for taking me with all the pros and cons that we share.

Annamaria, my daily companion in this voyage from the very beginning, to really the end. Rollercoaster for sure, but it was an interesting adventure.

Julia, for being such a curious and smart student who made me enjoy so much my teaching experience. Thanks for listening and learning so fast. Thanks for the help, the sharing time (and really long time courses nights at the microscope), the questions, the suggestions, the support, the presence and just the friendship you gave me. I will keep through life the meaning that knowing you and becoming so close assumed in these years.

Caro, always available to discuss life and science matters over a coffee or a beer. Thanks for all we shared and for being there for each other in sunny and grey days.

The people that inspired me during my first steps in science: Dr. Claudia Piagnani, Dr. Maurizio Molinari, Dr. Marcello Duranti, Dr. Emanuela Pedrazzini.

Particularly Dr. Jurgen Denecke for being such an enthusiastic, curious and motivating scientist as well as a real friend. And for the invaluable story of the leaves-swiping man, that when things become overwhelming always reminds me of taking them step by step

and with a smile, and turn around to look at the tasks accomplished to feel good and motivate the next.

All my lab mates (new and gone), colleagues and the peoples that, in the present and in the past, have shared with me the best and the worst of the lab experiences.

My family, the best support ever. Thanks for always being by my side through the years, positive, encouraging and supportive, for loving me also without always understanding me, for the listening, the patience, the perspective, the time, the hugs, the deserved kicks whenever required (or not), for teaching me how to always get back on my feet, for letting me be myself and express even in the craziest ways.

Andre, for the infinite patience, presence even in the distance, freedom, love, care, esteem and stubbornness that kept you close even when I struggled, ran and pushed you away. Thanks for always being positive and making it easier. Thanks for still dreaming and looking at me with such different beautiful eyes.

I Summary

Most cells store energy in lipid droplets (LDs), specialized storage organelles composed of a neutral lipid core that, during their biogenesis, is packaged into a single phospholipid monolayer decorated with specific proteins. Regulation of LDs size and number requires the function of the conserved ER protein Seipin/Fld1, however the molecular function of this protein remains poorly understood. Yeast seipin Fld1 is in complex with Ldb16, an uncharacterized ER protein. Like *fld1Δ* cells, *LDB16* deletion mutant displays a similar aberrant LDs morphology phenotype: lower number of supersized LDs (SLD) or tiny and clustered LD aggregates, depending on the absence or presence of the phospholipid precursor inositol in the media, respectively. The growth stage of cells also impacts on the relative distribution of these phenotypes: while LD aggregates predominate in dividing cells, SLDs are found primarily in stationary phase cells. We found that the complex formed by Ldb16 and Fld1 is required for normal LDs phenotype. In particular, this dual LD morphology is not observed for any other mutants studied so far suggesting that Fld1/Ldb16 have a unique role in LD biogenesis.

Combining mass spectrometry analysis on purified LDs with light microscopy, we found that the distribution of many ER and LDs proteins is altered in these mutants. Analysis of a subset of proteins enriched at LDs surface in mutant cells indicated that the physical properties of clustered LDs may differ from those of supersized LDs. Moreover our data obtained by following the process of LDs biogenesis in presence or absence of inositol points toward a role for Fld1/Ldb16 complex in organizing membrane domains at LDs assembly site. In the absence of the complex, the segregation between the two compartments could be lost and the assembly of LDs is impaired resulting in defects in phospholipid packing that is exacerbated in inositol presence. We propose a function in facilitating the establishment of LD identity by acting as a diffusion barrier at the ER-LD contact sites.

II Resumen

La mayoría de las células almacenan la energía en partículas lipídicas, también conocidas como “lipid droplets” (LD), unos orgánulos especializados compuestos por un núcleo de lípidos neutros que, durante su biogénesis, se empaqueta de forma coordinada en una monocapa de fosfolípidos decorada con proteínas específicas. La regulación del tamaño y número de LDs requiere la función de la proteína conservada de retículo endoplasmático (RE) Seipina/Fld1. Sin embargo, la función molecular exacta de esta proteína no está clara. La seipina/Fld1 de levadura está en complejo con Ldb16, una proteína de RE no caracterizada. Como las células *fld1Δ,* la deleción del gen correspondiente a esta proteína muestra la misma doble morfología aberrante de LDs: un LD individual y de tamaño gigante (SLD, “single and supersized LD”) o LDs pequeños y agrupados, en función de la ausencia o presencia, respectivamente, del precursor fosfolipídico inositol en el medio.

La fase de crecimiento de las células también influye en la distribución relativa de estos fenotipos: mientras que los agregados de LDs predominan en las células en división, los SLDs se encuentran principalmente en células en fase estacionaria. Observamos que el complejo formado por Ldb16 y Fld1 es necesario para el fenotipo de LDs normal. En particular, esta doble morfología de LDs no se observa en ningún otro mutante estudiado hasta ahora, lo que sugiere que Fld1 / Ldb16 tiene un papel único en la biogénesis de LDs.

Combinando el análisis de espectrometría de masas en LDs purificados con microscopía, se observó que la distribución de muchas proteínas de RE y LDs estaba alterada en estos mutantes. Los cambios observados en un subconjunto de proteínas enriquecidas en la superficie de las LDs, nos indicaron que las propiedades físicas de los LDs agrupados podrían diferir de las de los LDs gigantes. Los datos obtenidos siguiendo el proceso de biogénesis de LD sugieren que el complejo Fld1/Ldb16 organiza dominios de membrana en los sitios de ensamblaje de LDs, y en su ausencia la segregación entre RE y LDs pueden perderse. Proponemos que la función del complejo Fld1/Ldb16 es facilitar el establecimiento de la identidad del LD, actuando como una barrera de difusión en los sitios de contacto RE-LD.

III Preface

The work presented in this doctoral thesis was carried out in the Cell and Developmental Biology Program at the Centre for Genomic Regulation (CRG) in Barcelona, Spain under the supervision of Dr. Pedro Carvalho (CRG).

The content of this thesis provides novel insights on the function the yeast seipin as part of a previously uncharacterized complex and investigates the role of two of the binding partners, whose knock out give rise to the same phenotype, on lipid droplets biogenesis.

TABLE OF CONTENTS

1. INTRODUCTION

1.1 Lipid droplets relevance and function

Energy storage during periods of nutrient surplus is a universal strategy to cope with starvation. In almost every eukaryotic cells, energy is saved in form of neutral lipids (NLs) in a dedicated cellular compartment, the cytoplasmic lipid droplets (LDs) (Bartz et al., 2007b; Tauchi-Sato et al., 2002).These organelles, at first thought to be inert fat globules, have recently gained attention due to their broad roles in cellular homeostasis. They have a major function in energy metabolism and lipid homeostasis, as they allow assembly, storage and supply of cellular lipids. Nevertheless, they have also being implicated in infections and immunity (Anand et al., 2012), as well as in protein trafficking (Murphy et al., 2009), storage (Cole et al., 2002; Ohsaki et al., 2006) and degradation.
Importantly, impairment of lipid homeostasis and LD deregulation is a hallmark for different severe metabolic diseases as obesity, atherosclerosis and type II diabetes (Kopelman, 2000), that are increasingly concerning at level of global health. These diseases share, as common feature, the ectopic accumulation of fat in cells in which it is not normally stored.
Understanding the mechanisms underlying lipid synthesis and storage in microorganisms and plants is also critical for biofuel production and food security applications. For example LDs properties have been exploited for “molecular farming” (*i.e.* the production of valuable compounds through plant biotechnology), for food with enhanced nutritional value, for stress resistance and increased yield in crops, and for oil production (Andrianov et al., 2010; Bhatla et al., 2010; Divi and Krishna, 2009; Durrett et al., 2008; Mattoo et al., 2010).

1.2 Lipid droplets unique structure

At the structural level, LDs are distinct from any other membrane-bound organelle. (Figure 1). LDs consist of a highly hydrophobic core composed of NLs, primarily sterol esters (SE) and triacylglycerol (TAG), surrounded by a phospholipid monolayer in which specific proteins are inserted (Murphy and Vance, 1999; Zweytick et al., 2000). The number, the size, the lipid and protein composition of these organelles vary widely depending on the cell type and the metabolic state. For instance mammalian white adipocytes have a unilocular LD of 10-100 μM of diameter while in brown adipocytes

they range between 2 and 10 µM. Other tissues such as heart, liver, muscle, kidney, cultured fibroblasts and macrophages, have cells with smaller LDs. Importantly, LDs maintain tight interactions not only with the ER from which they are widely accepted to be generated but also with several other organelles including mitochondria, endosomes, peroxisomes and vacuoles (Beller et al., 2010)

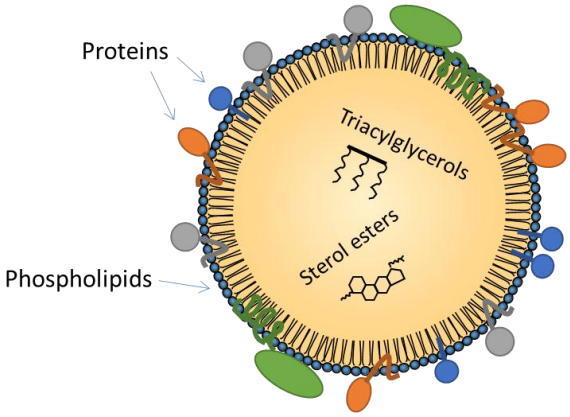

Figure 1. Schematic representation of a lipid droplet. A monolayer of phospholipid decorated with specific proteins surrounds the hydrophobic core of the LD.

1.3 Lipid composition

Although derived from the cytoplasmic surface of the ER and sharing with it some similarities, lipid analysis of LD composition also revealed a different composition compared to ER membrane (Leber et al., 1994; Tauchi-Sato et al., 2002). The phospholipid monolayer that covers LDs surface is mainly composed of phosphatidilcholine (PC), phosphatidylinositol (PI), phosphatidylethanolamine (PE), and phosphatidylserine (PS), however their relative *ratio* varies between cells and tissues. In mammalian cells above 90% of the LD surface is formed by PC (50-60%), PE (20-30%) and free cholesterol, with lower amounts of lyso-phosphatidylcholine (LPC) and lyso-phosphatidylethanolamine (LPE). In *Drosophila*'s S2 cells the amount of PE is higher (50-60%) than the one of PC (20-25%) (Jones et al., 1992; Krahmer et al., 2011). The composition of the hydrophobic core can also vary significantly: for instance in adipocytes TAG is the main component, in steroidogenic cells SE prevail and in murine hepatic stellate cells the most abundant lipid is retinyl ester (Blaner et al., 2009).

In budding yeast *Saccharomyces cerevisiae*, the model organism I focused on for this research, the hydrophobic core consists of TAG and SE in proportion of ~50% each in

wt cells (Leber et al., 1994). The surrounding monolayer contains ~50% PC, ~20% PE, ~30% PI, and other phospholipids in minor amount (Grillitsch et al., 2011; Leber et al., 1994). The fatty acid composition of these classes of lipids is mainly palmitic (C16:0), palmitoleic (C16:1) and oleic acid (C18:1). Importantly, gene KO causing alterations of the phospholipid composition dramatically affects the LDs morphology (Fei et al, 2011; Goodman et al, 2007; Guo et al, 2008; Krahmer et al, 2011) suggesting that phospholipid are key regulators in LDs size.

1.4 Lipid droplets proteins: composition and function

Mass spec analysis of LDs isolated from mammals and *Drosophila* cells (Cermelli et al., 2006; Krahmer et al., 2013b) revealed LDs proteomes ranging between 50 and 200 proteins (Yang et al., 2012b). The best characterized proteins associated with LDs include the adipose triglyceride lipase (ATGL and its activator CGI-58), the hormone sensitive lipase (HLS), catalyzing the hydrolysis of TAG and DAG (Zimmermann et al., 2009), and the PAT proteins, named after the major family members: Perilipin1, (Greenberg et al., 1991) Perilipin2/Adipophilin/ADRP (Adipocyte differentiation-related proteins) and Perilipin3/Tip47 (Tail-interacting protein of 47 KDa) (Kimmel et al., 2010). Other tissue specific proteins belonging to the PAT family are LSDP1 (Patel et al., 2005) and LSD2 (Gronke et al., 2003) in the fat body of insects, S3-12/Perilipin4 in the adipocytes (Wolins et al., 2003), and myocardial lipid droplet protein (MLDP/OXPAT/LSDP5)/Perilipin5. Additional mammalian LD proteins include vimentin, caveolin (Pol et al., 2001), cavin, phospholipase D (which catalyzes the hydrolysis of membrane glycerophospholipids to form PA) (Marchesan, 2003), some Rab proteins (*i.e.* Rab5, Rab11 and Rab18) (Liu et al., 2007) and proteins belonging to CIDE family (Cell Death Inducing DNA Fragmentation Factor45-like effector).

Most well-known LDs proteins from plants are found in seeds (Chapman et al., 2012). They are mainly structural proteins involved in regulating size and stability of LDs, as oleosins (Jolivet et al., 2004), caleosins (Naested et al., 2000), and steroleosins (sterol dehydrogenases) (Lin et al., 2002). These proteins were found to have specific functions in recruiting lipases for LDs breakdown, in calcium dependent degradation of polyunsaturated fatty acids and in brassinosteroid modulation and signaling, respectively.

Also in yeast LDs have been isolated, and their proteomes have been analyzed with increasingly sensitive methods in the last 15 years (Athenstaedt et al., 1999; Binns et al., 2006; Currie et al., 2014; Fei et al., 2011d; Grillitsch et al., 2011). Most recently, combined use of SILAC (Stable Isotope Labeling by Amino acids in Cell culture), proteins correlation profiling and high resolution mass spectrometry on purified LDs led to the assessment of 30 high confidence LD proteins. These were confirmed to localize to LDs by fluorescence microscopy (Currie et al., 2014). Functional annotations of LD proteins relate them to TAG, sterols, phospholipid and fatty acid biosynthesis and to lipolysis. Moreover, there are some proteins involved in other lipid-related function like synthesis of CoA or phytosphingosine or dolichol and a few uncharacterized proteins.

1.5 Lipid droplets proteins: localization and targeting

The peculiar architecture of LDs (*i.e.* the surrounding phospholipid monolayer and the absence of an aqueous lumen) imposes specific structural requirements to LD-localizing proteins. For example, proteins with multi membrane-spanning domains or hydrophilic regions on both sides are excluded from LDs recruitment, as placing a hydrophilic segment in the hydrophobic LDs core would be energetically unfavorable. On the other hand, proteins displaying lipid anchors, amphipatic helices or hydrophobic hairpins can be located at LDs either by interacting directly with the monolayer or by dipping segments into the hydrophobic phase (Thiam et al., 2013b). Positively charged amino acids in the flanking regions of the hydrophobic domain have been shown to be also necessary for targeting of certain proteins to LDs (Ingelmo-Torres et al., 2009).

Different mechanisms for protein targeting to LDs are emerging (Thiam et al., 2013b). Some proteins get recruited to LDs from the cytoplasm, like perilipins (Londos et al., 1999; Wolins et al., 2006), while others, liked ATGL, are first targeted to the ER and then localized to the LDs surface through their hydrophobic regions (Soni et al., 2009; Zehmer et al., 2009; Zehmer et al., 2008). This implies that they can diffuse between the two compartments independently from temperature and energy, as it was shown in yeast (Jacquier et al., 2011).

For example, mammalian PAT proteins share a common structural motif which consists of an N-terminal 11-mer repeats forming an amphipathic α-helical structure (Hickenbottom et al., 2004) which favors their interaction with LDs surface directly from the cytosol. On the other hand, a hydrophobic hairpin is necessary and sufficient for

GPAT4 (Glycerol-3phosphate acyltransferase 4) LDs targeting from the ER in *Drosophila* cells (Wilfling et al., 2013). This topology (*i.e.* two α-helices that dip into and out of a bilayer membrane without completely spanning it) is also found in plant oleosins, caleosins and steroleosins (Frandsen et al., 2001; Lin et al., 2002), and in mammalian caveolin (Ingelmo-Torres et al., 2009), DGAT2 and AGPAT3 (Stone et al., 2006; Wilfling et al., 2013).

It is also possible that alterations in membrane surface tension restricts or allows protein targeting to lipid droplets. Differently from the ER where bilayer membranes have very low surface tensions, the surface tension of LDs monolayers can vary a lot during growth or shrinking of this organelle. At higher surface tension, portions of the core components underlying the monolayer may be dynamically exposed to the cytosol, which could generate strongly hydrophobic patches that enable protein binding (Figure 2). These changes in phospholipid packing favor recruitment of amphipathic helices that detect differences in surface properties of oil–water interfaces (Thiam et al., 2013b). For instance CCT1 can detect and bind loose monolayer with high surface tension caused by low concentration of PC (Krahmer et al., 2011). On the contrary, APOC-I whose unfolded helix stays soluble in the cytosol until it can fold in a compressed monolayer (Meyers et al., 2012) binds more efficiently to densely packed PC regions. Besides recruitment of proteins from the cytoplasm, changes in LD surface tension could also regulate protein interchange with the ER.

In a recent study in *Drosophila* S2 cells, a mechanism of protein targeting that relies on altering the surface lipid composition of LDs was suggested (Thiam et al., 2013a; Wilfling et al., 2014b). In particular it was shown that Arf1/COPI proteins also localize to LDs and that their removal causes an increase in phospholipids content. This in turn reduces surface tension and leads to an impairment in the ER-LDs bridges that are required for targeting ATGL/Brummer and specific enzymes for TAG-synthesis to LD surfaces. Moreover, components of the Arf1/COPI machinery are sufficient to induce budding of nanodrops from purified LDs. The authors propose a function for Arf1/COPI in modulating the composition of the phospholipid layer around the droplet in a way that allows it to interact directly with the membrane of the ER.

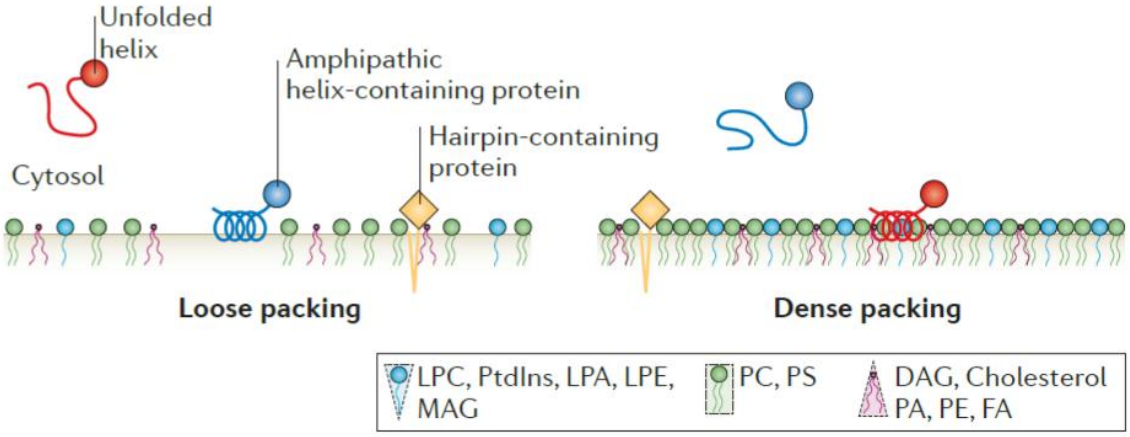

Figure 2: Protein targeting to LDs. The illustration shows the preferential binding of amphipathic α-helices and hairpin-containing proteins to LDs, depending on lipid packing. Left: a loose monolayer has higher surface tension and can be bound by a hairpin or by one type of helix. An unfolded helix, does not bind to lipid droplets under these conditions and stays soluble in the cytosol. Right: in a dense monolayer the hairpin can still be inserted, the helix that bound the loose monolayer gets expelled while the protein soluble in the cytosol can now fold its amphipathic helix by interacting, for example, with the head group of phospholipids. Adapted from (Thiam et al., 2013b).

1.6 Neutral Lipid Synthesis and LDs core formation

Because of their highly reduced and anhydrous nature, NLs are the major storage form of FA for energy production or reservoir for membrane lipids synthesis. They not only serve as acyl-donors for membranes biogenesis, but they buffer the excess lipids that are harmful for the cell, as free fatty acids (FFA) and sterols that at high concentrations perturb the membranes, and those as diacylglycerol that have roles as transcriptional activators/signal transducing molecules. Their hydrophobic nature makes them insoluble in the cytosol and not easy to accommodate into membranes in high amount, so they are stored within a phospholipid monolayer in LDs.

Reactions that produce NLs imply that fatty acids, derived either from acyl-coenzyme A (acyl-CoA) or phospholipids, are conjugated with free alcohols by an esterification reaction. TAG is synthesized *de novo* through the following four consecutive reactions (Figure 3):

1) glycerol-3-phosphate O-acyltransferase (GPAT in mammals and Sct1 and Gpt2 in yeast) catalyzes the reactions of glycerol-3-phosphate and acyl-CoA to form lysophosphatidic acid (LPA).
2) 1-acylglycerol-3-phosphate O-acyltransferase (mammalian AGPAT2, yeast Slc1 and Ale1) mediates the formation of phosphatidic acid (PA) from LPA and Acyl-CoA.
3) Phosphatidic acid phosphatase (PAP)/lipin (yeast Pah1) generates diacylglyerol (DAG).
4) The enzymes of DGAT family DGAT1 and DGAT2 (Dga1 in yeast, mainly active in stationary phase) and ER resident phospholipid:diacylglycerol O-acyltransferase (PDTA) (Lro1p in yeast, mainly active in logarithmic phase (Oelkers et al., 2002)) esterify DAG to triacylglycerol using Acyl-CoA and phospholipids (PE/PC) as acyl donors, respectively (Czabany et al., 2008; Chapman et al., 2012; Sturley and Hussain, 2012). Interestingly LDs localized DGAT2 was recently shown to form a TAG synthesizing complex with the ER acyl-CoA synthetase FATP1, promoting LDs expansion in *C. elegans* and mammalian cells (Xu et al., 2012).
FA are also stored in SE that are synthesized by ER resident acyl-CoA:cholesterol acyltransferases enzymes (ACATs) which in mammals are ACAT1 and ACAT2 and in yeast ARE1 and ARE2. Notably yeast strains lacking all the four acyl-transferases (*are1Δare2Δdga1Δlro1Δ*) are viable despite completely lacking LDs, indicating that cells adopt compensative mechanisms to maintain membrane homeostasis and that in normal conditions LDs are dispensable. However, these strains are markedly sensitive to unsaturated fatty acids induced lipotoxicity. Similarly, knockout studies in mammals showed that ACAT1, ACAT2, and DGAT1 are not essential for life. On the contrary DGAT2-deficient mice die shortly after birth due to the lack of energy stores and skin defects related to essential FA depletion.

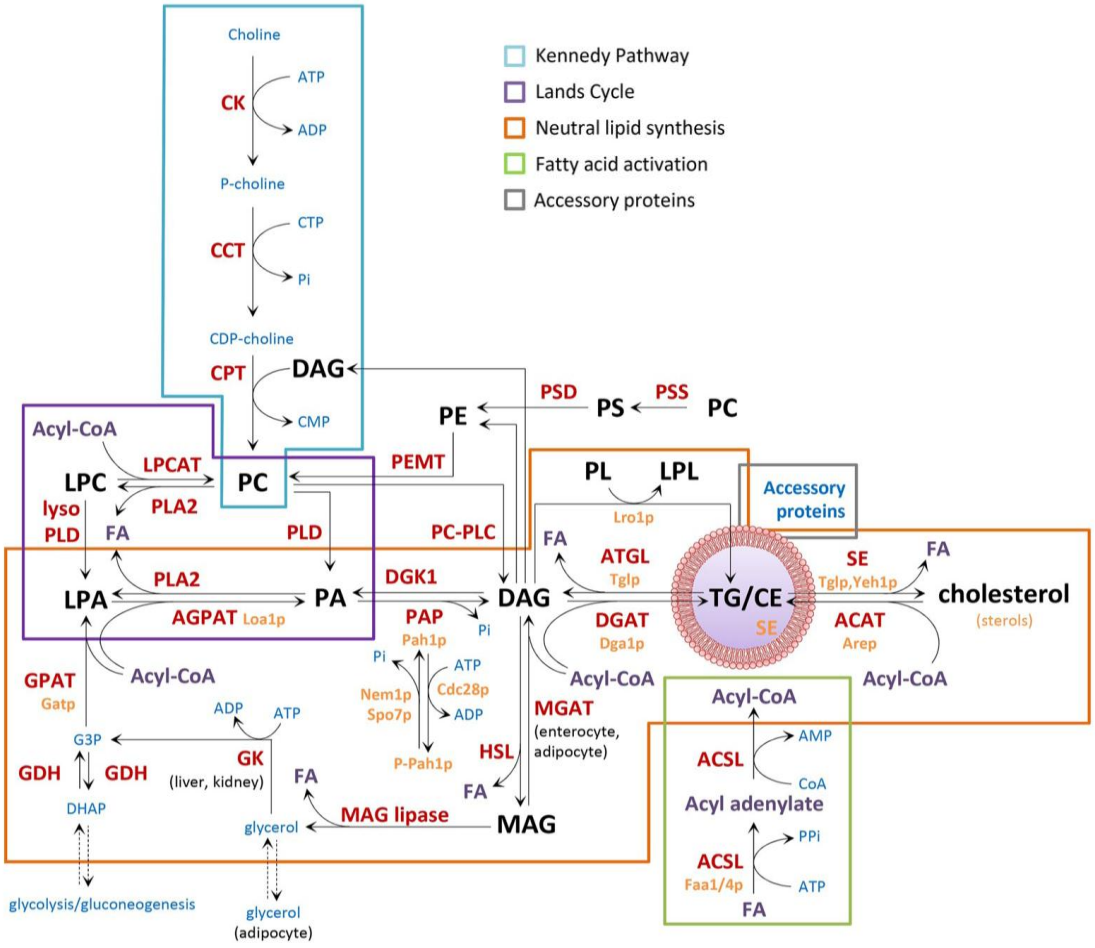

Figure 3. Lipid metabolism and LD formation. LD biogenesis requires coordination of several steps as indicated in the colored boxes. The enzymes involved in these pathways are shown with red (mammal) and yellow letters (yeast), the acyl-CoA with purple letters, the lipid intermediates with black letters, and other required molecules with blue letters. See text for abbreviations. Adapted from (Pol et al., 2014)

1.7 Lipid droplet biogenesis and growth

Several lines of evidence support a key role for the endoplasmic reticulum (ER) in the process of LD biogenesis. Indeed, the monolayer phospholipids and the neutral lipids in the core of LDs are primarily synthesized at the ER where most biosynthetic enzymes reside. Also, many of the LD proteins are targeted to the ER before concentrating in the LD monolayer. Moreover, a large fraction of LDs are in close proximity or connected to the ER membrane as revealed by both fluorescence and electron microscopy studies.

This is particularly evident in yeast, where LDs appear to always emerge from the ER and to remain in contact with it (Jacquier et al., 2011) allowing free diffusion of ER-LDs proteins between the two organelles. Nevertheless, the precise mechanisms of LD biogenesis are not well understood and different hypotheses have been proposed. Among them, the most widely accepted model involves budding from the ER: LDs grow from the ER bilayer and either remain connected or pinch off from the membrane. This would happen in a few steps including fatty acids activation and neutral lipid synthesis, intra-membrane accumulation of lipid lens. Coordinated phospholipid remodeling and biosynthesis allows the formation of the drop bulging towards the cytosolic leaflet (Pol et al., 2014; Wilfling et al., 2014a). In a recent review Thiam et al. propose for this model a dewetting mechanism in which a lipid lens would be converted to a nascent LD by gradually decreasing the angle at which a liquid interface (LD monolayer) meets a solid surface (in this case the ER). This depends on the phospholipid composition of both the bilayer membrane and the forming monolayer, and favors LDs budding when the surface tension between the two is lowered, for example by co-surfactants like DAG or FA. In this model, upon sufficient TAG accumulation LD formation is a spontaneous process, in which the type of surfactant determines the size of the budding LDs (Thiam et al., 2013b). To stabilize the membrane bending, it was suggested that lipids and proteins can contribute or even drive the process. In particular gradual lipid demixing at the nascent monolayer (Zanghellini et al., 2010) and local formation of conical lisophospholipids like LPA and LPC can generate stable positive membrane bending. These characteristics are likely sensed by ER localized proteins that are in proximity of the curvature through their amphipatic helices, which can also autonomously produce membrane bending. The hydrophobic interaction helix-membrane could provide the thermodynamic equilibrium to stabilize the nascent LD and mark the onset of its biogenesis (Pol et al., 2014).

From an experimental point of view, it was measured that TAG can be accumulated up to 3-7% (w/w) in ER membrane (Mackinnon et al., 1992). Above that threshold a lipid lens is formed, however how are the specific sites for this event determined, and if the process is facilitated by proteins, are still open questions. By increasing in size the lens becomes unstable and is predicted to form a drop and bud. Although it has been shown *in vitro* that a few nm globules can form stable membrane bends and that 12nm LDs are able to bud (Zanghellini et al., 2010), the minimal size for dropping out *in vivo* has not been determined due to technical limitations. However, LDs in the range of 50-100nm have been described to undergo this process.

Newly assembled LDs can expand by two general mechanisms: local lipid synthesis or coalescence/ripening. The localized synthesis of core TAG and of the phospholipid monolayer has to be tightly coordinated. Indeed, as core NL are deposed, phospholipid biosynthesis is also required to support the LD size increase. PC particularly has a determinant role in covering LDs and prevent coalescence. The rate limiting enzyme of the PC pathway, CCT, is recruited and activated by the lack of PC, and it uses phosphocholine and cytidine triphosphate (CTP) to form CDP-choline, that in turn is combined with DAG by cytidine diphosphate (CDP)-choline:1,2-diacylglycerol cholinephosphotransferase (CPT) to form PC. Since this last step takes place in the ER, it is still unclear how PC is then transferred to the growing LD. Another way to render PC available for this process is lipid remodeling thorough LPC-acyltransferases which can synthesize it from LPC and fatty acyl-CoA precursors.

Growth by coalescence is rare in normal conditions, however it is a fast process that can be triggered by LDs increased surface tension (for instance when PC availability is limiting and PA is increased), or by addition of a surfactant. The latter involves the formation of a pore between two membranes that depending on the properties and curvature of the phospholipid monolayer will allow fast fusion.

Ripening is a process in which molecules from one lipid droplet diffuse to another with a directionality determined by the difference in the Laplace pressures of the two LDs, the content of which travels from the smaller to the bigger. If the LDs are in contact this process is called permeation and it can be protein-mediated, as recently described for Fsp27 that in 3T3L1 adipocytes LD growth (Gong et al., 2011; Sun et al., 2013).

Alternative models for biogenesis have also been proposed. One of them, namely the “bicelle formation” (Ploegh, 2007) suggested that an entire lipid lens could be excised from the ER, however the transient hole that this event would create would likely cause the ER local collapse due to sudden calcium leaking out. Moreover, this model doesn’t explain what would direct the budding toward the cytosol. Another model is the “vesicular budding” (Walther and Farese, 2009) in which a bilayer secretory-like vesicle forms but remains tethered to the membrane where neutral lipids then would fill the bilayer intramembranous space and the extra layer would remain squeezed in the core. Finally there is an “eggcup” model in which a LD grows within a concave depression of the ER through transport of neutral lipids (Robenek et al., 2006).

1.8 Lipid Droplets breakdown

LD growth is counteracted by lipolysis which leads to LDs shrinkage and lipid mobilization for energy and membrane production. Esterification and lipolysis cycles are likely constitutively active in small droplets of most cells. When LDs undergo lipolysis, the liberated fatty acids (FA) can be oxidized in mitochondria (in mammals) or peroxisomes (in yeast) to generate ATP and the intermediates DAG and MAG that can be used or re-esterified. In mammalian adipocytes this process can be highly stimulated by the adrenergic hormones through PKA activation. PKA then phosphorylates perilipin leading to TAG hydrolysis by sequential action of the 2 lipases ATGL (activated by the perilipin dependent release of CGI-58), HSL and monoacylglycerol lipases, resulting in the progressive liberation of fatty acids chains and glycerol from the cell.
In yeast the NL mobilization is carried out by the sterol esters hydrolases Yeh1, Yeh2 and Tgl1 (Koffel et al., 2005) (of which Yeh2 localizes to plasma membrane) and by the TAG lipases Tgl3 (the major one), Tgl4 and Tgl5 (Athenstaedt and Daum, 2003, 2005) which also exhibit lysophospholipid acytransferase activity. What happens to the surface monolayer during LD regression is still an open question however proteins can localize back to the ER (Jacquier et al., 2011; Zehmer et al., 2009). One possibility is that phospholipids are removed enzymatically from the interface, which is supported by the presence of some phospholipases at LDs (Gubern et al., 2009; Nakamura et al., 2005). Another appealing possibility is that lipid transfer proteins are involved, like oxysterol binding proteins or StAR-related lipid transfer proteins, which could shuttle phospholipids from LD to other organelles.
It is also worth mentioning that recent evidences show that also lipophagy plays a relevant role in LDs turnover (Rambold et al., 2015; Singh et al., 2009; van Zutphen et al., 2014).

1.9 Supersized Lipid Droplets and phospholipid metabolism

Several genetic screens have been performed both in yeast KO collection and Drosophila S2 cells to identify gene products required for normal LD morphology (Fei et al., 2008; Guo et al., 2008; Szymanski et al., 2007). A major finding was that knockdown of enzymes important for phospholipid biosynthesis, as the two isoforms of the key enzyme for PC biosynthesis CCT, yielded cells with very large LDs (Guo et al., 2008).

Also in yeast, defects in pathways affecting phospholipid composition cause alterations in LDs morphology. Specifically, cells defective in genes required for PC synthesis by the phosphatidylethanolamine N-methyltransferase (PEMT) pathway display, at high frequency, supersized LDs when grown in minimal media, (*i.e.* in absence of the phospholipid precursors choline, inositol and ethanolamine) (Fei et al., 2011d). PC is synthesized in yeast via two pathways: the Kennedy pathway and the PEMT pathway (Figure 3). In the PEMT pathway, PE is methylated to PC in three sequential steps by the two methyltransferases Cho2p and Opi3p. Cells of strains defective in the genes encoding for these two enzymes display SLD when grown in minimal media. This pathway is positively regulated by the two transcription factors Ino2 and Ino4, so that *ino2Δ* and *ino4Δ* mutants are also defective in PC synthesis. The abnormal phospholipid composition of these mutants, particularly the decrease in PC (which acts as a surfactant to stabilize the LDs and prevents coalescence (Krahmer et al., 2011)), with a concomitant increase in levels of the fusogenic lipid PA, appears to favor the fusion/coalescence of LDs and therefore the formation of supersized LDs (Fei et al., 2011c). In agreement with this model, supplementation of PEMT mutants with exogenous choline, which stimulates PC biosynthesis through the alternative Kennedy pathway, restores PC levels and reverts the supersized LD phenotype. All these mutants were also rescued by inositol addition which is known to consume PA, so restoring the PC/PA ratio necessary for keeping LDs separated. Another mutant that was shown in the same screening (Fei et al., 2011d) to produce SLDs in minimal media was *TetO$_7$-CDS1*. However, SLDs in this mutant are not affected by choline supplementation while the addition of the phospholipid precursor inositol rescues Cds1 phenotype.

It is worth mentioning that besides genes involved in the phospholipid metabolism, many other components have been identified from these screening to affect the size or the number of LDs. Particularly relevant was the finding of components of ArfI-COPI vescicular transport machinery, as well as genes involved in neutral lipid metabolism. In addition, deletion of an array of genes causes either increased or decreased LD number (*i.e.* channels and transporters, cytoskeleton organization, metabolic enzymes, protein biosynthesis and degradation, signaling/transcription factors, vesicular transport) (Fei et al., 2008; Guo et al., 2008).

1.10 Lipid droplets and diseases

Many metabolic diseases that are impacting global health both in developed and developing countries are characterized by defects in lipid storage. If an excess of lipids accumulates, inflammatory responses are triggered. Obesity is a condition in which the exceeded adipose tissue storage capacity leads to ectopic fat deposition in non-dedicated organs, causing lipotoxicity and tissue disfunctions. On this line, obesity is often followed by hepatic steatosis, insulin resistance and fat liver, which in worst cases leads to fibrosis and liver failure. In many cases obesity gives raise to associated complications as type 2 diabetes mellitus. Another consequence of storage overloading is atherosclerosis, namely the cholesterol deposition in the arteries wall. Macrophages are responsible for the uptaking and esterification of cholesterol which is stored in their LDs until mobilization through high density lipoproteins which are transported to the liver and cleared by bile (Walther and Farese, 2012). Macrophages full of cholesterol ester–containing LDs are called foam cells and they can form the sclerotic plaques, the rupture of which can cause coronary heart diseases and stroke (Buers et al., 2011).

While the above-mentioned complications are have both a genetic and a lifestyle related components, the other side of the coin is represented by genetically inherited diseases related to the inability to store fat due to a dysfunctional adipose tissue, namely lipodystrophies. These are characterized by near total absence of adipose tissue, ectopic fat accumulation and altered glucose metabolism. Metabolic complications as hypertriglyceridemia and diabetes have early onset in the affected subjects.

Lypodistrophies can be classified in two categories: congenital generalized lipodystrophies (CGL) and familial partial lipodystrophies (FPL) (Fei et al., 2011a; Garg and Agarwal, 2009). FPL are caused by defects in Akt2/protein kinase B (AKT2), peroxisome proliferator-activated receptor-γ (PPARγ) (both involved in adipogenesis), lamin A/C (LMNA), and the metalloproteinase ZMPSTE24 which is essential for pre-LMNA processing. CGL include mutations in genes that encode for AGPAT2 (yeast SLC1), lipin (yeast PAH1), caveolin1/cavin (CAV1) that respectively catalyzes the formation of PA from LPA, the conversion from PA to DAG and the caveolae formation. The most severe form however is caused by seipin mutation (BCSL2, yeast FLD1), of which the function is still unclear.

1.11 Seipin and BSCL2

Seipin was originally identified as the product of a gene mutated in patients with the Berardinelli-Seip congenital lipodystrophy type II, the most severe form of this recessive disorder, which affects loss of both the metabolically active and the mechanical adipose tissues and it is characherized by severe insulin resistance and fatty liver (Magre et al., 2001). In mammals BSCL2/seipin has three transcripts two of which (1.6 and 2.2 kb) are ubiquitously expressed and one (1.8 kb) that is mostly found in brain and testis. However, seipin is maximally expressed in the adipose tissue. Indeed, it has been shown to strongly be induced during adipogenesis and to suppress adipocytes differentiation if knocked down in 3T3-L1 cells. This defect can be rescued by addition of the PPARγ agonist pioglitazone, suggesting an upstream function for seipin. (Chen et al., 2009; Payne et al., 2008). Differently from adipocytes, fibroblasts from BSCL2 patients contain many small LDs (Szymanski et al., 2007), suggesting a tissue/cell type dependent phenotype.

Targeted ablation of seipin in flies and mice remarkably recapitulates the features of the human disease. Bscl2-knockout (Bscl2-/-) mice show a lipodystrophic phenotype, with generalized loss of adipose tissues accompanied by hepatomegaly and most of the metabolic manifestations in type 2 BSCL patients, including hyperinsulinemia, insulin resistance and hepatosteatosis (Cui et al., 2011; Chen et al., 2012; Prieur et al., 2013).

In *drosophila,* dSeipin KO led to reduced lipid storage in the fat body and to ectopic LDs accumulation in salivary glands (Tian et al., 2011). This phenotype was suppressed either in *DGAT* or *Lipin* RNAi background, from which the authors deduced that *dSeipin* may act upstream of them. Also, they show synergistic interaction with the CDP diglyceride synthetase *CdsA*, both at cellular and organismal level. While LD size increases and the ectopic accumulation is worsened by *dSeipin* and *CdsA* double deletion, the overexpression of CdsA completely suppressed the mutant phenotype.

Seipin is a conserved ER membrane protein of 462 amino acid in its prevailing form (398 amino acids in a shorter isoform) that appears to play a role in LD formation and morphology. It contains two predicted transmembrane domains, the N- and C-termini in the cytosol and a big luminal loop (Lundin et al., 2006) glycosylated in mammals. Point mutantions (N88S, S90L) at glycosylation sites are responsible for autosomal-dominant distal hereditary motor neuropathy type V and Silver syndrome (Windpassinger et al., 2004). Another point mutation, A212P cause the protein loss of function leading to BSCL2 (Magre et al., 2001).

Two independent screenings identified yeast Seipin homolog Fld1 (Fei et al., 2008; Szymanski et al., 2007). Fld1 is a 285 amino acids protein with conserved structure. At the cellular level, the major defect of seipin mutation is observed in LDs. In *fld1Δ* LDs appear either as disorganized, amorphous clusters of very tiny LDs or drastically reduced in number and abnormally large LDs (previously termed “supersized”, SLDs). How mutations lead to these defects in LD formation is unclear, however genetic studies have suggested a link to PA metabolism (Fei et al., 2011d; Tian et al., 2011). Interestingly two mutations in yeast have been identified corresponding to mammalian A212P (S224P and G225P) that cause Fld1 loss of function giving rise to the same LD phenotype as the KO mutant. mCherry-tagged Fld1 co-localized at the ER with GFP-HDEL and it was enriched at the ER-LDs contact sites. In contrast, the nonfunctional SeipinG225P localized at aberrant LDs clusters, in which membrane proliferation is likely as GFP-HDEL and the LDs marker ERG6-cherry overlap (Szymanski et al., 2007). The authors proposed that Fld1 could be involved in communication between ER and LDs, providing a junction for exchange of phospholipids and proteins during periods of rapid lipolysis or LDs expansion, so coupling NL synthesis and LDs assembly. Recently, Fld1 isolated from yeast was shown form a discrete homo-oligomer of nine copies which by negative staining electron microscopy looks like a toroid (Binns et al., 2010). It was postulated that seipin/Fld1 forms a collar with structural role at the ER–LD contact site to facilitate LD assemble or regulate their size.

Another study favored a role of Fld1p in phospholipid/fatty acid metabolism. This was based on a shift from long to medium/short acyl chains in lipid analysis of whole cells and on the LDs spontaneous fusion, suggesting a role for phospholipids in this event (Fei et al., 2008). Despite these potential connections to lipid metabolism, the protein contains no known domain or enzymatic activity. Therefore, the role of Seipin in lipid droplet biogenesis is still poorly understood and requires further investigation. In this thesis I aimed to understand the function of Seipin in the biogenesis and maintenance of LDs.

2. OBJECTIVES

Seipin is a conserved protein of unknown function that localizes at ER-LD contact sites and whose absence causes a strong lipid droplets phenotype across species. It is therefore a good candidate to have a central role in the mechanisms of lipid droplets biogenesis and dynamics at the ER. The aim of the research presented here is to provide new insights on the role of Fld1 in this process, using yeast as a model system.

To achieve this we aimed to first identify eventual binding partners and then study the contribution of the uncovered complex to lipid metabolism and LD assembly. Moreover, once uncovered a common phenotype for the deletion mutants of two components of the complex (Fld1 and Ldb16), and found that this phenotype can be altered by the phospholipid precursor inositol in most cases, we wanted to investigate how LDs aberrancies may affect the proteome of these organelles, and how the seipin complex controls lipid droplets formation.

3. RESULTS

Chapter 3.1

3.1.1 The seipin complex: identification of the binding partners

To address the role of yeast seipin Fld1 in lipid droplet formation, we started by identifying its binding partners. To this purpose the endogenous Fld1 protein was C-terminally fused to a TAP (tandem affinity purification) tag, consisting of a calmodulin binding peptide and an IgG interaction module, separated by a TEV cleavage site (Rigaut et al., 1999). Cells expressing Fld1-TAP as the unique source of Fld1, displayed LDs morphologically indistinguishable from *wt* control cells, indicating that the fusion protein is functional and complements the deletion phenotype (data not shown). Fld1-TAP was isolated from a crude membrane fraction by solubilization in the mild detergent digitonin, followed by single affinity purification with IgG-coupled magnetic beads. The eluted proteins were precipitated and analyzed by tandem mass spectrometry. *Wild-type* cells expressing untagged Fld1 were used as control.

This led to the identification of three previously uncharacterized proteins, encoded by *LDB16, YMR147W and YMR148W/OSW5*. Reciprocal pull-down on LDB16 or OSW5 C-terminally fused with TAP-TAG followed by mass spec analysis, identified the same components, strongly suggesting that these candidates are part of a protein complex, that we named “seipin complex”. To further confirm these results we performed immunoprecitation followed by western blotting with specific antibodies (Figure 4). Ldb16-TAP co-precipitates Fld1-Myc and Ymr148w-3xHA but not Usa1, an unrelated ER protein, indicating that this interactions are specific. We observed that in absence of Fld1, the levels Ldb16 in the lysate are strongly reduced. In contrast, in absence of *LDB16*, Fld1 levels are not affected. So the presence of Fld1 appears to be important for normal Ldb16 levels.

We also expressed the mutants Fld1 (S224P or G225P) instead of the *wt* Fld1-13Myc in the same genetic background. These loss of function point mutations are homolog to those causing lipodystrophy in human and were previously shown to cause a SLD phenotype in yeast (Szymanski et al., 2007). They are still able to interact with Ldb16-TAP and, accordingly, Ldb16-TAP levels in the lysate are only moderately reduced.

We also noticed that the presence of YMR148w is dispensable for the interaction between Fld1 and Ldb16. Interestingly we observed two bands in the anti-HA blots,

suggesting that ymr148w is present is two forms. We initially thought that the higher molecular weight one was preponderant in the interaction, however this was not confirmed in following experiments, and in the conditions tested both forms appear to bind equally.

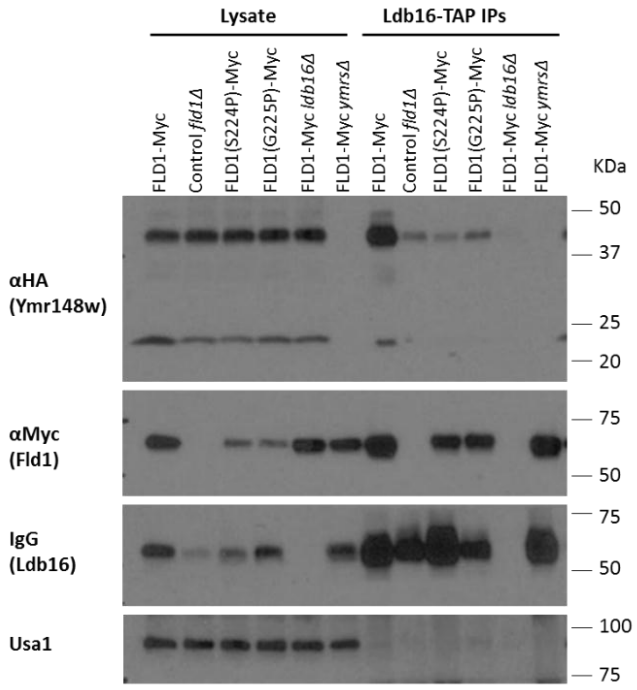

Figure 4. Yeast seipin Fld1 forms a complex with two other proteins of unknown function. Yeast *fld1Δ* cells co-expressing Fld1–13Myc (or its C-terminally tagged loss of function mutants), Ymr148-3HA and Ldb16-TAP were lysed and subjected to pulldown. Input and pull-down fractions were analyzed by immunoblotting with antibodies against Myc, HA, IgG (TAP) and Usa1.

3.1.2 Phenotype of Fld1-binding partners knock-out cells

In order to investigate the function of the components of the Fld1p complex, we have generated *S. Cerevisiae* knock-out strains for the genes *LDB16, YMR147W*, *YMR148W/OSW5*.

Cells of each genotype have been grown in minimal media to early stationary phase, to better highlight the LDs differences between *wild type* and mutants. Cells have then been stained with the neutral lipid dye MDH and examined at the microscope for altered LDs morphology. The acquired high resolution images were deconvolved and analysed through an automated algorithm developed by Raul Gomez at our institute, allowing us

to count large number of cells. We found that, like previously reported for *fld1Δ* (Fei et al., 2008; Szymanski et al., 2007), in these conditions *ldb16Δ* cells show decreased number of droplets together with a striking increase in size when compared to *wt* cells. Depending on growth stage, they display a different LDs phenotype that will be described later in further detail. On the other hand, the knock-out strains *ymr147wΔ, ymr148w/osw5Δ,* did not display a LDs phenotype clearly distinguishable from *wt* (Figure 5 and data not shown).

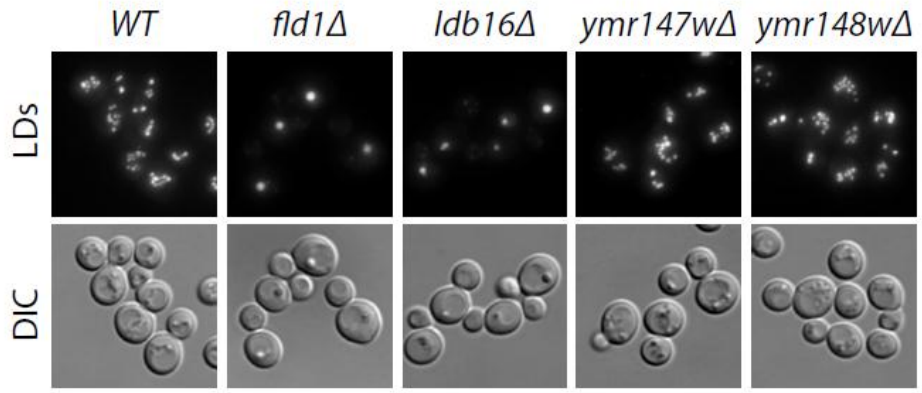

Figure 5. LD phenotype of knock-out mutants of the seipin complex. Cells were harvested in early stationary phase and stained with the neutral lipid dye MDH before imaging. Z projections of LDs channel are shown. Scale bar 5µm.

3.1.3 Subcellular distribution of the seipin complex proteins

To assess the subcellular distribution of the proteins constituting the Fld1 complex, we endogenously tagged them at C-terminus with green fluorescent protein (GFP) and visualized them together with the neutral lipid dye MDH. It has been previously shown that by fluorescence microscopy, Fld1-GFP displays a punctuate pattern along the ER that is adjacent to LDs (Fei et al., 2011c; Szymanski et al., 2007) and it was therefore proposed that Fld1 marks ER-LD contact sites. Like Fld1, endogenously expressed Ldb16-GFP appears as small *foci* apposed to LDs (Figure 6A). Moreover, it was recently reported that Lbd16-GFP displays 50% colocalization with C-terminally tagged Fld1-mCherry (Wang et al., 2014). Thus, Ldb16 is a novel component of the ER-LD contact sites.

The uncharacterized protein Ymr148w/Osw5-GFP, containing a predicted N-terminal TMD, was distributed both at LDs surface and at *foci* apposed to LDs (Figure 6A). Consistently the co-localization of Ldb16-GFP with Osw5-Cherry shows contact but not complete overlap between their signals (Figure 6A).

As we could not detect any signal for Ymr147w-GFP, neither under the control of its endogenous promoter nor overexpressed under the strong TEF promoter (Mumberg et al., 1995), we tagged it at its N-terminus controlled by promoters of different strength (Janke et al., 2004). The obtained GFP-Ymr147w appeared to localize at LD-like structures. Interestingly, these cells displayed a higher number of LDs, in particular when GFP-Ymr147w expression was driven by the strongest TEF and GPD promoter (Figure 6B). Consistently, cells expressing CYCp-GFP-Ymr147w showed a weak GFP staining at LDs, reminiscent of YMR148w/Osw5 localization and displayed normal LD phenotype (Figure 6B).

To test if manipulating the levels of Ymr147wp could lead to a change in LDs number, we placed Ymr147p under the control of Gal1 promoter (inducible on galactose) (Janke et al., 2004; Longtine et al., 1998). Compared with *wt*, MDH staining of cells overexpressing Ymr147wp showed an induced proliferation and clustering of LDs. Moreover, the distribution of the overexpressed N-terminal GFP-tagged protein at LDs was not homogeneous. Indeed, when co-expressed with ERG6-mCherry the overlap between the fluorescent signals was incomplete and only present in subpopulations of clustered LDs. Notably, under the strongest level of overexpression, as for GPD and Gal promoter, Erg6 was partially redistributed at the ER (Figure 6B). Importantly, overexpression of Fld1 or Ldb16 or both of them together under the control of the strong GPD promoter did not affect the LDs morphology or distribution (Figure 6C).

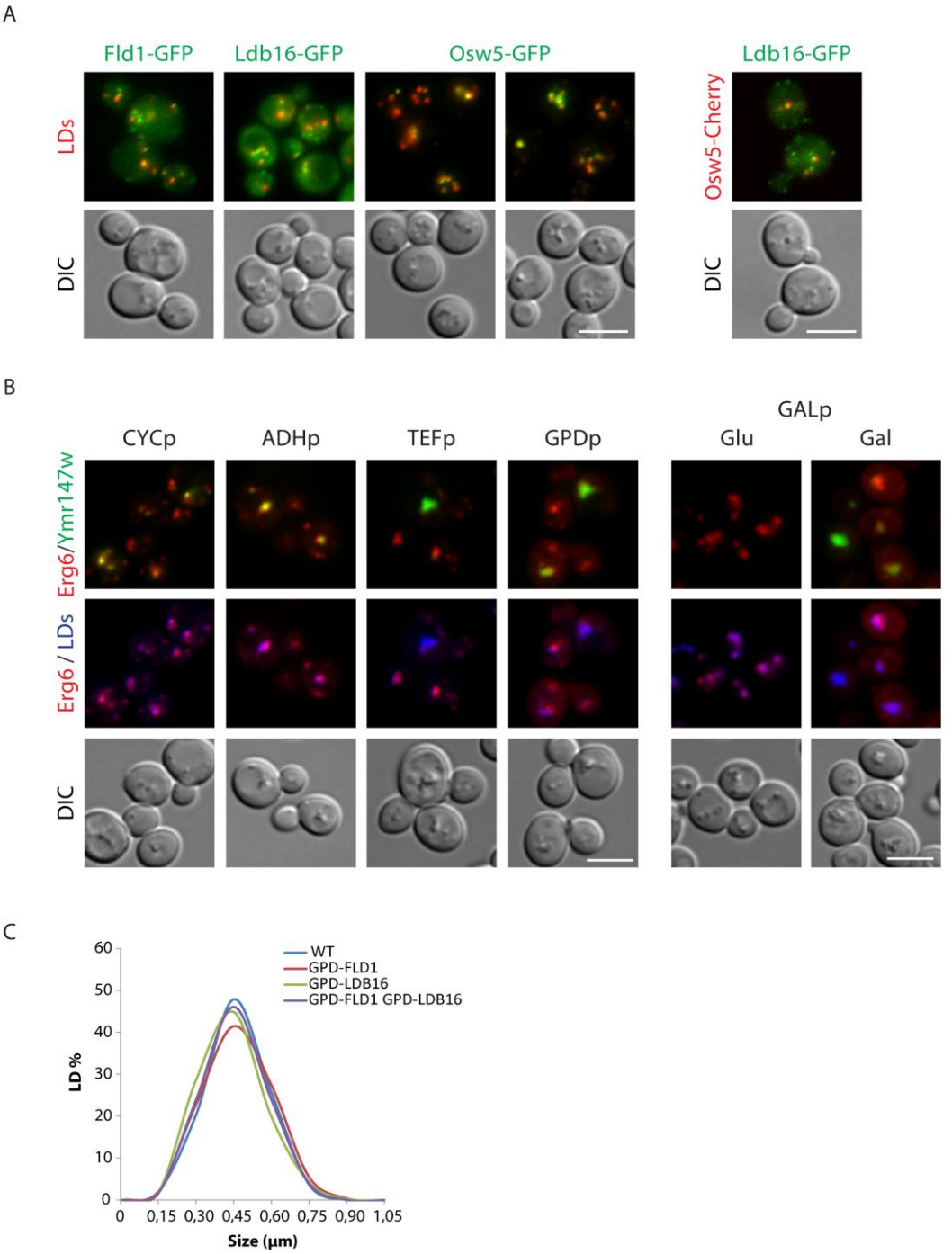

Figure 6 – Localization of GFP-tagged proteins of the seipin complex. A) Fld1, Ldb16 and Ymr148w/Osw5 localization relatively to the LDs dye MDH, and Ldb16 localization relatively to Osw5-Cherry. B) N-terminally GFP tagged Ymr147w under the control of different constitutive or inducible promoters. For Gal1p both repressive (Glu) and induced (Gal) conditions are shown. C) LD quantification of Fld1 and Ldb16 overexpression under constitutive strong GPD promoter.

3.1.4 Ymr147w and Ymr148 form a single protein originating from alternative splicing

As indicated by the systematic name, YMR147W and YMR148W are adjacent *loci* in the genome. A previous cDNA deep sequencing analysis to explore the yeast transcriptome of cells exponentially growing in minimal medium reported that heat-shock induces alternative splicing of the intragenic sequence that connects YMR147W and YMR148W ORFs, suggesting that YMR147W is a not independent ORF upstream of YMR148W (Miura et al., 2006). The new protein isoform deriving from this splicing is a combination of both ORFs and part of the intragenic region, excluding the last 29 amino acids of Ymr147w (Figure 7A).

To characterize in more detail the two bands noticed in the IP (Figure 4), we tested if Ymr147w-Ymr148w was detectable as a unique protein in yeast cells by western blot (Figure 7). Indeed, we observed proteins corresponding to the size of either Ymr148w, approximately 20kD, or the fusion protein Ymr147-148w of approximately 45kD. We could not detect Ymr147w alone, unless Ymr148w was deleted (Figure 7). Ymr148w alone is likely expressed from its own promoter and deletion of YMR147W (including the promoter region) did not have an effect on Ymr148w expression. On the contrary, upon Ymr147w overexpression, no unspliced Ymr148w was detected, indicating that the control of a strong promoter led to the exclusive expression of the full length protein. It is likely that strong transcription through YMR147W prevents binding of transcription factors at YMR148w promoter.

How the splicing and the expression of the two isoforms is regulated, what is the effect of the relative abundance of these two species on LDs dynamics as well as what is their role in the Fld1 complex will require additional investigation.

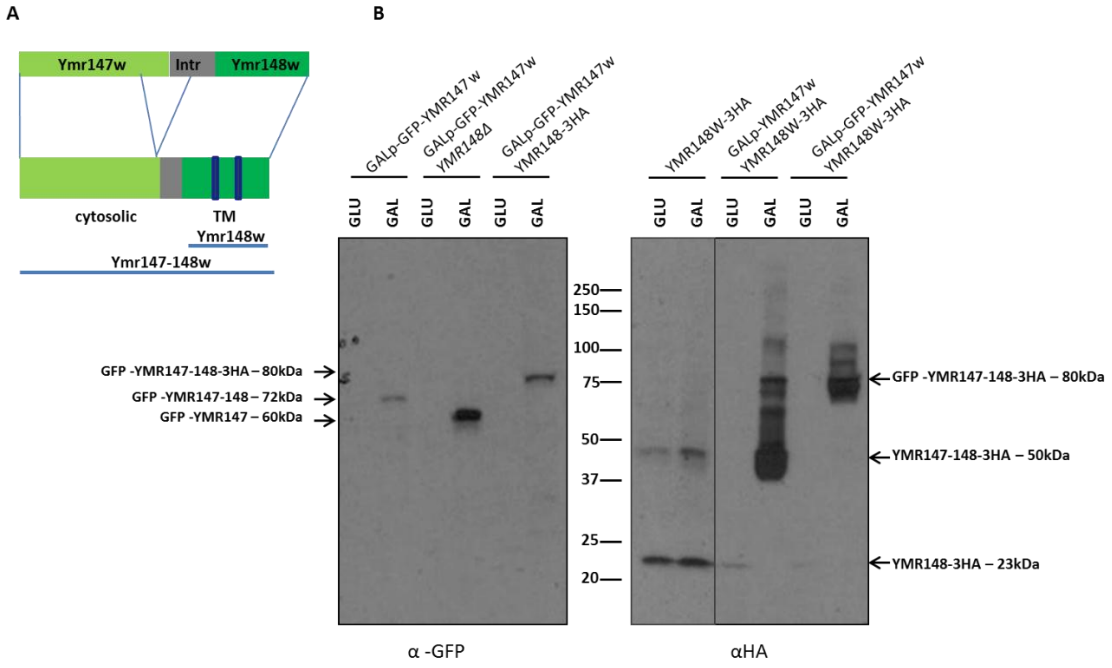

Figure 7. Ymr147w and Ymr148w can originate a single protein. Strains carrying GFP N-terminally tagged Ymr147w under the control of the Gal promoter, and Ymr148w C-terminally tagged with 3xHA, as indicated, were grown till OD1 in glucose or galactose-containing media. Blot against GFP and HA are shown, respectively.

3.1.5 As Fld1, Ldb16 is required for normal LD morphology

Deletion of Ldb16 exhibited a LD phenotype very similar to *fld1Δ* or Fld1 (S224P and G225P) loss of function mutants. For this reason we decided to focus specifically on Fld1/Ldb16 complex characterisation, aiming to further investigate the role of this unknown protein in yeast LDs biogenesis.

In stationary phase, *wt* yeast cells display 5-7 LDs that have on average a diameter of ~0.4µm. In contrast, cells lacking *FLD1* show a reduced number of LDs per cell (Figure 8A and (Fei et al., 2008; Szymanski et al., 2007)). As in *fld1Δ* mutants, LDs in *ldb16Δ* fall into morphologically distinct classes. Plotting in a graph LDs sizes of early stationary phase cells grown in minimal media, we observed a population of LDs with diameter similar to the ones found in *wt* cells or smaller, and a population of LDs with large diameter (>0.8µm), termed “supersized” LDs (SLD) (Fei et al., 2011c) that are virtually absent from *wt* cells. By observing the deletion strains at ultrastructural level using electromicroscopy (EM), we again found that supersized LDs in *fld1Δ* and *ldb16Δ* mutants are also indistinguishable (Figure 8B). When cells were observed in logarithmic

growth phase or in rich media, LDs were very small and aggregated in clusters containing the ER marker GFP-HDEL, as shown previously for *fld1Δ* cells (Szymanski et al., 2007). Altogether, these data show that Ldb16, in complex with Fld1, is required to control LD morphology.

A

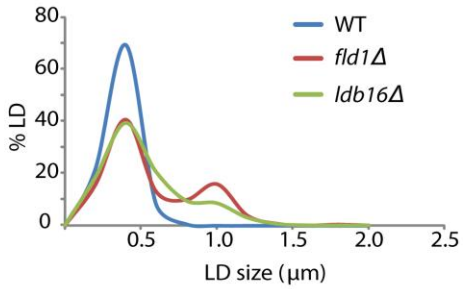

n > 200	Av nr	Av diam	St Dev nr	St Dev diam
WT	5.04	0.270	±2.28	±0.10
fld1 Δ	1.84	0.477	±1.62	±0.29
ldb16 Δ	1.92	0.428	±1.79	±0.26

B

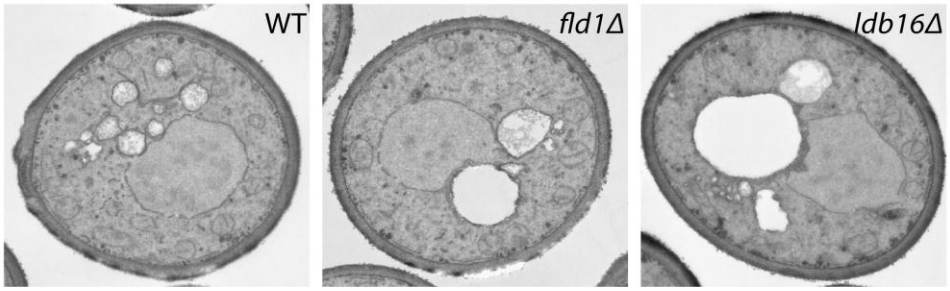

Figure 8. Ldb16 deletion strain displays the same phenotype as *fld1Δ* cells. A) LD diameters of cells stained with MDH have been analyzed and plotted in the graph. Average LD number and sizes are reported in the table. N>100. B) EM images of cells of the indicated genotypes.

3.1.6 Characterization of Ldb16p

Yeast seipin/Fld1 is composed of two TM segments separated by an ER luminal loop that comprises most of its polypeptide sequence with very short the N- and C-termini in the cytoplasm (Lundin et al., 2006). Ldb16 is a 256 amino acids protein also predicted to bear the N-terminus in the cytoplasm followed by two membrane-spanning segments and an extended cytoplasmic C-terminal domain (Figure 9A-B).

To further characterize the interaction between Fld1 and Ldb16 we generated different Ldb16 alleles, progressively truncating the protein at its C-terminus, which is also predicted to carry phosphorylation sites at positions 241 and 255. This prediction was

confirmed by mass spectrometry, however point mutations on these sites did not affect LDs morphology, suggesting that these modifications are not directly linked to LDs size regulation, at least under the condition tested. We analyzed by light microscopy strains carrying Ldb16(1-98), (1-112), (1-133), (1-191) and (1-225) truncations, all C-terminally tagged with 3xFLAG. We also generated the TM deletions Ldb16(Δ25-132) and Ldb16(Δ1-133) which only preserved the cytosolic tail and, as expected, failed to complement the SLD phenotype (data not shown). Ldb16(1-98), which is close to the end of the predicted TM (aa1-94), displayed a marked shift towards increased size LDs (Figure 9C). LDs analysis of cells bearing these truncations showed that Ldb16(1-112), although not affecting the LDs distribution in the overall population, already had a slight increase in size when observed at the microscope, displaying more medium sized LDs than *wt* (Figure 9C and data not shown). The Ldb16 truncated allele Ldb16(1-133) preserves the predicted Ldb16 TMs and lacks virtually the whole C-terminal cytosolic domain. Cells expressing Ldb16(1-133) had LDs indistinguishable from *wt* cells (Figure 9C). Moreover, the localization pattern observed in cells expressing Ldb16(1-133)-GFP is the same of the full length Ldb16-GFP (Figure 9E) indicating that this localization is likely mediated by Ldb16 membrane domain via interaction with Fld1.

Indeed, when expressed from the endogenous *LDB16* locus, this truncated protein still co-immunoprecipitated Fld1, confirming that the interaction between the two proteins likely occurs through their membrane domains (Figure 9D). Altogether, these data indicate that Ldb16(1-133) is the minimal fragment maintaining the functionality of the seipin complex. Consistently, similar findings were described in a recent paper by Wang et al., 2014.

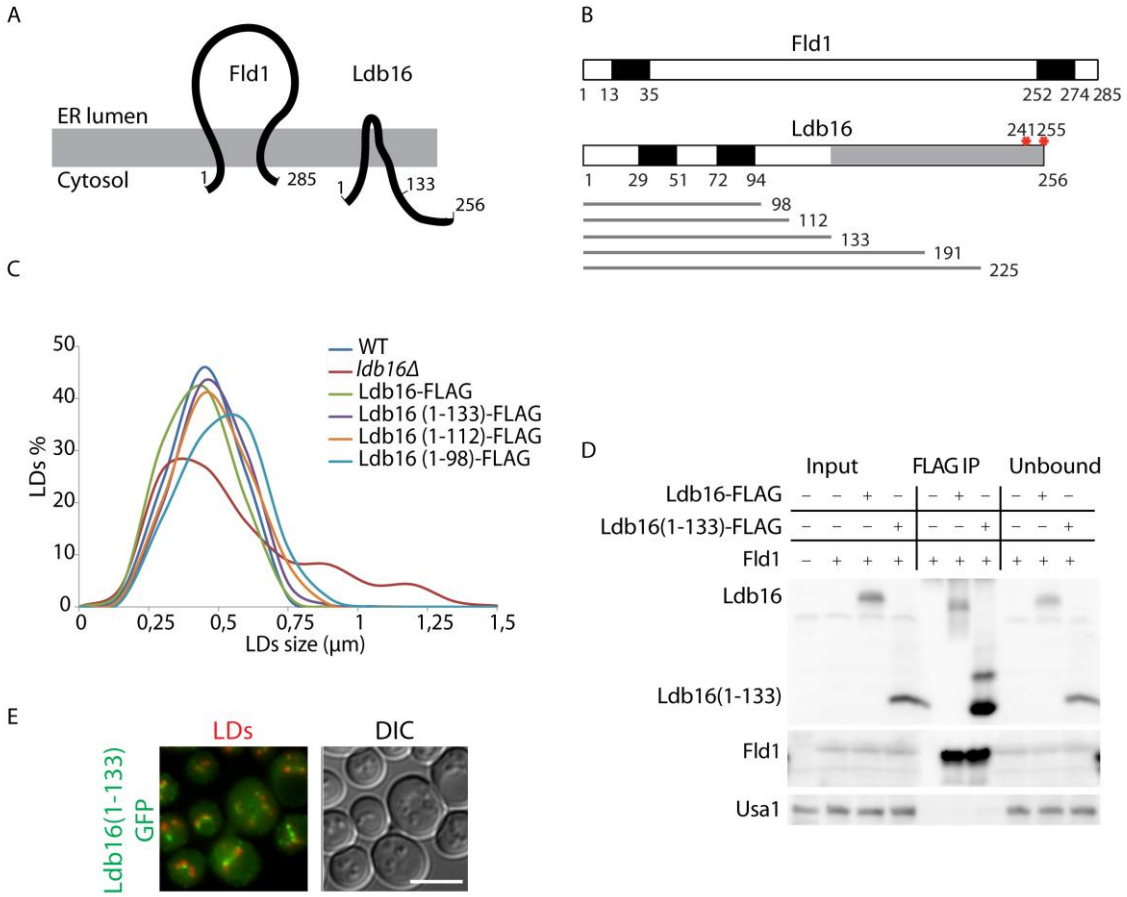

Figure 9. Characterization of Ldb16. A-B) Schematic representation of the seipin complex. Black boxes represent the TM domains. Gray part represent the deleted portion in Ldb16(1-133). Red asterisks represent Ldb16 phosphorilation sites. The cytosolic part of Ldb16 has been progressively shortened to study its functional domain. The constructs used are represented. C) Deletions not affecting the TM domain do not affect LDs morphology. The graph represents LDs sizes distribution in cells with the indicated genotypes grown to early stationary phase in minimal media. N>200. D) Ldb16(1-133) is sufficient to immunoprecipitate Fld1**.** E) C-terminally GFP tagged Ldb16(1-133) retains its localization. Ldb16 TM domain C-terminally tagged with GFP is expressed under its endogenous promoter in early stationary cells grown in minimal media. LDs are stained with MDH. Scale bar 5µm.

In absence of Fld1, the steady state levels of Ldb16 protein are highly reduced (Figure 4 and 10A). This decrease of Ldb16 in *fld1Δ* cells is due to proteasome-dependent proteolysis by ER-associated degradation pathway (ERAD). Indeed we observed that in absence of Fld1, Ldb16 is degraded through the ubiquitin ligase Doa10 (our unpublished data and (Wang et al., 2014)). All the tested truncations preserving the *wt* LDs phenotype

are still expressed in *fld1Δ* background, while the full length Ldb16 is degraded, suggesting that the degradation signal is comprised between residues 191 and 256. We further tested whether in *fld1Δ* cells Ldb16 levels can be rescued either by deleting Doa10 or by overexpressing the protein under GAL1 promoter. This was indeed the case in both conditions, however this did not complement the LDs phenotype in this strain (Figure 10B). We concluded that the two proteins are not redundant. In contrast, deletion of *LDB16* did not affect the levels of Fld1 protein (Figure 10C). Consistently, Fld1-GFP still localizes to LDs in its binding partner absence (Figure 10D and (Wang et al., 2014)). As aforementioned (Figure 6C), the overexpression of Fld1 or Ldb16 from strong constitutive GPD promoter did not alter the LDs phenotype in *wt* cells. In contrast, the overexpression of Ldb16(1-133) in *wt* background caused SLDs phenotype (Figure 10E). This effect was anyway suppressed in a background overexpressing also Fld1 (Figure 10E). This suggests that in absence of its regulatory portion the overexpression of Ldb16 (*i.e.* its TM domain) causes a dominant negative effect.

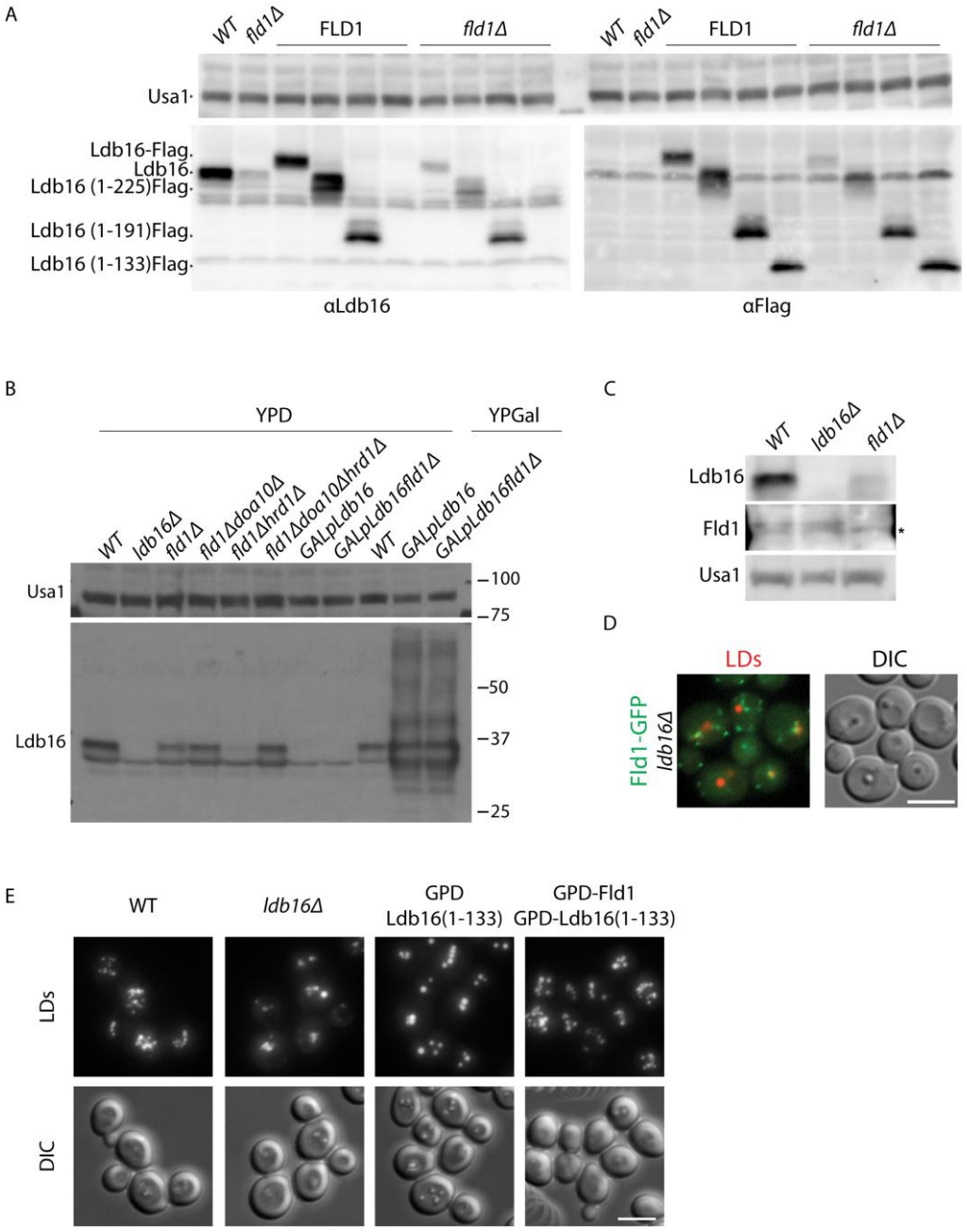

Figure 10. Ldb16 is destabilized in absence of Fld1. A) Ldb16 truncations are more stable than the full length protein. Steady state levels of C-terminally FLAG-tagged Ldb16 truncations. Proteins are immuno-detected with anti-Ldb16 and anti-Flag antibody. Usa1 is used as loading control. B) Doa10 deletion and Ldb16 overexpression rescue the protein level. Usa1 (top panel) is used as loading control. C) Fld1 is not destabilized in Ldb16 absence. Proteins are detected with Ldb16 or Fld1 antibody. Loading control: Usa1. Asterisk indicates a non-specific band. D) Fld1-GFP can still localize at LDs in absence of Ldb16. LDs are visualized with MDH, scale bar 5µm. E) Overexpression of the TM domain of Ldb16 cause an altered LDs phenotype. Z projection of cells are shown. LDs are stained with MDH, scale bar 5µm.

3.1.7 Conclusions

Searching for yeast seipin binding partners by reciprocal immunoprecipitations and western blot, we identified a previously uncharacterized protein complex. We show that the localization of the members of this complex, and in particular Ldb16, follows the same punctuate pattern at ER-LDs contact sites.

By generating knock out mutants and by analyzing them by light and electro-microscopy, we found the deletions of FLD1 and LDB16 ORFs lead to a common defect that morphologically displays in two ways: cells present either small and clustered LDs or few and supersized LDs. To address the role of the complex in LDs biogenesis we chose to focus specifically on characterizing these two binding partners. We found that Ldb16 is a phosphorylated protein and that its stability depends on Fld1 presence. The truncated versions of Ldb16, Ldb16(1-133) was more stable than the full-length protein, suggesting a regulatory function for the C-terminal tail that does not affect the LDs phenotype. We found that Ldb16 TM domain is necessary and sufficient for the complex integrity and for normal LDs morphology. Further studies will be required to address the role of the other binding partners in the Seipin complex.

Ymr148w/Osw5-GFP is both found in *foci* co-localizing with Ldb16 and distributed at LDs surface. Deletions of ymr147w, ymr148w (or ymr147/148w) did not affect the LDs phenotype compared to *wt* cells. We showed that Ymr147w and Ymr148/Osw5 are in fact a single protein that undergoes alternative splicing, which is present in two forms: a long one of around 45kD comprising both the ORFs and a short one of 18kD comprising only the TM domain-containing sequence Ymr148w. Moreover a strong promoter in front of the Ymr147w ORFs leads to the exclusive expression of the full length protein and it induced accumulation and clustering of lipid droplets. Although fascinating, these results were preliminary and need to be addressed in depth in further research projects.

Chapter 3.2

3.2.1 Distinct mechanisms leading to supersized LD formation

In a screen for genes required for normal LD morphology, components involved in phospholipid synthesis were identified. These components were not found in previous screenings performed in rich media (Fei et al., 2008; Szymanski et al., 2007). When cells are grown in minimal media, which lacks the phospholipids precursor inositol, choline and ethanolamine, strains defective in genes of the *de novo* phospholipid biosynthetic pathway form supersized LDs that strongly resemble those observed on in *fld1Δ* or *ldb16Δ* cells (Fei et al., 2011c). In particular cells with mutations in *CHO2*, *OPI3* or *INO2*, required for phosphatidylcholine (PC) synthesis by the phosphatidylethanolamine N-methyltransferase (PEMT) pathway, and in the essential gene *CDS1*, (CDP-Diacylglycerol synthase) that catalyzes the generation of CDP-DAG from phosphatidic acid (PA) and CTP (Figure 11A) display, at high frequency, supersized LDs (Fei et al., 2011c).

The abnormal phospholipid composition of these mutants, and particularly the decrease in the surfactant PC with a concomitant increase in phosphatidic acid (PA) levels, (a conic shaped negatively charged phospholipid, known to favor membrane fusion) appears to prompt the coalescence of LDs and therefore the formation of supersized LDs (Fei et al., 2011c). In support of an effect of the phospholipid imbalance, supplementation of the growth media with choline, which stimulates PC biosynthesis through the Kennedy pathway (Figure 11A) restores PC and PA levels in PEMT mutants and reverts the supersized LD phenotype in *cho2Δ* and *opi3Δ* but not in *cds1Δ* (Fei et al., 2011c). All these data indicate a close connection between the levels of PC in cells and LD morphology. However, analysis of total lipid extracts of *fld1Δ* and *ldb16Δ* cells do not show any significant changes in phospholipid composition (Fei et al., 2011b; Fei et al., 2008; Fei et al., 2011c; Szymanski et al., 2007; Wang et al., 2014) suggesting that, in these mutants supersized LDs are not a consequence of a general phospholipid imbalance at cellular level. Moreover, the frequency of supersized LDs in FLD1 or LDB16 mutants is insensitive to choline supplementation (Figure 11B), a condition that reverted the LD phenotype in *opi3Δ* cells (Figure 11B), as previously reported (Fei et al., 2011c). These data suggest that Fld1/Ldb16 control LD size by a mechanism distinct from genes in the CDP-DAG pathway. In agreement with this, cells lacking simultaneously *OPI3* or *CHO2* and *FLD1* or *LDB16* display an additive phenotype in LD morphology. In

opi3Δfld1Δ or *opi3Δldb16Δ* double mutants the population of SLDs increases and the individual LDs are bigger than in each one of the single mutants (Figure 11C-D). Moreover, choline supplementation to these double mutants only rescues the part of the phenotype, likely the contribution of the PEMT pathway mutation. Altogether these data shows that supersized LDs in PEMT and *fld1Δ/ldb16Δ* mutants are formed by distinct mechanisms.

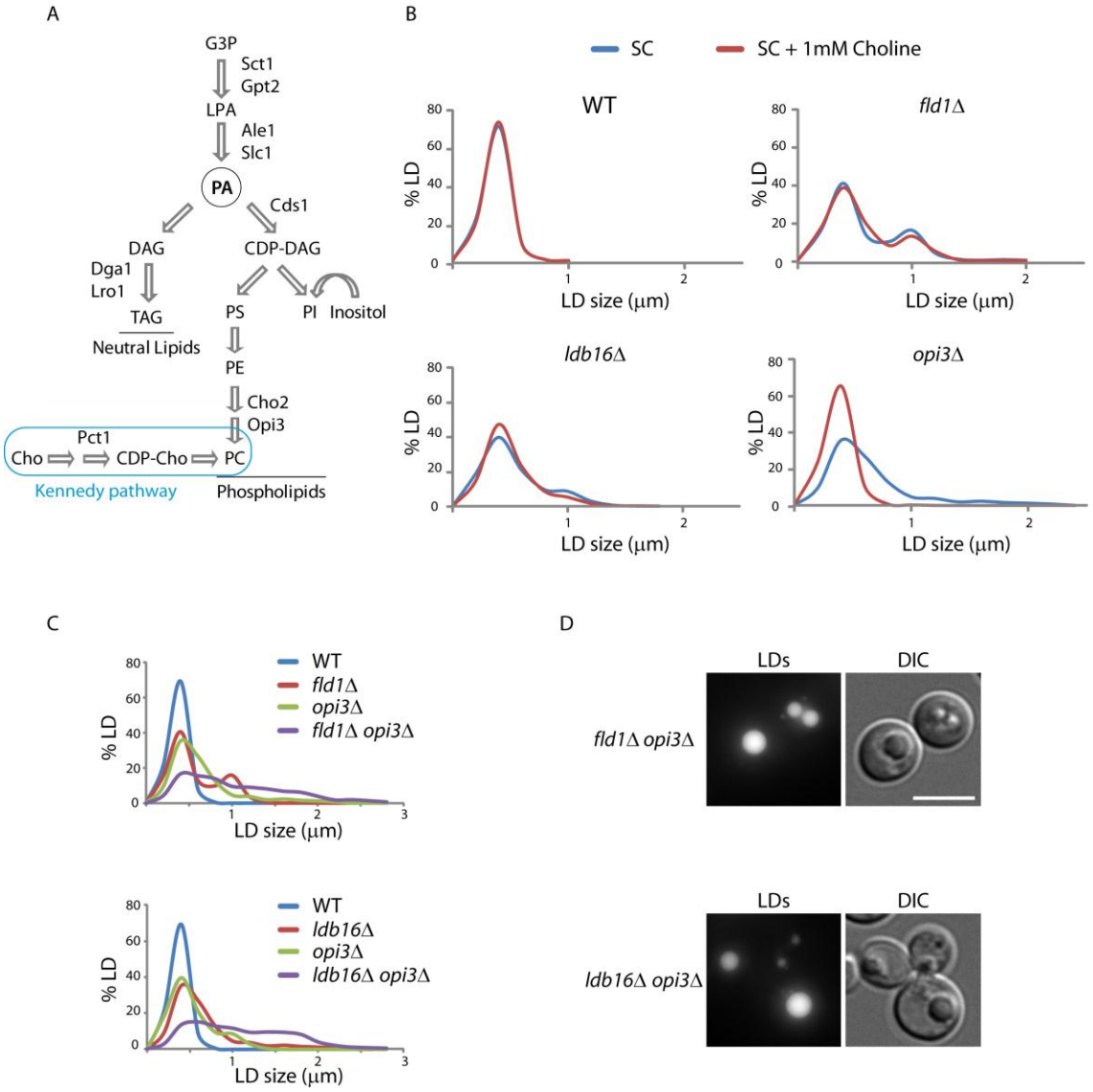

Figure 11. SLDs are formed by distinct mechanisms in PEMT pathway and FLD1/LDB16 mutants. A) Lipid metabolic pathway. A scheme of phospholipids and neutral lipids derived from PA is shown. Kennedy pathway is highlighted in blue. G3P, glycerol-3-phosphate. LPA, lysophosphatidic acid. PA, phosphatidic acid. DAG, diacylglycerol. TAG, triacylgycerol. PS, phosphatidylserine. PI, phosphatidylinositol. PE, phosphatidylethanolamine. PC, phsphatidylcholine. Cho, exogenous choline. B) Seipin complex deletion SLD phenotype is not

rescued by choline addition. Cells were grown in minimal media supplemented or not with 1mM choline till early stationary phase. LDs were stained with MDH for imaging and analyzed. Size distributions are plotted in the graphs. C-D) *fld1Δ* and *ldb16Δ* have additive effect with deletion strains of CDP-DAG pathway. Cells of the indicated genotype grown till early stationary in SC have been stained with MDH, imaged and analyzed. The diameters are plotted in the graph. Representative image are shown. Scale bar 5µm.

3.2.2 LD biogenesis in the *ldb16Δ* mutant

Since choline has no role in the defect that leads to abnormal LDs in the Seipin complex mutants, we set out to dissect the nature of the defect in *fld1Δ* and *ldb16Δ* mutants by following the process of LD biogenesis in presence or absence of the only phospholipid precursor that affects their morphology, *i.e.* inositol. Towards this goal we took advantage of the quadruple mutant strain *are1Δ are2Δ dga1Δ lro1Δ*, lacking the acyltransferases required for the synthesis of neutral lipids, and therefore deprived of LDs (Oelkers et al., 2002; Sandager et al., 2002). We produced strains bearing deletions on *ARE1*, *ARE2*, *LRO1* and in which *DGA1* expression, under the control of the strong inducible GAL1 promoter. The presence of a plasmid encoding for the estradiol responsive GAL4-ERE-VP16 chimeric protein allowed DGA1 expression in minimal media (*i.e.* without changing the carbon source from glucose to galactose). This construct provides the inducible transcriptional activation of genes driven by *GAL* promoters in response to β-estradiol (Louvion et al., 1993). We termed these cells LD^{switch}. At time 0, there are no visible LDs in *ldb16Δ*^{switch} cells. On the other hand *wt*^{switch} already displayed LDs in 30% cells due to ADGEV plasmid presence, affecting the interpretation of the result (Figure 12A). Induction of Dga1 expression with β-estradiol 100nM leads to the formation of LDs that are labeled by the neutral lipid dye MDH. Following the process for up to 6 hours, we observed that the dynamics of biogenesis and growth through time in the mutant are altered depending on the presence or absence of inositol in the media. Indeed while 60 minutes after induction around 75% of *wt*^{switch} cells displayed LDs both in minimal media and upon inositol addition, *ldb16Δ*^{switch} cells in SC reached about 60% of cells with LDs versus about 35% in presence of inositol, suggesting that the normal dynamics of LDs formation are impaired in this mutant and the defect can be alleviated by inositol depletion. Indeed, although shifted due to leakage in *wt*, the kinetics of LD initiation in *LD*^{switch} cells in minimal media appear similar (with *wt* going from 30% to 70% of cells displaying LDs in the first 30 min, and *ldb16Δ* going from 0 to 45%) irrespective of

whether the cells contain a *wt* or a mutant *LDB16* allele. From 2h to 6h *wt* number of cells displaying LDs remain stable reaching up to 87% in SC and to 78% in inositol presence (Figure 12B). *ldb16Δ* cells in minimal media reach 76% in 2 hours *versus* 78% in *wt,* and up to 6 hours remain stable. In presence of inositol however, although after 6 hours nearly 70% of cells display LDs, the initial kinetics are clearly delayed. Indeed, only 16% of the cells form LDs in the first 30 min, reaching 36% in one hour. This indicates that the seipin complex has a function in LDs biogenesis, particularly in conditions where there is an increased availability of newly synthesized phospholipids due to the presence of inositol in the media.

A

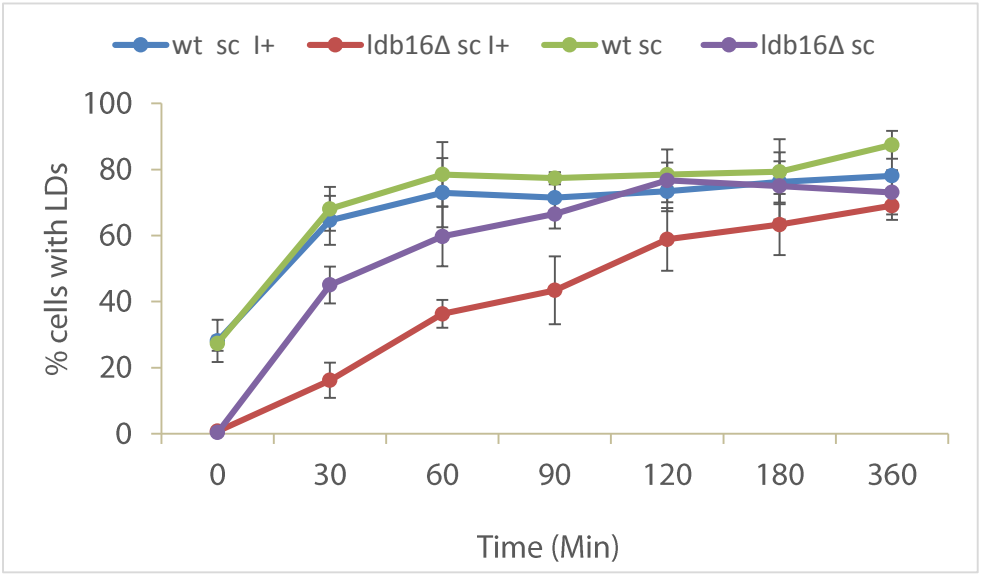

B

	sc I+				sc			
	AV		SD		AV		SD	
Time (min)	***wt***	***ldb16Δ***	***wt***	***ldb16Δ***	***wt***	***ldb16Δ***	***wt***	***ldb16 Δ***
0	28,10	0,77	6,44	1,01	27,36	0,38	2,25	0,44
30	64,62	16,18	7,41	5,32	68,08	45,04	6,65	5,58
60	72,95	36,28	10,46	4,21	78,48	59,73	9,77	9,04
90	71,43	43,38	4,78	10,27	77,36	66,49	1,86	4,37
120	73,40	58,83	3,33	9,50	78,43	76,67	3,70	9,36
180	76,22	63,31	6,29	9,25	79,32	75,00	9,81	10,14
360	78,09	69,01	8,05	4,27	87,45	73,05	4,23	6,68

Figure 12. LDs biogenesis is slower in ldb16Δ mutant cells, particularly in presence of inositol. A) LDs have been induced with 100nM βestradiol, in cells GalDGA1 *are1Δ are2Δ lro1Δ* in *wt* or *ldb16Δ* background. Time courses have been performed to monitor LDs appearance in presence or absence of 75µM inositol during 6 hours. The graph represents the number of cells displaying LDs at each indicated time point. Error bars represent the SD calculated on four independent experiments. B) Table relative to the graph. Averages and SD are shown. More than 100 cells have been counted for each time point.

3.2.3 Conclusion

We found that *ldb16Δ* strain displays the same LDs phenotype as *fld1Δ, i.e.* LDs distribution in two populations of either very small and aggregated or large LDs. This evidence suggests that these interacting partners function is involved in the same process and we focused on investigating their role in LDs regulation. Based on phenotypes similarity with the mutants in the PEMT pathway that leads to PC biosynthesis, it was proposed that absence of *FLD1* may also increase the PA/PC ratio. However, SLDs in *fld1Δ/ldb16Δ* cells are not rescued by choline supplementation to the growth media, as observed for *opi3Δ*. To further look into this aspect we generated the double KO *opi3Δfld1Δ* and *opi3Δldb16Δ*. Observing these mutant cells by light microscopy, we found that there is an additive increase in size combining the two mutations. These results suggest that Fld1 and its new interacting partner Ldb16 generate SLDs by a mechanism that is independent from the PC biosynthetic pathway. Moreover, time courses experiments in mutant cells revealed that in absence of the seipin complex proteins there is a defect in LDs biogenesis which is alleviated by inositol removal.

Chapter 3.3

The seipin complex Fld1/Ldb16 establishes a diffusion barrier at the ER-lipid droplet contact sites

Alexandra Grippa[1,2], Laura Buxó[1,2],Gabriel Mora[1,2], Francesco Mancuso[1,2], Raul Gomez[1,2], Júlia Muntanyà, Eduard Sabidó[1,2] and Pedro Carvalho[1,2]

[1]Cell and Developmental Biology Programme, Centre for Genomic Regulation (CRG), Dr. Aiguader, 88 08003 Barcelona, Spain

[2]Universitat Pompeu Fabra (UPF), Dr. Aiguader, 88 08003 Barcelona, Spain

Correspondence should be sent to:

Pedro Carvalho (pedro.carvalho@crg.eu; phone: +34-933-160-286)

Character count: 36,581

Abstract

Lipid droplets (LDs) are storage organelles consisting of a neutral lipid core surrounded by a phospholipid monolayer and a set of LD specific proteins. Most LD components are synthesized in the endoplasmic reticulum (ER), an organelle that is often physically connected with LDs. How LD identity is established while maintaining biochemical and physical connections with the ER is not known. Here, we show that the yeast seipin Fld1, in complex with the ER membrane protein Ldb16, has a role in preventing equilibration of ER and LD surface components. In the absence of the Fld1/Ldb16 complex, assembly of LDs results in phospholipid packing defects leading to aberrant distribution of lipid-binding proteins and abnormal LDs. We therefore propose that the Fld1/Ldb16 complex facilitates the establishment of LD identity by acting as a diffusion barrier at the ER-LD contact sites.

Introduction

In virtually all eukaryotic cells, LDs play central roles in lipid and energy metabolism and their deregulation is associated with metabolic disorders such as obesity, diabetes and lipodystrophy (Krahmer et al., 2013a). At structural level, LDs are rather unique: a hydrophobic core composed of neutral lipids, mainly triglycerides (TAG) and sterol esters (SE), surrounded by a monolayer of phospholipids acting as surfactants and a specific set of proteins (Fujimoto and Parton, 2011; Pol et al., 2014; Thiam et al., 2013b). This structural organization of LDs favors the binding of proteins with hydrophobic α-helical hairpins or amphipathic helices (AHs) while it precludes the association of integral membrane proteins with luminal domains. Proteins with AHs are recruited to LDs directly from the cytosol whereas the ones with hydrophobic hairpins are first targeted to the ER before concentrating at the LD monolayer (Pol et al., 2014; Thiam et al., 2013b). In both cases, the targeting appears to be highly regulated. This set of LD-specific proteins, mostly consisting of lipid modifying enzymes and regulatory proteins, to large extent determines many of the LD properties. The ER is also involved in the synthesis of most of the lipids both at the surface and in the hydrophobic core of LDs. Moreover, a large fraction (in mammals) or all (in yeast) LDs are continuous with the ER (Jacquier et al., 2011; Wilfling et al., 2013). Therefore, how these biochemically and physically connected organelles achieve and maintain their identity is a major question in cell biology.

Depending on the cell type or metabolic state, LDs vary widely in their number, size and composition (Yang et al., 2012a). The molecular mechanisms controlling these aspects of LD biology are largely unknown, but changes in phospholipid biosynthesis were shown to play a role in LD morphology (Fei et al., 2011c; Guo et al., 2008; Krahmer et al., 2011). Phospholipid imbalances, particularly defects leading to a decrease in the levels of phosphatidylcholine (PC), induce the formation of abnormally large LDs (*i. e.* "supersized"). For example, mutations in *CHO2* or *OPI3*, components of the phosphatidylethanolamine N-methyltransferase (PEMT) pathway for PC biosynthesis, lead to supersized LDs in the yeast *S. cerevisiae* (Fei et al., 2011c). In this case, the supersized LDs appear to form by coalescence of smaller ones as a consequence of both a decrease in levels of PC, which acts as a surfactant to prevent LDs coalescence (Krahmer et al., 2011), together with increased amounts of phosphatidic acid (PA), which is thought to have fusogenic properties (Chernomordik and Kozlov, 2005; Zeniou-Meyer et al., 2007). Consistent with these data, the stimulation of an alternative pathway for PC biosynthesis –the Kennedy pathway- restores the PA/PC ratio and LD morphology.

Similarly, depletion of the Kennedy pathway rate limiting enzyme CTP:phospho-choline cytidylyltransferase (CCT1) in *Drosophila* cells also induces the coalescence of small into supersized LDs (Guo et al., 2008; Krahmer et al., 2011). Whether a general imbalance in phospholipid composition is the only or the major mechanism leading to the formation of supersized LDs is unclear.

Seipin is an evolutionarily conserved ER membrane protein that has been implicated in regulating LD morphology but whose function is not well understood. It was originally identified as being mutated in patients with Berardinelli-Seip congenital lipodystrophy (Magre et al., 2001). These patients display almost complete absence of adipose tissue, ectopic fat accumulation and altered glucose metabolism, a phenotype recapitulated in mice and flies upon targeted ablation of seipin (Cui et al., 2011; Chen et al., 2012; Prieur et al., 2013; Tian et al., 2011).

At the cellular level, the major defect caused by seipin mutations is observed in LDs, which appear smaller and aggregated (Boutet et al., 2009; Fei et al., 2011b; Szymanski et al., 2007). In *S. cerevisiae* lacking the seipin homolog Fld1 similar LD defects are displayed, however only in a fraction of the cells (Fei et al., 2008; Fei et al., 2011c; Szymanski et al., 2007; Wang et al., 2014). In the rest of *fld1Δ* cells LDs are still abnormal, but instead of small and aggregated, they appear in reduced numbers and supersized. While resembling those observed in the PEMT pathway mutants *opi3Δ* or *cho2Δ*, supersized LDs in *fld1Δ* cells are not rescued by stimulation of the Kennedy pathway, indicating that they are caused by a different defect (Fei et al., 2011c; Wang et al., 2014). Interestingly, the distinct morphologies of abnormal LDs in *fld1Δ* cells can be manipulated by inositol, a phospholipid precursor with a central role in glycerolipid metabolism (Henry et al., 2012). At low inositol concentrations supersized LDs are seen in a large fraction of *fld1Δ* cells; in contrast, if inositol concentration is high the frequency of supersized LDs decreases with a concomitant increase in LD aggregates (Fei et al., 2011c; Wang et al., 2014). This observation suggests that the LD defects in *FLD1* mutants might derive from abnormal phospholipid homeostasis. However, robust and consistent changes in global phospholipid composition have not been detected in seipin mutants, in yeast or in any other cell type (Fei et al., 2011b; Fei et al., 2008; Fei et al., 2011c; Szymanski et al., 2007; Wang et al., 2014).

In yeast Fld1 binds to Ldb16, another ER membrane protein (Wang et al., 2014). Ldb16 localizes with Fld1 to ER-LD contact sites and is necessary for the stability of Fld1. Moreover, the LD phenotypes of *fld1Δ* and *ldb16Δ* are remarkably similar further

indicating that they have a common unknown function in LD formation (Wang et al., 2014).

Here we show that the Fld1/Ldb16 complex is required for the identity of LDs in *S. cerevisiae*. In the absence of this complex, incorporation of phospholipids into the monolayer of nascent LDs is entirely dependent on the ER phospholipid pools leading to the generation of membrane defects and abnormal localization of ER, LD and other lipid-binding proteins. We propose that the Fld1/Ldb16 complex contributes to LD identity by acting as a diffusion barrier at the ER-LD contact sites.

Results

Lipid-driven relocalization of Opi1 in Fld1/Ldb16 complex mutants

As a first step in dissecting the function of the Fld1/Ldb16 complex we analyzed the protein composition of the LDs in *fld1Δ* and *ldb16Δ* mutants. LDs were isolated from *wt*, *fld1Δ* and *ldb16Δ* cells grown in rich media to late logarithmic phase, a condition in which the mutant cells display equivalent amounts of supersized and aggregated LDs (Fei et al., 2008; Szymanski et al., 2007; Wolinski et al., 2011). Label-free quantitative mass spectrometry revealed that the proteomes of LDs isolated from *fld1Δ* and *ldb16Δ* cells were similar between them but very distinct from the one of *wt* LDs. Both a dramatic decrease of LD-specific proteins and an increase of proteins that do not associate with LDs from *wt* cells were detected in LDs isolated from *fld1Δ* and *ldb16Δ* mutants. We will describe the two phenotypes separately starting with the latter as it provides insights on the function of the Fld1/Ldb16 complex in LD formation.

		fld1Δ		***ldb16Δ***	
ID	**Description**	**logFC**	**P.Value**	**logFC**	**P.Value**
YHL020C	Opi1	5.489566	1.46E-04	4.20386	6.32E-06
YPR097W	Ypr097w	3.716108	1.17E-04	2.281816	6.38E-04
YLL040C	Vps13	2.827194	6.16E-04	2.056947	2.57E-03
YLR380W	Csr1	2.803219	4.00E-04	1.653667	1.12E-02
YGR202C	Pct1	2.473526	8.19E-04	2.180898	3.08E-04
YIL041W	Gvp36	2.371785	9.15E-03	2.775928	8.10E-05
YPL145C	Kes1	1.918121	5.72E-03	1.21771	6.65E-02

Table S1- Peripheral membrane proteins increased in LDs isolated from *fld1Δ* and *ldb16Δ* cells, as determined by label free quantitative mass spec and confirmed by fluorescence microscopy.

The LD proteomic analysis revealed a group of peripheral membrane proteins that in *wt* cells do not associate with LDs but that are highly enriched in LDs isolated from *ldb16Δ* and *fld1Δ* mutants (Table S1). The most abundant of these proteins was Opi1, a transcriptional repressor whose activity is controlled by association with the membrane of the ER (Loewen et al., 2004). In the nucleus, Opi1 represses the activation of many genes, including phospholipid biosynthetic genes (Henry et al., 2012). Under conditions of active phospholipid synthesis, Opi1 is bound to the ER membrane in an inactive state.

The membrane association of Opi1 involves a bipartite signal: through its FFAT motif, Opi1 binds to the ER membrane protein Scs2; through a short lysine-rich segment (Q2), Opi1 is thought to bind to PA, a precursor for most cellular phospholipids as well as TAG (Loewen et al., 2004; Loewen et al., 2003). To validate the mass spec data, we analyzed the localization of endogenous Opi1 C-terminally tagged with mCherry (Opi1-Cherry). In *wt* cells, Opi1-Cherry was uniformly distributed at the nuclear ER as expected (Loewen et al., 2003) (Fig. 1A). In cells lacking Ldb16 or Fld1, Opi1-Cherry still overlapped with the nuclear ER marker Hmg1-GFP, however its distribution was uneven forming 1-3 *foci*/cell (Fig. 1A and data not shown). These Opi1-rich *foci* were often apposed to abnormal aggregated or supersized LDs and, based on our proteomic analysis, likely co-purify with LDs.

Next, we investigated the determinants leading to Opi1 relocalization in *ldb16Δ* and *fld1Δ* cells. First, we tested the involvement of its membrane-bound partner Scs2. In *scs2Δ* cells, Opi1-GFP is mostly nuclear (Fig. 1B), as previously shown (Loewen et al., 2003). In contrast, the localization of Opi1-GFP in *ldb16Δ scs2Δ* and *fld1Δ scs2Δ* double mutants is similar to that in single *ldb16Δ* and *fld1Δ* mutants (Fig. 1B) suggesting that Scs2 is not involved in Opi1 *foci* formation. Moreover, despite localizing to LD aggregates in *ldb16Δ* and *fld1Δ* mutants, Scs2 is normally distributed throughout the ER (Fig. S1A). A similar distribution is observed for a GFP-fusion of the Opi1 FFAT domain (GFP-Opi1^{FFAT}) (Fig. S1B). Thus, the aberrant distribution of Opi1 in *ldb16Δ* and *fld1Δ* mutants is independent of Scs2.

Next we tested whether the abnormal Opi1 distribution in the mutants relied on its lipid-binding activity, putatively to PA. A short Opi1 fragment rich in basic amino acids, Opi1^{Q2}, was shown to bind to PA both in vivo and in vitro (Loewen et al., 2004). In *wt* cells, Opi1^{Q2} fused to GFP (GFP-Opi1^{Q2}) localized mostly to the nucleus as previously shown (Loewen et al., 2004). In *ldb16Δ* cells, besides the nuclear localization, GFP-Opi1^{Q2} formed *foci* resembling the Opi1-GFP although at a much lower frequency (Fig. S1C). These results suggested that abnormal PA distribution could be the cause of Opi1 relocalization in Seipin complex mutants. Therefore we analyzed the distribution of GFP-Spo20$^{51-91}$, a 40 amino acid fragment containing the AH of the SNARE Spo20 widely used as a PA biosensor (Nakanishi et al., 2004). In *wt* cells, GFP-Spo20$^{51-91}$ localizes at the cell periphery (Fig. 1C), as expected (Nakanishi et al., 2004). Besides this peripheral staining, *fld1Δ* and *ldb16Δ* mutant cells frequently displayed additional GFP-Spo20$^{51-91}$

foci. These were often apposed to LDs and were reminiscent of those observed for Opi1-GFP.

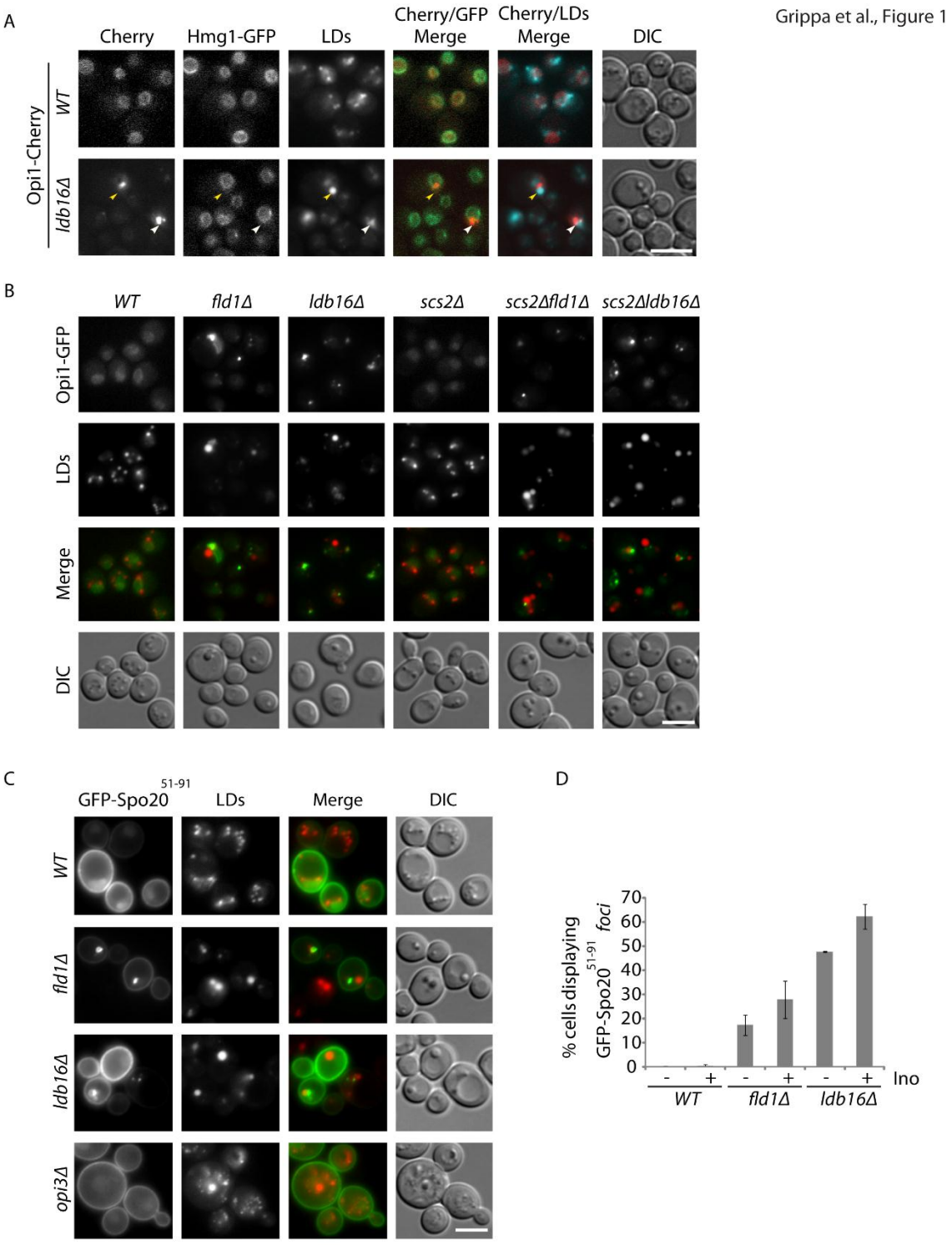

Figure 1. Lipid-driven relocalization of Opi1 in Fld1/Ldb16 complex mutants. (A) Localization of Opi1 in *wt* and *ldb16Δ* cells grown in SC media to early stationary phase. Opi1 was expressed from the endogenous locus as C-terminal mCherry fusion (Opi1-Cherry). Nuclear envelope was labeled by endogenously expressed Hmg1-GFP. LDs were stained with the neutral lipid dye MDH. Yellow arrowheads indicate supersized LDs; white arrowhead indicates LD aggregates. Scale bar: 5µm. (B) Localization of endogenously expressed Opi1-GFP in cells with the indicated genotype grown to early stationary phase in SC media. LDs were stained with the neutral lipid dye MDH. Scale bar: 5µm. (C) Localization of GFP-Spo20$^{51-91}$ expressed from a 2µ plasmid in cells with the indicated genotype. LDs were stained with the neutral lipid dye MDH. Scale bar: 5µm. (D) Percentage of cells with the indicated genotype displaying abnormal *foci* of GFP-Spo20$^{51-91}$. Late logarithmic cells grown in SC media (-) or SC supplemented with 75 µM of inositol (+) are shown. The average of 2 independent experiments is graphed; error bars represent the standard deviation of the mean. For each genotype and condition, at least 100 cells/experiment were analyzed.

Figure S1. Distribution of Scs2, Opi1 protein and lipid binding domain and PA in *fld1Δ* and *ldb16Δ* mutants. (A) Localization of GFP-Scs2 in *wt*, *ldb16Δ* and *fld1Δ* cells grown in SC media to early stationary phase. LDs were stained with the neutral lipid dye MDH. Scale bar: 5µm. (B) Localization of GFP-Opi1^{FFAT} in *wt*, *ldb16Δ* and *fld1Δ* cells grown in SC media to early stationary phase. LDs were stained with the neutral lipid dye MDH. Scale bar: 5µm. (C) Localization of GFP-Opi1^{Q2} in cells with the indicated genotype. Plasmid-borne GFP-Opi1^{Q2} expression was driven by the constitutive *PRC1* promoter. LDs were stained with the neutral lipid dye MDH. Scale bar: 5µm. (D) Amount of PA in cells with the indicated genotype and grown in SC media or SC supplemented with inositol (75 µM). Lipids were labeled to steady state with $^{[1\text{-}14C]}$acetate, extracted and analyzed by thin layer chromatography. The content of PA, relative to *wt* cells grown in SC media, is presented as the average of 3 independent experiments, error bars represent standard deviation of the mean.

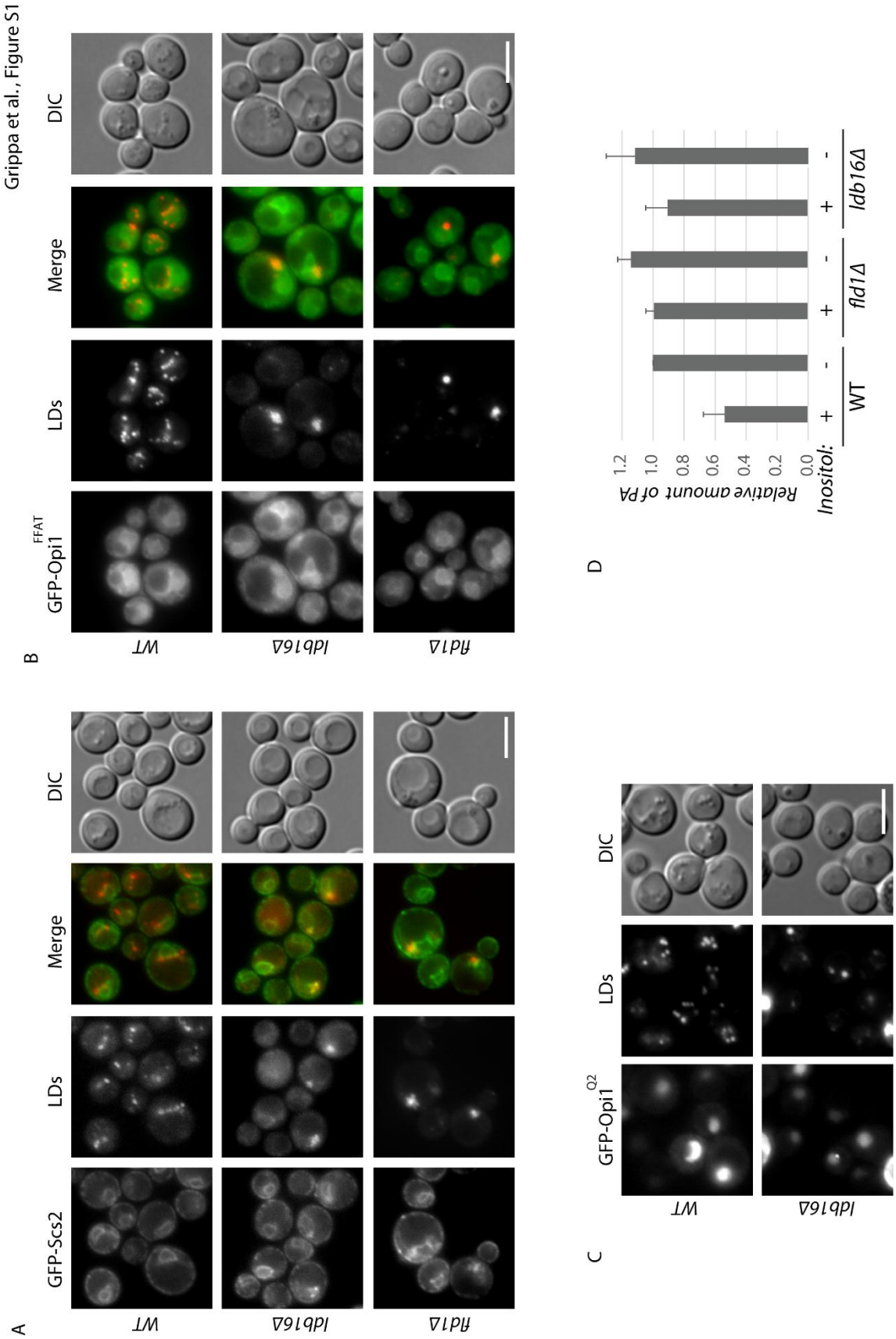
Grippa et al., Figure S1
A
GFP-Scs2
LDs
Merge
DIC
WT
Idb16Δ
fld1Δ
B
GFP-Opi1FFAT
LDs
Merge
DIC
WT
Idb16Δ
fld1Δ
C
GFP-Opi1Q2
LDs
DIC
WT
Idb16Δ
D
Relative amount of PA
1.2
1.0
0.8
0.6
0.4
0.2
0.0
Inositol:
+
-
+
-
+
-
WT
fld1Δ
Idb16Δ

The GFP-Spo20$^{51-91}$ spots were specific to *fld1Δ* and *ldb16Δ* cells and were not present in other mutants displaying supersized LDs, such as *opi3Δ* (Fig. 1C). Curiously, cells grown in inositol-supplemented media showed higher percentage of GFP-Spo20$^{51-91}$ *foci* (Fig. 1D). Altogether these data indicate that abnormal Opi1 distribution is driven by its lipid-binding domain. However, it is unlikely that abnormal PA accumulation is the cause of the defect as the relocalization of both Opi1-GFP and GFP-Spo20$^{51-91}$ increases in presence of inositol, a condition that favors PA consumption (Fig. S1D) (Loewen et al., 2004).

Table 1. Amphipathic helix (AH) containing proteins ectopically localized to LDs in *ldb16Δ* and *fld1Δ* cells.

Protein	Localization	Function	Type of AH	Ref.
Pct1	Nuclear Envelope / Nucleus	Cholinephosphate cytidylyltransferase	"canonical"	(Cornell and Taneva, 2006)
Kes1	Cytoplasm/ Golgi	Oxysterol binding protein	ALPS	(Drin et al., 2007)
Vps13	Cytoplasm / Endosomes (?)	Unknown	ALPS	(Drin et al., 2007)
Gvp36	Cytoplasm / Golgi Vescicles	Unknown (BAR-domain containing protein)	AH (ALPS type) in N-BAR domain	(Gautier et al., 2008)

Relocalization of amphipathic helix-containing proteins in seipin complex mutants

The other peripheral membrane proteins co-purifying ectopically with *ldb16Δ* and *fld1Δ* LDs were very diverse in function and normal subcellular localization. However, they all contain or are predicted to contain an AH, a common motif involved in membrane association (Table 1)(Gautier et al., 2008). These AH-containing proteins were expressed from their endogenous *loci* as C-terminal fusions to GFP and their distribution was analyzed by fluorescence microscopy (Fig. S2A). When compared to *wt* cells, in *ldb16Δ* and *fld1Δ* mutants all the tested proteins were dramatically relocalized appearing as 1-3 *foci*/cell overlapping or proximal to LDs (Fig. S2A and data not shown). These results confirmed the proteomic analysis of isolated LDs. Next, we asked whether the change in localization of those proteins required their AHs. In all tested cases, deletion of the AH abolished or dramatically decreased the relocalization of the proteins in *ldb16Δ* and *fld1Δ* mutants (Fig. 2A). The drop in ectopic localization was observed irrespective of the inositol concentration (Fig 2A), which influences the morphology of LDs in the mutants, and was not due to changes in the steady state levels of proteins (Fig. S2B).

Finally, expression from the endogenous promoter of the AH of one of these proteins (Kes1) fused to GFP was sufficient for LD relocalization in *ldb16Δ* and *fld1Δ* cells (Fig. 2B). Altogether, these results indicate that the relocalization of several proteins in *ldb16Δ* and *fld1Δ* cells is mediated by their AHs.

Grippa et al., Figure 2

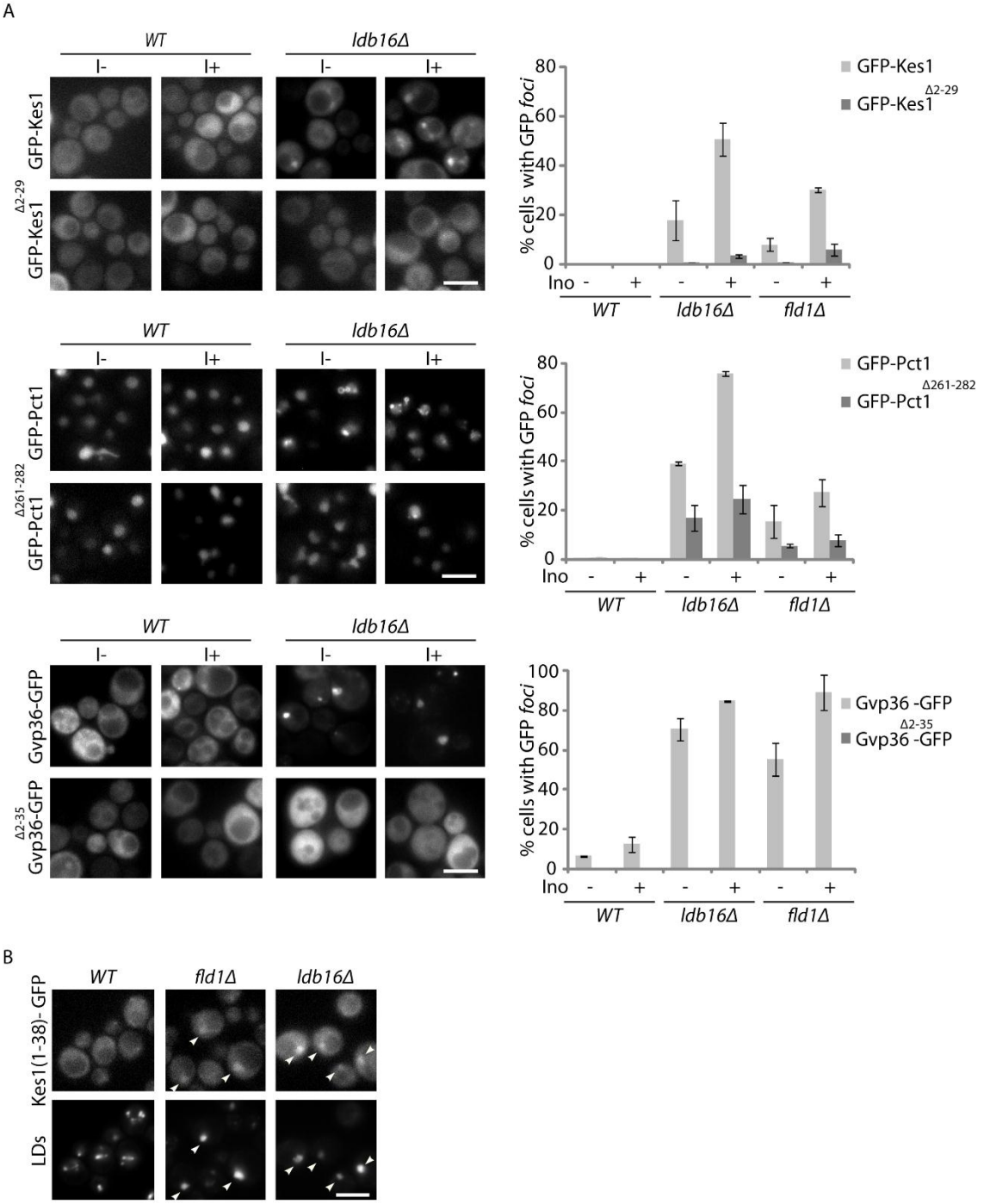

Figure 2. Relocalization of amphipathic helix-containing proteins in seipin complex mutants. (A) Localization of GFP-tagged Kes1, Pct1, Gvp36, and the corresponding counterparts lacking the AH Kes1$^{\Delta 2\text{-}29}$, Pct1$^{\Delta 261\text{-}282}$ and Gvp36$^{\Delta 2\text{-}35}$ in cells with the indicated genotype. The GFP fusion proteins were expressed from a centromeric plasmid. Cells in early stationary phase grown in SC media (-) or SC supplemented with 75 µM of inositol (+) were imaged. LDs were stained with the neutral lipid dye MDH. Scale bar: 5µm. On the right the percentage of cells with the indicated genotype displaying abnormal *foci* of GFP-tagged proteins. The average of 3 independent experiments is displayed; error bars represent the standard deviation of the mean. At least 100 cells/experiment were analyzed per genotype. (B) Localization of Kes1(1-38)-GFP in cells with the indicated genotype grown in SC supplemented with inositol. Kes1(1-38)-GFP was expressed from the endogenous *KES1 locus* and encodes for Kes1 AH. LDs were stained with the neutral lipid dye MDH. Scale bar: 5µm.

Figure S2. Amphipathic-helix containing proteins are specifically relocalized in seipin complex mutants. (A) Localization of the proteins Opi1, Pct1, Kes1, Gvp36 and Vps13 in *wt* and *ldb16Δ* cells. All proteins were expressed from their endogenous locus as C-terminal GFP fusions. Scale bar: 5µm. (B) Steady state levels of full length Pct1, Kes1, Gvp36 (FL) and the corresponding counterparts lacking the AHs (ΔAH) in cells with the indicated genotype. Protein extracts of cells grown in the indicated media were subjected to SDS page and analysed by western blotting with anti-GFP antibody. Phosphoglycerate kinase 1 (Pgk1) was used as loading control and detected with anti-Pgk1 antibody. (C) Localization of the AH-containing proteins Gvp36 and Vps13 in *wt* and *ldb16Δ* cells grown in SC media to early stationary phase. Proteins were expressed from their endogenous locus as C-terminal mCherry fusions. Nuclear envelope is labelled by endogenously expressed Hmg1-GFP. LDs are stained with the neutral lipid dye MDH. Yellow arrowheads indicate supersized LDs; white arrowheads indicate LD aggregates. Scale bar: 5µm.

Grippa et al., Figure S2

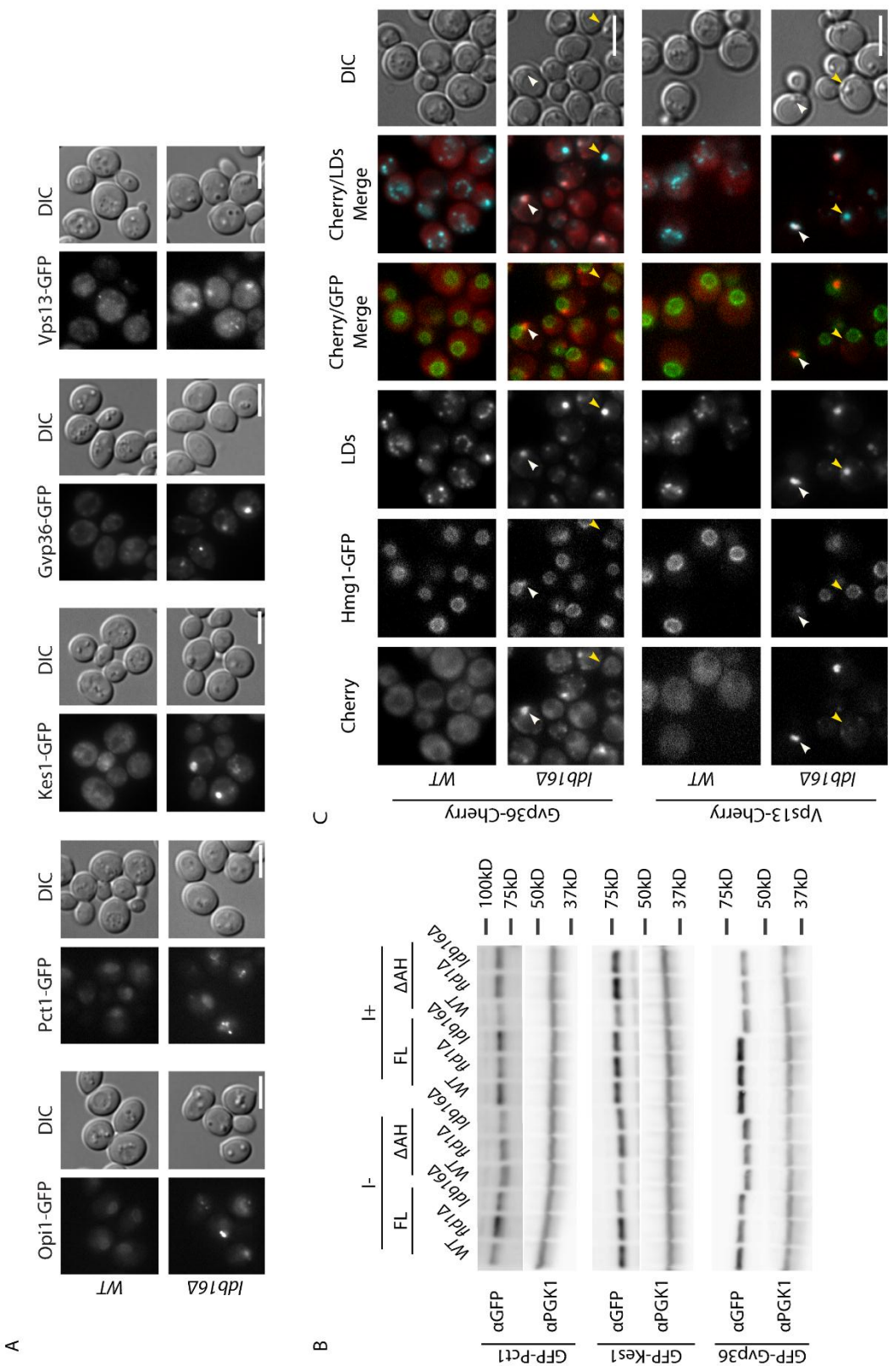

Seipin complex mutants display phospholipid-packing defects

AHs do not act as simple membrane anchors but can play an active role in deforming lipid membranes or sensing membrane packing defects, thereby controlling membrane-related processes (Campelo and Kozlov, 2014; Drin and Antonny, 2010). Moreover, the chemical properties of AHs can vary significantly and determine the binding preferences to target membranes. Intriguingly, Kes1 and Pct1, two of the ectopically localized proteins in the mutant cells, contain AHs with very distinct chemical properties. The AH of Pct1, the yeast CTP:phospho-choline cytidylyltransferase, has a highly charged polar face (Fig. 3A). In contrast, the AH of the lipid transfer protein Kes1 has a polar face enriched in serine/threonines and poor in charged residues (Fig. 3A). This latter type of AH is also known as ALPS (amphipathic lipid packing sensor) domain and was shown to recognize lipid packing defects arising either from membrane curvature or accumulation of conical lipids in flat membranes (Campelo and Kozlov, 2014; Drin et al., 2007; Vamparys et al., 2013; Vanni et al., 2013).

Given the distinct properties of their AHs, the distribution of Kes1 and Pct1 was analyzed in detail. In *wt* cells both Pct1-Cherry and Kes1-Cherry had a diffuse distribution as expected (MacKinnon et al., 2009) (Fig. 3B). In *ldb16Δ* and *fld1Δ* mutants, Pct1-Cherry formed *foci* overlapping with the nuclear envelope marker Hmg1-GFP and that were frequently apposed to abnormal LDs, both supersized and aggregated (Fig. 3B). In mutant cells Kes1-Cherry also formed *foci*, however these were distinct from the ones of Pct1. Kes1-Cherry *foci* were juxtaposed to the nuclear envelope and perfectly overlapping with the LD aggregates (Fig. 3B). Remarkably, Kes1-Cherry was never seen at supersized LDs indicating that the monolayers of aggregated and supersized LDs have different properties.

In cells co-expressing Pct1 and Kes1 as Cherry and GFP fusions respectively we confirmed that these proteins relocalize to proximal but distinct regions in *ldb16Δ* and *fld1Δ* mutants, likely as a consequence of the different chemical properties of their AHs (Fig. 3C). Accordingly, Vps13 and Gvp36, that like Kes1 contain AHs of the ALPS type also localize to LD aggregates (Fig. S2C). In sum, these data indicate that in *ldb16Δ* and *fld1Δ* mutants, LDs and proximal regions of the nuclear envelope display phospholipid packing defects that are recognized by AHs with different specificities.

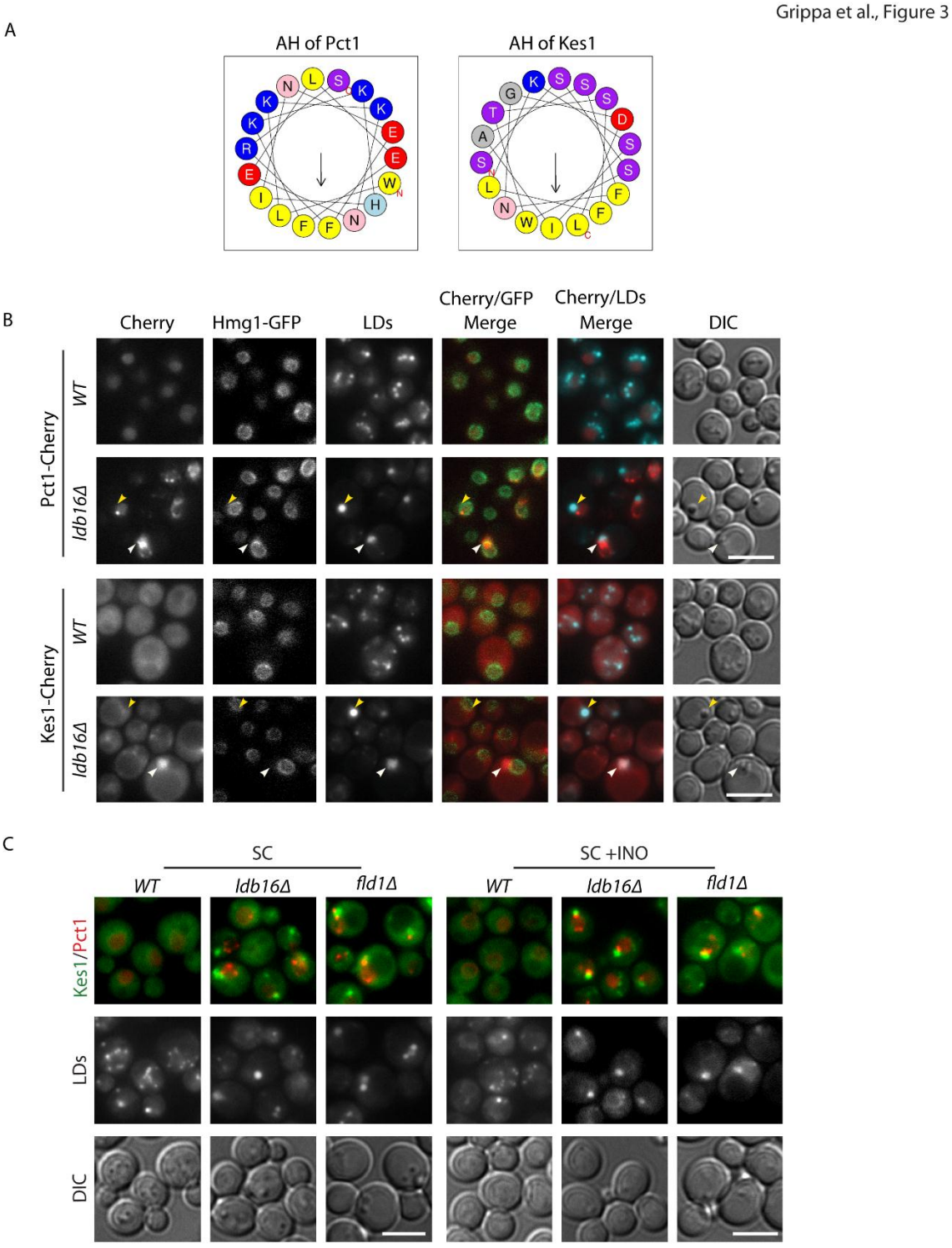

Figure 3. Phospholipid packing defects in Fld1/Ldb16 complex mutants. (A) Helical-wheel representation of the AH of Pct1 and Kes1 as predicted and drawn by Heliquest (Gautier et al., 2008). Both AHs display a well-defined face enriched in hydrophobic residues (yellow). In contrast, the polar faces are very distinct: in Pct1 it is enriched in charged residues (blue and red) while in Kes1 the abundance of non-charged serine and threonine residues (purple) dominates.

(B) Localization of Pct1 and Kes1 in *wt* and *ldb16Δ* cells grown in SC media to early stationary phase. Proteins were expressed from their endogenous locus as C-terminal mCherry fusions. Nuclear envelope is labeled by endogenously expressed Hmg1-GFP. LDs are stained with the neutral lipid dye MDH. Yellow arrowheads indicate supersized LDs; white arrowheads indicate LD aggregates. Scale bar: 5µm. (C) Localization of endogenously expressed Kes1-GFP and Pct1-mCherry in *wt*, *ldb16Δ* and *fld1Δ* cells. Late logarithmic cultures in SC media or SC supplemented with 75 µM of inositol (SC + INO) were imaged. LDs are stained with the neutral lipid dye MDH. Scale bar: 5µm.

Membrane defects in Seipin complex mutants are caused by LD assembly

Mutations on *FLD1* and *LDB16* might have a general effect on membrane properties causing the observed defects in LD morphology and protein localization. Alternatively, the membrane defects might derive specifically from abnormal LD assembly in these mutants. To discriminate between these possibilities we analyzed the distribution of Pct1, GFP-Spo20$^{51-91}$ and Kes1 in cells lacking LDs, as is the case of the quadruple mutant *are1Δ are2Δ dga1Δ lro1Δ* (*Qmut*) unable to synthesize neutral lipids (Sandager et al., 2002; Sorger et al., 2004). The distribution of these proteins was indistinguishable between *wt* and *Qmut* cells (Fig. 4A and S3A-B). Importantly, the abnormal localization of Pct1, GFP-Spo20$^{51-91}$ and Kes1 induced by *ldb16Δ* and *fld1Δ* mutations was completely reverted in the absence of LDs, such as the quintuple mutants *are1Δ are2Δ dga1Δ lro1Δ ldb16Δ* and *are1Δ are2Δ dga1Δ lro1Δ fld1Δ* (Fig. 4A and S3A-B).

Next we followed LD assembly in cells lacking *are1Δ are2Δ lro1Δ* in which *DGA1* is under the control of an inducible promoter (LD^{Switch}) either in presence or absence of *LDB16* and *FLD1*. Time course experiments showed that relocalization of Pct1 and Kes1 follows the appearance of LDs (Fig 4B-C). Moreover, the abnormal LD morphology in seipin complex mutants was not reverted by additional deletion of Pct1 or any of the other proteins localizing ectopically to LDs (Fig. S3C and data not shown). These data show that the membrane defects are a consequence of abnormal LD formation in *ldb16Δ* and *fld1Δ* mutants. Moreover, they suggest that the Seipin complex organizes ER membrane domains required specifically during LD assembly.

Grippa et al., Figure 4

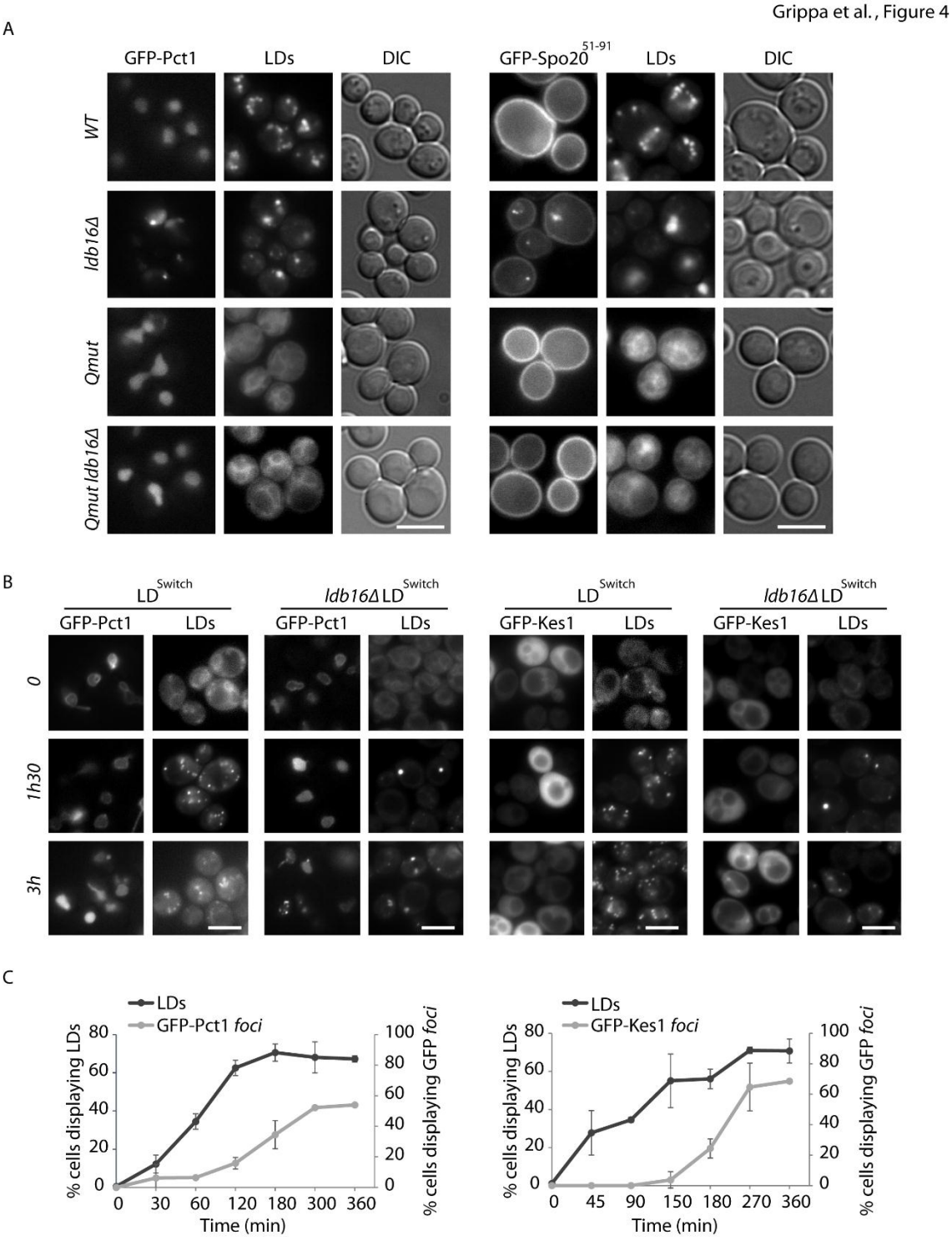

Figure 4. LD assembly causes phospholipid-packing defects in Seipin complex mutants. (A) Localization of GFP-Pct1 and GFP-Spo20$^{51-91}$ in cells with (*wt* and *ldb16Δ*) and without LDs (*are1Δ are2Δ dga1Δ lro1Δ* and *are1Δ are2Δ dga1Δ lro1Δ ldb16Δ*). Cells were grown in SC media up to early stationary phase. LDs were stained with the neutral lipid dye MDH. Scale bar: 5µm. (B) Localization of GFP-Pct1 and GFP-Kes1 at the indicated time points upon induction of LD formation. LDs were induced by expression of the TAG synthesizing enzyme Dga1 from a regulatable promoter in *are1Δ are2Δ lro1Δ* (LD^{Switch}) or *are1Δ are2Δ lro1Δ ldb16Δ* (*ldb16Δ* LD^{Switch}) cells. LDs were stained with the neutral lipid dye MDH. Scale bar: 5µm. (C) Kinetics of LD formation and appearance of GFP-Pct1 (left) or GFP-Kes1 (right) *foci* in *ldb16Δ* LD^{Switch} cells. Cells were grown in minimal media supplemented with 75µM inositol until early stationary phase. The percentages of *ldb16Δ* LD^{Switch} cells displaying LDs (black line) or *foci* of the indicated GFP-tagged protein (grey line). Expression of Dga1 was induced at time zero. The average of 2 independent experiments is displayed; error bars represent the standard deviation of the mean. At least 100 cells/timepoint were analyzed in each experiment.

Figure S3. LD assembly causes phospholipid-packing defects in Seipin complex mutants. (A) Localization of GFP-Kes1 in cells with (*wt*, *ldb16Δ* and *fld1Δ*) and without (quadruple mutant *are1Δ are2Δ dga1Δ lro1Δ*, *are1Δ are2Δ dga1Δ lro1Δ ldb16Δ* and *are1Δ are2Δ dga1Δ lro1Δ fld1Δ, i.e. Qmut Δ, Qmut Δ ldb16Δ and QmutΔ fld1Δ*) LDs. Cells were grown in SC media up to early stationary phase. LDs were stained with the neutral lipid dye MDH. Scale bar: 5µm. (B) Localization of GFP-Pct1 in cells with the indicated genotype. LDs were stained with the neutral lipid dye MDH. Scale bar: 5µm. (C) Deletion of *KES1* or *PCT1* does not affect LD morphology in presence or absence of *LDB16*. LDs of single and double mutants were stained with the neutral lipid dye MDH. Scale bar: 5µm.

Grippa et al., Figure S3

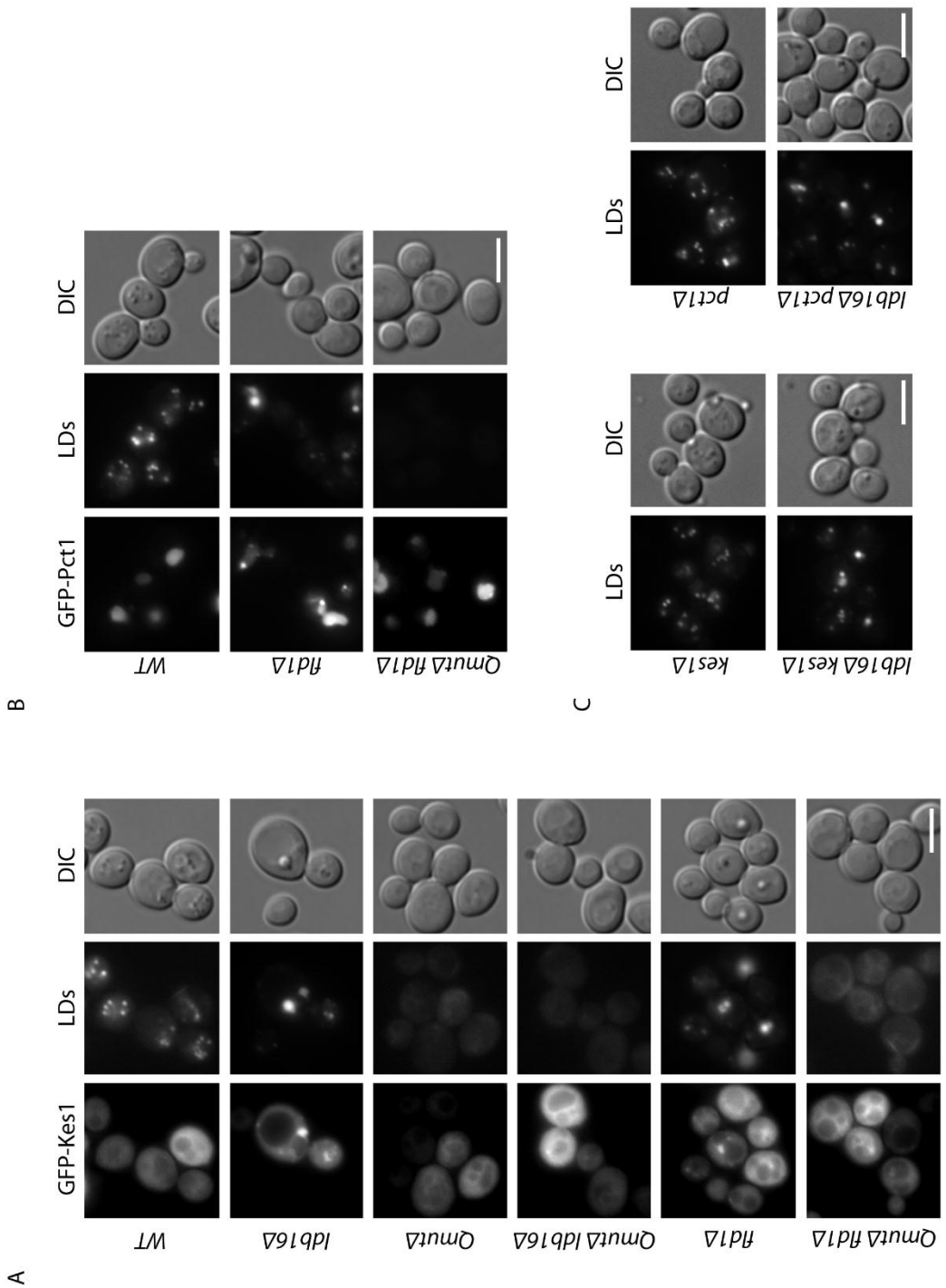

Seipin complex prevents equilibration of ER and LDs

The proteomic analysis also revealed a general increase of ER integral membrane proteins in LDs from *fld1Δ* and *ldb16Δ* cells. In agreement with this finding, the ER fatty acid elongase Elo3 (also known as Sur4) was shown to associate with abnormal LDs in *fld1Δ* cells (Wolinski et al., 2011). While in *wt* cells Elo3-GFP localizes exclusively to the ER, it is enriched in regions adjacent to supersized LDs and co-localizes with LD aggregates both in *fld1Δ* (Wolinski et al., 2011) and *ldb16Δ* cells (Fig. 5A). Several other ER membrane proteins such as Sec63 or Scs2 (Fig. 5A and Fig. S1A) were shown to co-localize with LD aggregates present in *fld1Δ* and *ldb16Δ* mutants while retaining their normal ER distribution. This ectopic localization of ER membrane proteins to aggregates but not to supersized LDs further indicated that these morphologically distinct LDs have different properties.

Multispanning membrane proteins, with their luminal loops and/or domains, are strongly disfavored in the phospholipid monolayer of LDs (Thiam et al., 2013b). Therefore, the presence of multispanning membrane proteins in the LD aggregates indicates that these structures likely contain regions with lipid bilayers. Indeed, ultrathin section EM analysis showed that LD aggregates in *ldb16Δ* or *fld1Δ* mutants are highly connected to the ER membrane and contained regions formed by phospholipid bilayers (Fig. 5B). While in *wt* cells LDs are also continuous with the ER (Jacquier et al., 2011), such membranous structures are never seen.

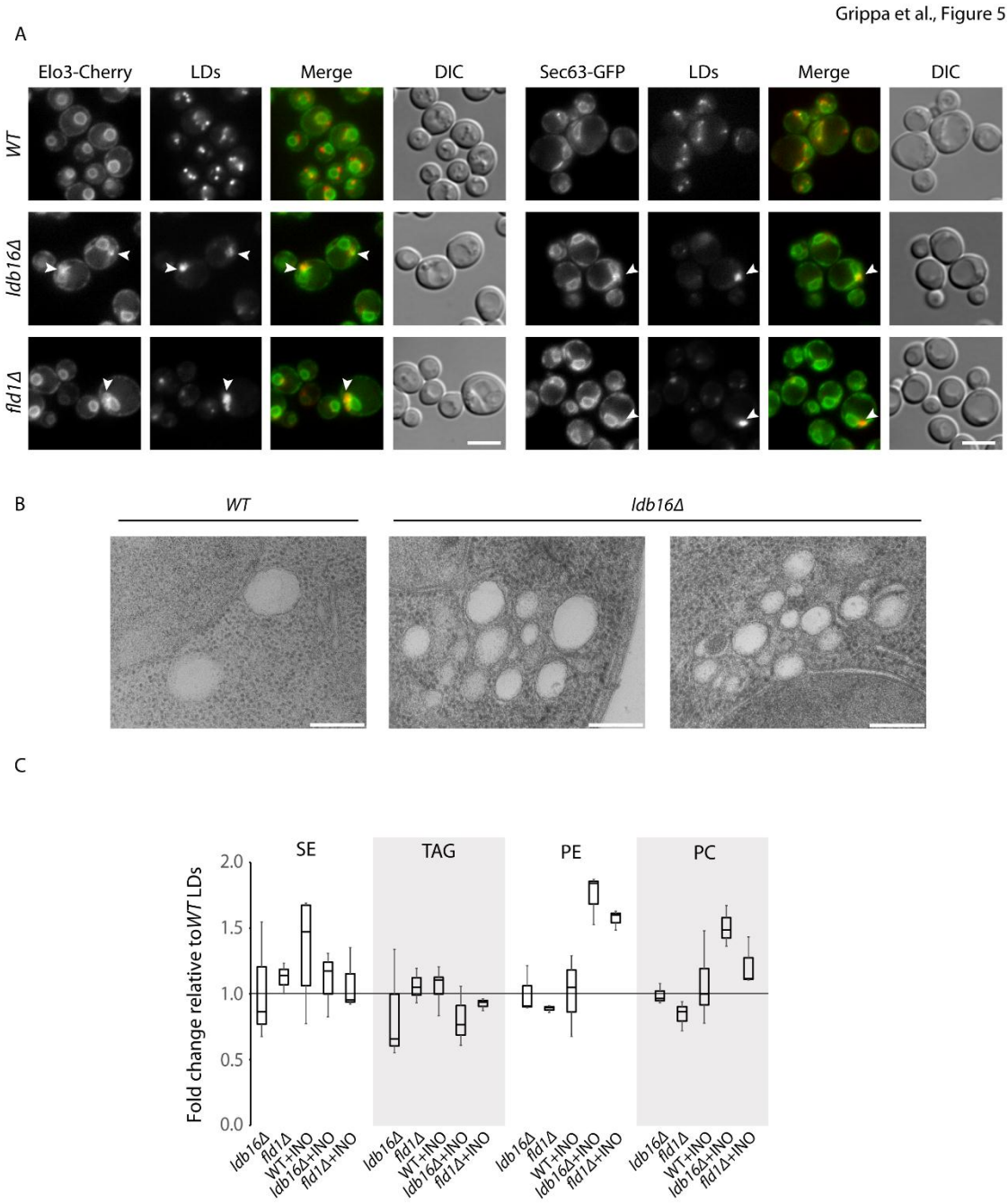

Figure 5. ER integral membrane proteins and phospholipids localize to LD aggregates formed in Seipin complex mutants. (A) Localization of the ER integral membrane proteins Elo3 and Sec63 in *wt*, *ldb16Δ* and f*ld1Δ* cells grown to early stationary phase. Elo3 and Sec63 were expressed from the endogenous promoters as mCherry and GFP fusion proteins. LDs were stained with the neutral lipid dye MDH. Arrowheads indicates LD aggregates. Scale bar: 5µm. (B) Ultrathin section electron micrographs of *wt* and *ldb16Δ* cells grown in YPD media to early stationary phase. Scale bar: 200nm. (C) Lipid composition of LDs isolated from cells with the indicated genotype and grown in SC or SC supplemented with 75 µM of inositol (+INO). LDs from

wt cells grown in SC media were used as reference. The result of at least 3 independent experiments is shown in the graph; whiskers represent the maximum and minimum values.

Grippa et al., Figure S4

A

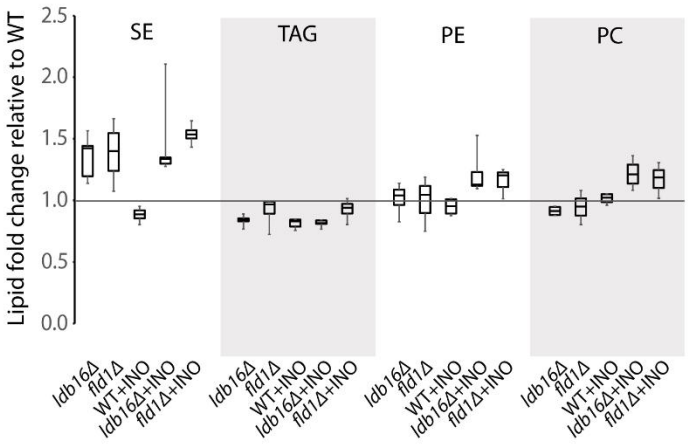

B

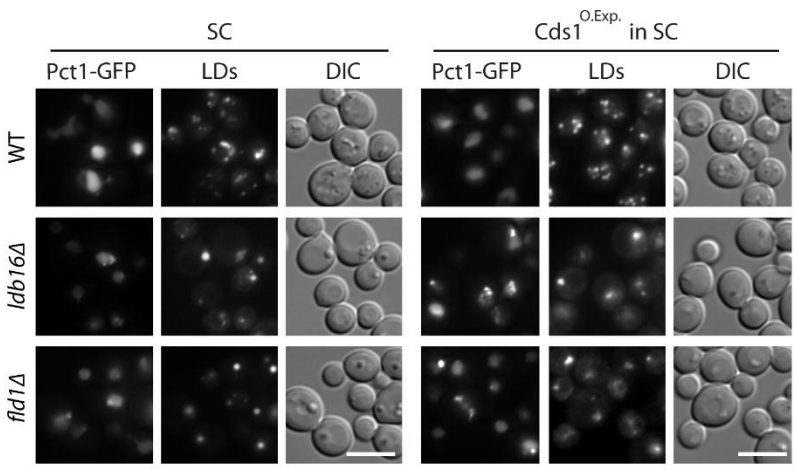

Figure S4. Seipin complex controls incorporation of phospholipids into LDs. (A) Lipid composition of cells with the indicated genotype and grown in SC or SC supplemented with 75 µM of inositol (+INO). Lipid extracts from *wt* cells grown in SC media were used as reference. The result of at least 3 independent experiments is shown in the graph; whiskers represent the maximum and minimum values. (B) Localization of endogenously expressed Pct1-GFP in cells with the indicated genotype. Early stationary cells grown in SC were analyzed. LDs were stained with MDH. Scale bar: 5µm.

To further characterize the LDs of *ldb16Δ* or *fld1Δ* cells we determined their lipid composition. Given that morphologically distinct LDs have different properties, we analyzed LDs from cells grown in regular or in inositol-supplemented minimal media, which favor the formation of supersized or aggregated LDs, respectively. The LDs isolated from *wt* and mutant cells grown in regular minimal medium showed a similar composition, both at the level of phospho- and neutral lipids (Fig. 5C). In contrast, LDs isolated from *ldb16Δ* or *fld1Δ* cells grown in inositol supplemented medium, while maintaining similar neutral lipid content, were highly enriched in the major ER phospholipids PC and PE (Fig 5C). The changes were specific to the LD fraction as whole cell lipid composition was indistinguishable between mutant and *wt* cells (Fig. S4A). These data indicate that in *fld1Δ* and *ldb16Δ* cells LDs maintain an abnormally strong connection with the ER and that integral membrane proteins and phospholipids can freely exchange between the two organelles, in particular in the case of the LD aggregates.

To more directly assess the continuity between the ER membrane and LD aggregates in *fld1Δ* and *ldb16Δ* mutants we used FRAP (fluorescence recovery after photobleaching). In mutant cells, endogenously expressed Sec63-GFP labeling aggregated LDs was photobleached and the fluorescence recovery was measured over time (Fig. 6A-B). Control FRAP experiments were conducted by photobleaching a small pool of Sec63-GFP in the nuclear envelope (Fig. 6A). In all cases, Sec63-GFP fluorescence recovered to a similar extent and with comparable kinetics (Fig. 6B) indicating that ER integral membrane proteins can freely diffuse between the ER and LD aggregates in *fld1Δ* and *ldb16Δ* mutants. Altogether these data indicate that the Fld1/Ldb16 complex plays a key role in preventing the equilibration between the ER and LD membranes.

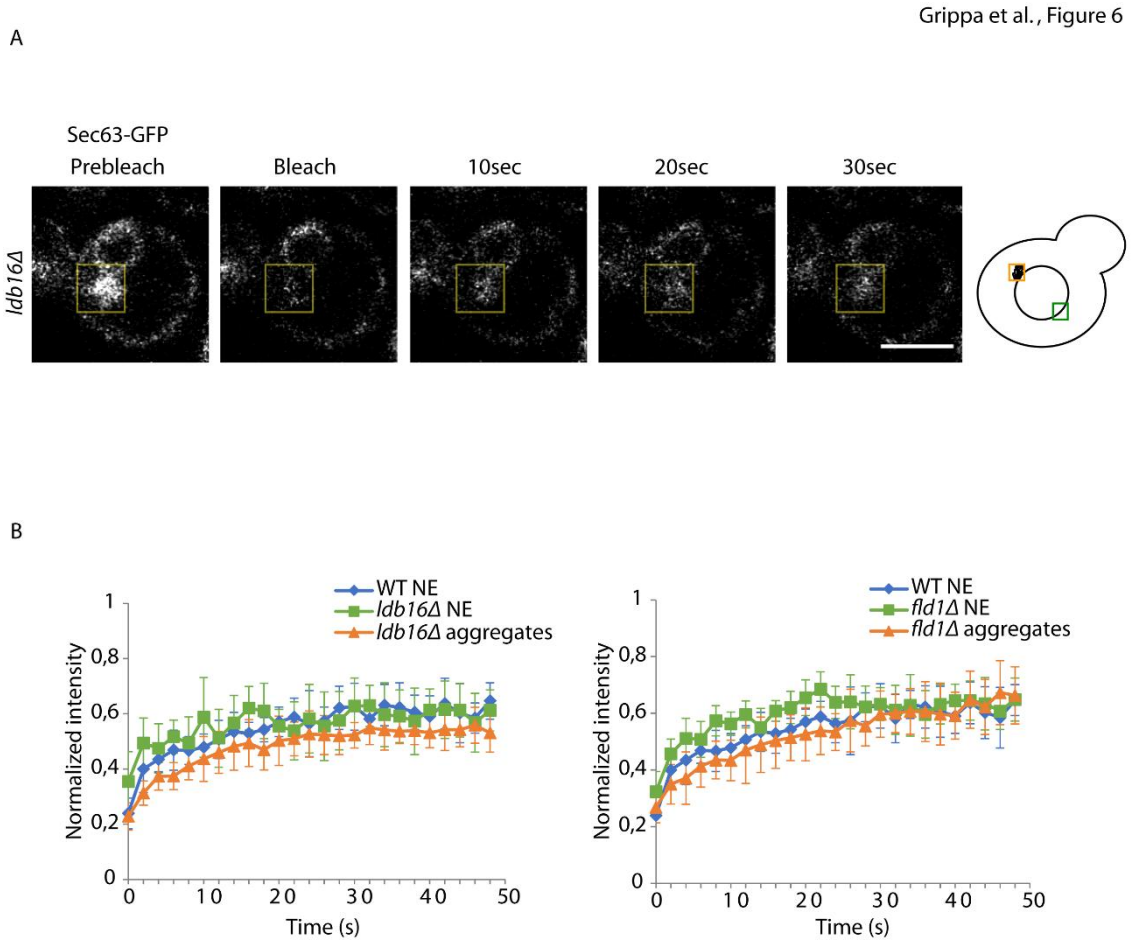

Figure 6. Rapid exchange of the integral membrane protein Sec63 between the ER and LD aggregates formed in Seipin complex mutants. (A) FRAP of Sec63-GFP expressed from endogenous promoter. Images were taken before and at the indicated time after photobleaching. The boxed region shows photobleached area. On the right side a scheme of the regions of the nuclear envelope (Green) or LD aggregates (Orange) that were photobleached. Scale bar 3µm. (B) Average fluorescence intensities of Sec63-GFP over time. Sec63-GFP was photobleached in a small region of the nuclear envelope (NE) in *wt*, *ldb16Δ* and *fld1Δ* cells or in the LD aggregates present in the mutants. Intensity values were normalized to prebleach Sec63-GFP fluorescence. At least 6 cells were analyzed per genotype per condition. Error bars represent the standard deviation of the mean.

ER phospholipid pools determine LD morphology in Fld1/Ldb16 complex mutants

Inositol is a precursor of phosphatidylinositol (PI) and its presence strongly stimulates the synthesis of this phospholipid *in vivo* (Henry et al., 2012). Moreover, in *fld1Δ* and *ldb16Δ* cells inositol strongly impacts the morphology (Fei et al., 2011c; Wang et al., 2014) and the protein composition of LDs. Therefore we asked whether general ER phospholipid pools are a major determinant of LD morphology in *fld1Δ* and *ldb16Δ* mutants. To manipulate phospholipid biosynthesis in an inositol-independent manner we overexpressed the CDP-diacylglycerol synthase *CDS1* which catalyzes the conversion of PA into CDP-DAG, a key step in the synthesis of most phospholipids in yeast (Shen et al., 1996). Overexpression of *CDS1* did not affect LD morphology in *wt* cells (Fig. 7A). In contrast, increasing Cds1 levels in *fld1Δ* and *ldb16Δ* cells resulted in the formation of LD aggregates indistinguishable from the ones induced by inositol (Fig. 7A). Moreover, *CDS1* overexpression also led to the ectopic relocalization of Kes1 and Pct1 to LD aggregates and proximal regions of the nuclear envelope, respectively (Fig. 7A and Fig. S4B). We also analyzed how a reduction in phospholipid pools, as it is the case of *opi3Δ* and *cho2Δ* mutants defective in PC synthesis by the CDP-DAG pathway (Henry et al., 2012), affects LDs in *fld1Δ* and *ldb16Δ* cells. As previously shown (Fei et al., 2011c), *opi3Δ* and *cho2Δ* cells display supersized LDs (Fig. 7B-C). Combination of CDP-DAG pathway mutations with deletion of *FLD1* or *LDB16* results in even bigger LDs (Fig. 7B-C), suggesting that the enlargement of LDs in *fld1Δ* and *ldb16Δ* cells is due to a local shortage of phospholipids. Altogether, these data indicate that the Fld1/Ldb16 complex is important to uncouple LD growth from ER phospholipid pools.

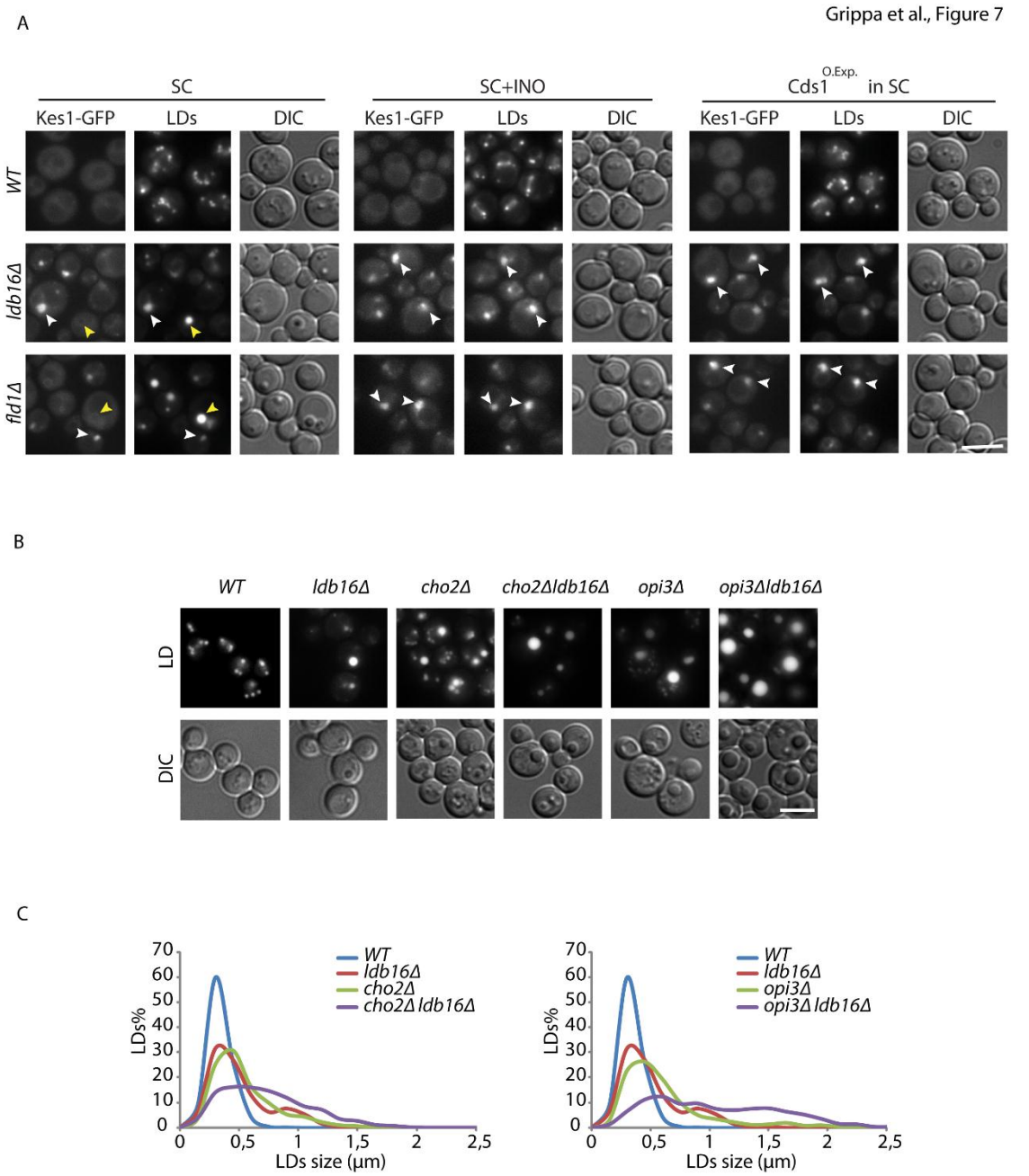

Figure 7. ER phospholipid pools determine LD morphology in Fld1/Ldb16 complex mutants. (A) Localization of endogenously expressed Kes1-GFP in cells with the indicated genotype. Early stationary cells grown in SC or SC supplemented with 75 µM of inositol were analyzed. Yellow arrowheads indicate supersized LDs; white arrowheads indicate LD aggregates. LDs were stained with MDH. Scale bar: 5µm. (B) LD morphology in cells with the indicated genotype grown in SC medium until early stationary phase. LDs were stained with the neutral lipid dye MDH. Scale bar: 5µm. (C) Size distribution of LDs in cells with the indicated genotype grown in SC medium until early stationary phase. The cells were fixed, LDs were stained with the neutral lipid dye MDH and quantification was performed using an in-house developed ImageJ macro. LDs from 200-400 cells per genotype per experiment were analyzed.

Localization of LD specific proteins requires the Fld1/Ldb16 complex

The second important result of our LD proteomic analysis was a dramatic decrease of LD-specific proteins. We detected that out of the 30-40 high-confidence LD proteins (Currie et al., 2014; Grillitsch et al., 2011), 27 were strongly reduced or completely absent from *ldb16Δ* and *fld1Δ* LDs (Table S2). To validate the proteomic data some of these proteins were expressed from their endogenous locus as C-terminal GFP fusions and their localization evaluated by fluorescence microscopy. In agreement with the mass spectrometric data, all tested LD proteins were strongly reduced or completely absent from the LD surface in *ldb16Δ* or *fld1Δ* mutants (Fig. 8A and data not shown). The changes did not appear to be due to an overall decrease in protein levels, which for the tested proteins were comparable in *wt* and mutant cells (data not shown). Importantly, the magnitude of the defect varied depending on the LD morphology. While LD proteins were decreased but still visible in supersized LDs, they were undetectable in LD aggregates (Fig. 8A). Thus, Ldb16 and Fld1 are required for the localization of LD specific proteins.

Table S2- LD-specific proteins reduced in LDs isolated from *fld1Δ* and *ldb16Δ* cells, as determined by label free quantitative mass spec.

		fld1Δ		***ldb16Δ***	
ID	**Description**	**logFC**	**P.Value**	**logFC**	**P.Value**
YLL012W	Yeh1	-7.78649	1.13E-05	-5.05418	8.77E-04
YOL048C	Rrt8	-3.7425	1.27E-04	-3.41304	2.63E-05
YDL193W	Nus1	-3.49958	9.97E-05	-2.40426	1.02E-04
YOR246C	Yor246c	-3.25081	6.85E-05	-2.45812	1.60E-05
YGR263C	Say1	-3.24911	3.83E-04	-2.25961	2.05E-04
YMR313C	Tgl3	-3.24879	8.08E-05	-2.54358	6.01E-05
YMR148W	Osw5	-3.08516	2.28E-04	-2.58567	1.97E-03
YKL140W	Tgl1	-3.06946	2.61E-04	-2.43399	1.78E-04
YBR041W	Fat1	-3.00532	3.26E-04	-2.1922	7.36E-04
YPL206C	Pgc1	-2.9476	1.41E-04	-3.1552	8.86E-05
YIL124W	Ayr1	-2.94212	8.75E-04	-1.77792	8.77E-03
YKR046C	Pet10	-2.88843	1.59E-04	-2.14085	2.34E-04
YPR139C	Vps66	-2.88325	2.22E-04	-1.64523	2.15E-02
YHR072W	Erg7	-2.6831	1.10E-03	-3.13586	3.00E-06
YDL052C	Slc1	-2.33422	4.94E-04	-1.43428	9.79E-03
YLR100W	Erg27	-2.32554	5.69E-04	-1.90138	1.72E-03
YOR245C	Dga1	-1.98278	6.85E-03	-1.19096	5.91E-02
YKR067W	Gpt2	-1.78775	1.62E-02	-1.69292	1.24E-01
YMR246W	Faa4	-1.46686	1.10E-02	-1.74005	1.13E-02
YIL009W	Faa3	-1.44055	2.29E-02	-1.91776	1.62E-02
YMR110C	Hfd1	-1.34235	3.15E-02	-1.99597	3.29E-03
YML008C	Erg6	-1.27227	1.43E-02	-1.62012	4.79E-03
YKL094W	Yju3	-1.26406	1.66E-02	-1.23556	2.12E-02
YBR002C	Rer2	-3.43938	1.27E-04	-2.42116	5.27E-03
YIL124W	Ayr1	-2.94212	8.75E-04	-1.77792	8.77E-03
YBR265W	Tsc10	-3.11278	9.39E-05	-2.55269	3.41E-04

Grippa et al., Figure 8

A

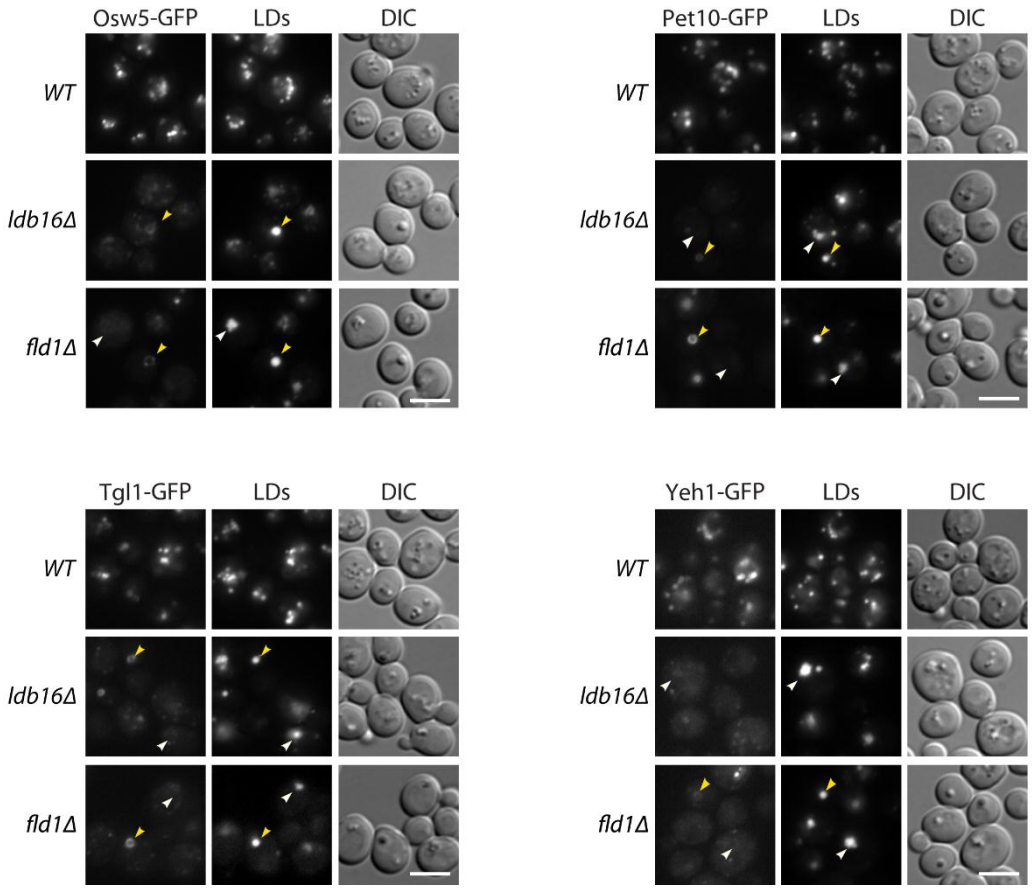

Figure 8. Localization of LD specific proteins requires the Fld1/Ldb16 complex. (A) Localization of the LD-specific proteins Osw5, Pet10, Tgl1 and Yeh1 in *wt*, *ldb16Δ* and *fld1Δ* cells grown in YPD until early stationary phase. All proteins were expressed from their endogenous locus as C-terminal GFP fusions. Yellow arrowheads indicate supersized LDs, white arrowheads indicate LD aggregates. LDs are stained with the neutral lipid dye MDH. Scale bar: 5µm.

Discussion

Here we characterized the function of the yeast seipin complex in LD biogenesis. LD assembly in absence of Fld1/Ldb16 led to membrane defects in LDs and proximal regions, and to abnormal LDs, which were either supersized or small and aggregated. Moreover, we showed that the determinant between these contrasting LD morphologies is the availability of ER phospholipid pools, indicating that Fld1/Ldb16 is important to couple the amounts of monolayer and core lipids during LD biogenesis. We propose that the seipin complex, at the ER-LD contact sites, serves as a diffusion barrier controlling LD assembly and membrane identity (Fig. 9).

Grippa et al., Figure 9

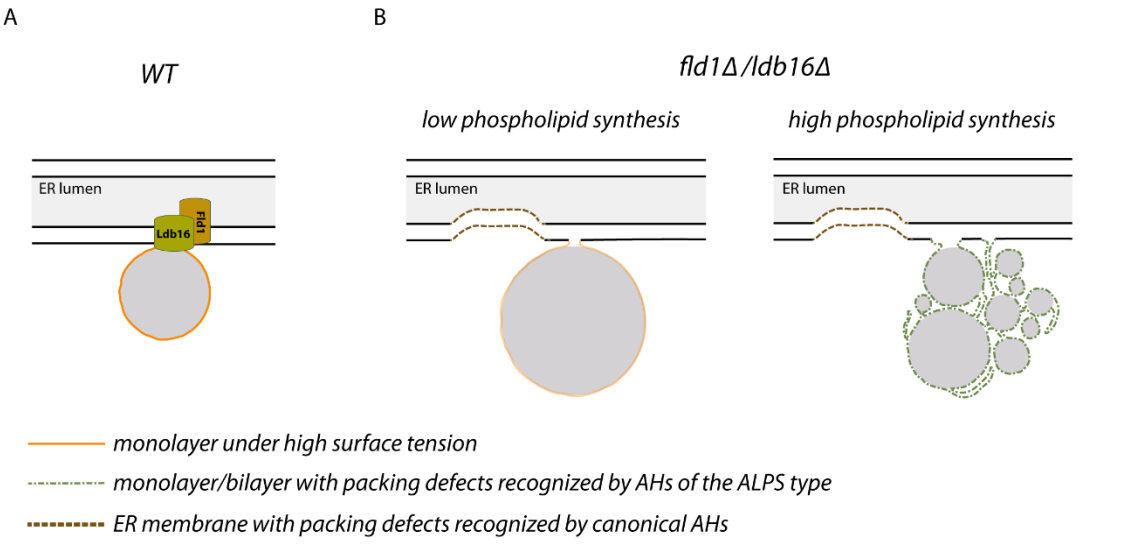

Figure 9. Fld1/Ldb16 complex acts as a diffusion barrier at the ER-LD contact sites. (A) The scheme illustrates a contact site between the ER and a LD. Although connected with the ER membrane, the LD monolayer has different properties such as a higher surface tension (in orange). The presence of the Fld1/Ldb16 complex at the contact sites prevents the equilibration of the two membrane systems. (B) In the absence of this complex, phospholipids freely diffuse between the two organelles. Under low synthesis conditions, phospholipids can become limiting and LDs coalesce into a supersized one. The mild surface tension (faint orange) in these LDs still allows the targeting of LD proteins, albeit at lower efficiency (left panel). Under high phospholipid synthesis conditions, ER membrane and LDs equilibrate. The low surface tension of these LDs prevents their coalescence and the recruitment of LD proteins. Instead, these aggregates are enriched in ER-like membranes and display phospholipid packing defects (in green) which recruit ER integral membrane proteins and ALPS motif-containing proteins (right panel). Both low and high phospholipid synthesis lead to phospholipid defects in membranes adjacent to LDs which are recognized by proteins containing canonical AHs (in brown).

Imbalances in cellular phospholipid composition, in particular defects in the synthesis of PC such as in yeast *opi3Δ* or *cho2Δ* cells, lead to supersized LDs (Fei et al., 2011c). However, we and others could not detect significant global changes in the lipid composition of *fld1Δ* and *ldb16Δ* cells, arguing that supersized LDs in these mutants are distinct (Fei et al., 2008; Fei et al., 2011c; Wang et al., 2014). Given that the LD morphology in *fld1Δ* and *ldb16Δ* can be manipulated by inositol, a regulator of phospholipid synthesis, it is likely that localized lipid imbalances exist.

Lipid analysis of LDs isolated from *wt* and mutant cells under conditions favoring formation of either supersized or small aggregated LDs (i.e. *minus* or *plus* inositol) showed similar composition at the level of neutral lipid and phospholipid classes. The most noticeable difference between *wt* and mutant LDs was at the level of their phospholipid content, particularly the major ER phospholipids PC and PE. Importantly, the amounts of neutral lipids were unaffected. This dramatic rise in phospholipid content cannot simply be explained by the increase in surface-to-volume ratio of LDs in aggregates. Accordingly, there is a massive enrichment of ER-like membranes in the aggregates, indicating increased connectivity between ER and LDs in *fld1Δ* and *ldb16Δ* mutants. This likely facilitates the free diffusion of phospholipids between the two compartments, placing LD morphology on a strict dependence of ER phospholipid pools in these mutants. This is further supported by the changes in LD morphology upon manipulation of the phospholipid levels in an inositol-independent manner, such as *CDS1* overexpression or mutations in the CDP-DAG pathway. In agreement with these observations, unperturbed *fld1Δ* and *ldb16Δ* cells display mainly LD aggregates during logarithmic growth, a condition favoring phospholipid synthesis, while the supersized LD phenotype dominates as cells approach stationary phase, when phospholipid synthesis is reduced [(Wang et al., 2014) our unpublished data]. The high degree of connectivity between ER and LDs in these mutants also allows the free diffusion of ER integral membrane proteins into the membrane-rich LD aggregates, as confirmed by FRAP studies. In fact, even the ER luminal marker GFP-HDEL has been previously observed at the LD aggregates found in these mutants (Cartwright et al., 2015; Szymanski et al., 2007). Thus, Fld1 and Ldb16 are important to prevent equilibration of ER and LDs.

Another consequence of the loss of Fld1/Ldb16 is the ectopic recruitment of AH-containing proteins to LD aggregates and proximal regions. In all the tested cases, the AH was necessary and sufficient for protein relocalization. In general, AHs adsorb to membranes exposing phospholipid packing defects (Campelo and Kozlov, 2014; Drin

and Antonny, 2010) suggesting the presence of such membrane defects in *fld1Δ* and *ldb16Δ* mutants. Although the precise nature of the membrane defects is in not entirely clear (see below) they are a direct consequence of LD assembly, as demonstrated by time course experiments following LD biogenesis.

With a well-developed hydrophobic face but very few charged residues on their polar face, the AH of Kes1 binds to membranes primarily through hydrophobic interactions (Drin et al., 2007). As such, this prototypical ALPS motif has a marked preference for binding to membranes with phospholipid packing defects generated by high curvature or accumulation of conical phospholipids (such as PE) in a flat membrane (Drin et al., 2007; Vamparys et al., 2013; Vanni et al., 2013). *In vitro* studies demonstrated that Kes1 ALPS domain binds to small liposomes (in the range of 30-40nm in diameter) but not to bigger ones (Drin et al., 2007). Crude measurements from thin section EM suggest that the diameter of individual LDs in the aggregates are bigger (>80nm). Therefore, it is possible that the ectopic recruitment of ALPS-containing proteins to LD aggregates in *fld1Δ* and *ldb16Δ* LDs are due to the combined effect of curvature and increased levels of PE, a conic shaped lipid, present in these structures.

Based on their sequences, the AHs of Pct1 and Spo20 appear canonical AHs and likely associate with membranes by a combination of both hydrophobic and electrostatic interactions (Drin and Antonny, 2010). While the Pct1 AH has not been extensively characterized biochemically, the AH of Spo20 ($Spo20^{51-91}$) was shown to bind to PA-rich membranes *in vivo* (Horchani et al., 2014; Nakanishi et al., 2004), however recent *in vitro* studies suggest a general preference for anionic phospholipids and not necessarily for PA (Horchani et al., 2014). A preference for PA, preferably with shorter acyl chains, was also observed for the Q2 region of Opi1 (Hofbauer et al., 2014; Loewen et al., 2004). We detected only a small increase in whole-cell levels of PA and no enrichment in LD lipid fractions therefore we favor that $Spo20^{51-91}$ and $Opi1^{Q2}$ recognize some other feature at the nuclear envelope of *fld1Δ* and *ldb16Δ* mutants. The fact that conditions stimulating PA consumption, such as inositol supplementation or Cds1 overexpression, augment the relocalization of $Spo20^{51-91}$ and Opi1 to *foci* at the nuclear envelope further argue against a PA-driven process. In sum, while it is clear that AHs of different chemistry are recognizing different features in adjacent but distinct membranes, the exact nature of the membrane defects upon LD biogenesis in *fld1Δ* and *ldb16Δ* mutants is unclear. It is possible that the spatial segregation of the different AHs reflects differences in membrane curvature. However, we cannot exclude that LD assembly in these mutants

leads to the formation of membrane subdomains, with different phospholipid composition for example at the levels of acyl chains.

The ectopic clustering of several proteins at LDs aggregates and proximal regions observed in *fld1Δ* and *ldb16Δ* mutants can have several consequences. On one hand, it can deplete proteins from their site of function, potentially leading to a "loss of function" phenotype. This appears to be the case of Opi1, a negative regulator of Ino2/Ino4 required for transcription of most phospholipid biosynthetic genes (Henry et al., 2012). In fact, several Ino2/Ino4 targets, such as *INO1* or *OPI3*, are upregulated in *fld1Δ* and *ldb16Δ* mutants [(Fei et al., 2011c; Hancock et al., 2006; Wang et al., 2014) our unpublished data]. However, upregulation of Ino2/Ino4 target genes is not the main cause of *fld1Δ* and *ldb16Δ* phenotype as LDs are mostly normal in *opi1Δ* cells. On the other hand, ectopic concentration of certain proteins in the proximity of LDs can lead to local "gain of function" of these proteins. The phenotype of *fld1Δ* and *ldb16Δ* mutations was not modified by deleting individually Pct1, Kes1, Gvp36 or Vps13 suggesting that the ectopic recruitment of each one of these proteins *per se* is not responsible for the LD defects. This was further supported by time course experiments showing that protein recruitment followed the formation of abnormal LDs in *fld1Δ* and *ldb16Δ* cells.

Another important consequence of the loss of Fld1/Ldb16 is reduction of most LD-specific proteins at the monolayer of these organelles. Many LD proteins are originally targeted to the ER before concentrating in the LD monolayer (Thiam et al., 2013b; Yang et al., 2012a). It is possible that the crowding of the LD monolayer due to ectopic localization of AH-containing proteins precludes proper targeting of LD proteins. However, under conditions of overexpression, the LD-specific protein Dga1 was shown to localize normally in *fld1Δ* cells (Jacquier et al., 2011) suggesting that the targeting of this protein is not defective. An alternative appealing possibility is that LD-specific proteins are able to target but are not retained/concentrated at the LD monolayer as a consequence of changes in surface tension due to the free diffusion of phospholipids from the ER into LDs in *FLD1* and *LDB16* mutants. This is also in agreement with the stronger defect in protein targeting to LD aggregates, which have a higher content of phospholipids. In LDs that are not connected to the ER, the regulation of monolayer surface tension is essential in recruiting soluble proteins from the cytoplasm (Krahmer et al., 2011; Thiam et al., 2013a), in facilitating ER-LD re-attachments (Wilfling et al., 2014b) and consequently in generating LD identity. We propose that in LDs that remain

connected to the ER, the Fld1/Ldb16 complex serves as a diffusion barrier allowing the regulation of LD surface tension.

The Fld1/Ldb16 complex has been previously shown to localize to ER-LD contact sites (Fei et al., 2008; Szymanski et al., 2007; Wang et al., 2014). Moreover, both Fld1 and Ldb16 form oligomers, which in the case of Fld1 appear to have a toroid shape (Binns et al., 2010; Wang et al., 2014). Therefore, it is well positioned to prevent equilibration of the ER and LDs. Given the similarity of phospholipid classes between the two organelles, the control of monolayer surface tension might thus be a unifying feature determining LD identity.

Materials and methods

Reagents

The LD dyes Bodipy$^{493/503}$ (Invitrogen) and monodansyl pentane (MDH) (Abgent) were used at 1µg/ml and 0.1mM, respectively. Anti-HA (rat 3F10 monoclonal) antibody was purchased from Roche, anti-PGK1 (mouse) from Life Technologies, anti-GFP (rabbit) from Santa Cruz and anti-RFP (mouse) from Abcam. Rabbit polyclonal anti-Usa1 antibody was previously described (Carvalho et al., 2006). Polyclonal antibodies anti-Dga1 and anti-Pet10 were raised in rabbits from recombinant protein fragments and affinity purified.

Yeast strains and plasmids

Protein tagging, promoter replacements and individual gene deletions were performed by standard PCR-based homologous recombination (Janke et al., 2004; Longtine et al., 1998). Strains with multiple gene deletions were made either by PCR-based homologous recombination or by crossing haploid cells of opposite mating types, followed by sporulation and tetrad dissection using standard protocols (Guthrie and Fink, 1991). The strains used are isogenic either to BY4741 (*Mata ura3Δ0 his3Δ1 leu2Δ0 met15Δ0*) or to BY4742 (*Matα his3Δ1 leu2Δ0 lys2Δ0 ura3Δ0*) unless otherwise specified and are listed in the Supplementary file 1. Plasmids and primers used in this study are listed in Supplementary files 2 and 3, respectively.

Growth Conditions

Strains were grown at 30°C in synthetic complete (SC) (0.17% yeast nitrogen base, 5g/l ammonium sulphate, 2% glucose, and amino acids) or YPD liquid media (1% yeast extract, 2% peptone, and 2% glucose). For analysis of protein localization and LD morphology both late logarithmic phase (OD_{600} 2-3) and early stationary phase (OD_{600} 4-6) cultures were used. For phospholipids precursor treatment (I+), SC medium was supplemented with 75µM inositol as described (Gaspar et al., 2006).

Lipid Droplet Induction System

For LD induction time courses, strains *GAL1-DGA1 are1Δ are2Δ lro1Δ* and *GAL1-DGA1 are1Δ are2Δ lro1Δ ldb16Δ*, bearing a plasmid encoding for the chimeric Gal4-VP16 transcription factor fused to the hormone-binding domain of the human estrogen receptor

were used (Louvion et al., 1993). This chimeric GAL4-ERE-VP16 protein provides galactose-independent activation of transcription of genes driven by *GAL* promoters (*DGA1* in this study) in response to β-estradiol. Cells were pre-cultured in SC media lacking the appropriate amino acids until early stationary phase, diluted to OD 0.15 in 10 ml of fresh media in 25ml flasks at 30°C and stimulated by addition of 100nM β-estradiol. Time point 0 was imaged before induction with β-estradiol and samples were acquired at the indicated time points, stained with MDH and immediately imaged by live cell fluorescence microscopy.

Fluorescence microscopy

Fluorescence microcopy was performed at room temperature in a wide-field Leica AF6000LX microscope with an Andor iXon EMCCD camera and controlled by Leica LAS AF software, or in a Zeiss Cell Observer HS with a Hamamatsu CMOS camera ORCA-Flash4.0 controlled by 3i Slidebook6.0 software. A 100x 1.40 oil immersion objective was used. GFP and Bodipy$^{493/503}$, mCHERRY, and MDH signals were detected using GFP filter, RFP filter cube and DAPI filters, respectively, with standard settings. For LD measurements, stacks of images spaced 0.2µm (36 slices) were acquired and deconvolved using Huygens Essential software package. Statistical analysis of LDs was performed by in-house developed ImageJ macro. The distribution of LD size is presented as an histogram. Statistical analysis of LDs was performed using 200-400 cells per genotype per experiment, unless otherwise indicated.

Fluorescence Recovery After Photobleaching

Photobleaching experiments were performed on yeast cells grown in SC media supplemented with inositol 75µM. Early stationary cells were diluted into the same media to OD_{600} 0.5 and grown up to OD_{600} 2 before being transferred to a concanavalin A pretreated chamber. Live imaging was performed on a confocal Leica TCS SP5 microscope using a HCX PL APO CS 100.x1.40 oil objective and controlled by the LAS AF software. Bleaching experiments were performed using the point bleach option of the FRAP module. Photobleaching was applied to a small region of the nuclear envelope or clustered LDs. Three pre-bleach images were acquired followed by photobleaching. Images were acquired every 2 seconds. The fluorescence recovery values of the bleached region were background subtracted and normalized to the average of the

prebleaching values. The normalized recovery values were plotted after adjusting for the slow decay of fluorescence caused by imaging using areas of the image distant from the bleached region as described (Shibata et al., 2008). At least 7 photo- bleaching events were recorded for each strain to calculate averages and standard deviations.

Lipid droplet isolation

LD purification was carried out as previously described (Connerth et al., 2009; Leber et al., 1994) with minor modifications. Briefly, cells were grown in 500ml YPD until stationary phase and 3000 ODs of cells were centrifuged in a JLA 10500 rotor, washed in milliQ water, preincubated in 0.1M Tris-HCl pH9.5, 10 mM DTT for 10minutes at 30°C, washed and resuspended to 50OD_{600}/ml in spheroplast buffer (1.2M sorbitol, 50mM TRIS, pH7.4). For spheroplast preparation Zymolyase (Seikagaku Biobusiness) 20T from 10mg/ml stock was added (10 µg/OD_{600} unit cells) followed by incubation in waterbath (30°C, 1-2h). Spheroplasts were recovered by centrifugation (1000g, 4°C) washed with spheroplast buffer and resuspended in breaking buffer (BB: 10 mM MES-Tris (pH 6.9) - 12% (w/w) Ficoll400- 0.2mM-EDTA) at a final concentration of 0.3g of cells (wet weight)/ml. PMSF (1mM) and Complete (Roche) were added before homogenization (loose-fitting pestle, 40 strokes) in a Dounce homogenizer on ice. The homogenate was diluted with 1 volume of BB and centrifuged (5000g, 5') in J26-XP using rotor JS13.1. The resulting supernatant was transferred into 38ml Ultra-Clear™ centrifuge tubes (Beckman), overlaid with an equal volume of BB and centrifuged (45', 30000rpm) in an SW-32 swinging bucket rotor (Beckman). The floating layer was collected from the top of the gradient and following purification steps were performed as described in (Connerth et al., 2009). The recovered high purity top LDs fraction was snap frozen, stored at -80°C and used subsequently for proteomics and lipid analysis.

Electron Microscopy

Cells were cryoimmobilized by high pressure freezing using a EM HPM100 (Leica Microsystems, Vienna). Freeze-substitution of frozen samples was performed in an Automatic Freeze substitution System EM AFS-2 (Leica Microsystems, Vienna), using acetone containing 0.1% of uranyl acetate and 1% water, for 3 days at -90°C. On the fourth day, the temperature was slowly increased, by 5°C/hour, to -45°C. At this

temperature, samples were rinsed in acetone, and then infiltrated and embedded in Lowicryl HM20 for 3 days. Ultrathin sections from the resin blocks were obtained using a Leica Ultracut UC6 ultramicrotome and mounting on Formvar-coated copper grids. They were stained with 2% uranyl acetate in water and lead citrate. Thin sections were observed in a Tecnai Spirit (FEI Company, The Netherlands).

Mass Spectrometry Protein Analysis

Trichloroacetic acid precipitated proteins were resuspended in 6M Urea and 200mM ammonium bicarbonate prior to reduction (dithiothreitol 10 mM) and alkylation (iodoacetamide 20mM). Samples were diluted to 2M Urea and digested with trypsin (1:10 w:w) overnight at 37º C. Tryptic peptide mixtures were desalted using a C18 UltraMicroSpin column as described (Rappsilber et al., 2007).

Samples were analyzed in a LTQ-Orbitrap Velos Pro mass spectrometer (Thermo Fisher Scientific, San Jose, CA, USA) coupled to nano-LC (Proxeon, Odense, Denmark) equipped with a reversed-phase chromatography 12-cm column with an inner diameter of 75 µm, packed with 5 µm C18 particles (Nikkyo Technos Co., Ltd. Japan). Chromatographic gradients were set from 93% buffer A, 7% buffer B to 65% buffer A ,35% buffer B in 60 min with a flow rate of 300 nl/min. Buffer A: 0.1% formic acid in water and buffer B: 0.1% formic acid in acetonitrile. The instrument was operated in DDA mode and full MS scans with 1 micro scans at resolution of 60,000 were used over a mass range of m/z 250-2,000 with detection in the Orbitrap. Following each survey scan the top twenty most intense ions with multiple charged ions above a threshold ion count of 5000 were selected for fragmentation at normalized collision energy of 35%. Fragment ion spectra produced via collision-induced dissociation (CID) were acquired in the linear ion trap. All data were acquired with Xcalibur software v2.2.

Acquired data were analyzed using the Proteome Discoverer software suite (v1.3.0.339, Thermo Fisher Scientific) and the Mascot search engine (v2.3, Matrix Science) was used for peptide identification. Data were searched against an in-house generated database containing all proteins corresponding to yeast in the Genome Database plus the most common contaminants as previously described (Bunkenborg et al., 2010). A precursor ion mass tolerance of 7 ppm at the MS1 level was used, and up to three miscleavages for trypsin were allowed. The fragment ion mass tolerance was set to 0.5 Da. Oxidation of methionine and protein acetylation at the N-terminal were defined as variable

modifications. Carbamidomethylation on cysteines was set as a fix modification. The identified peptides were filtered using a FDR < 5 %.

Protein areas were normalized intra- and inter-samples by median of the Log-area. A linear modeling approach implemented in *lmFit* function and the empirical Bayes statistics implemented in *eBayes* and *topTable* functions of the Bioconductor *limma* package (Gentleman et al., 2004; Smyth, 2004) were used to perform a differential protein abundance analysis. The normalized protein areas of different yeast mutants were compared to *wt* samples. Protein p-values were calculated with *limma* and were adjusted with Benjamini–Hochberg method (Benjamini and Hochberg, 1995). A value of 0.05 was used as cutoff.

Lipid analysis

Lipids from whole cells (lysed with glass beads) or LDs (isolated as described above) where extracted with chloroform:methanol 2:1 v/v by the single-step modification of (Folch et al., 1957) described by (Atkinson et al., 1980) and washed with 0.9% NaCl. The extracts were dried, dissolved in chloroform:methanol 2:1 v/v and analyzed by TLC on silica gel 60 plates (Merk). Phospholipids were resolved with chloroform:ethyl acetate:acetone:isopropanol:ethanol:methanol:water:acetic acid (30:6:6:6:16:28:6:2 v/v). Neutral lipids were resolved with hexane:diethyl ether:acetic acid (80:20:1 v/v) to 3/5 of the plate, dried and followed by hexane:chloroform (9:1 v/v) to 4/5 of the plate. DAG and free sterol were resolved with toluene:ethyl acetate:ethyl ether:ammonia (25%) (80:10:10:0.2 v/v). Bands were stained in a chamber saturated with iodine vapor, scanned and quantified by densitometry with Quantity One (Bio-Rad). Known standards were included on all plates for identification.

Steady state lipid labeling for PA quantification: Cultures in SC were diluted to OD_{600} 0.1 in SC or SC supplemented with 75 µM of inositol and grown for 24 hours at 30°C in presence of 1 µCi/ml [1-^{14}C]acetate (45-60 mCi/mmol. Perkin Elmer). Lipids were extracted as described above in presence of 5 mM HCl, resolved by TLC with chloroform:methanol:acetic acid (65:25:8 v/v), scanned on a Typhoon Trio phosphorimager (Amersham Biosciences) and quantified with Quantity One (Bio-Rad).

Acknowledgements

Cryo-Electron Microscopy was performed at the CCiT University of Barcelona (C.Lopez-Iglesias Lab). Mass spectrometric measurements and data analysis were performed in the CRG/UPF Proteomics Unit, part of the “Plataforma de Recursos Biomoleculares y Bioinformàticos (ProteoRed-Instituto de Salud Carlos III, PT13/0001)”. FRAP experiments were performed at the CRG advanced light microscopy unit. We thank S. Abreu and F. Reggiori for preliminary EM studies. We thank A. Curwin, T. Levine, F. Posas and W. Prinz for reagents. We thank F. Campelo, O. Foresti, F. Idrissi, R. Klemm and W. Prinz for discussions and critical reading of the manuscript. P.C. is supported by CRG, an International Early Career Award from the HHMI, the EMBO Young Investigator Program and grants from the Spanish MCCIN and ERC.

References

Atkinson, K.D., B. Jensen, A.I. Kolat, E.M. Storm, S.A. Henry, and S. Fogel. 1980. Yeast mutants auxotrophic for choline or ethanolamine. *J Bacteriol*. 141:558-564.

Benjamini, Y., and Y. Hochberg. 1995. Controlling the false discovery rate: a practical and powerful approach to multiple testing. *J. R. Stat. Soc. Ser. B*:289–300.

Binns, D., S. Lee, C.L. Hilton, Q.X. Jiang, and J.M. Goodman. 2010. Seipin is a discrete homooligomer. *Biochemistry*. 49:10747-10755.

Boutet, E., H. El Mourabit, M. Prot, M. Nemani, E. Khallouf, O. Colard, M. Maurice, A.M. Durand-Schneider, Y. Chretien, S. Gres, C. Wolf, J.S. Saulnier-Blache, J. Capeau, and J. Magre. 2009. Seipin deficiency alters fatty acid Delta9 desaturation and lipid droplet formation in Berardinelli-Seip congenital lipodystrophy. *Biochimie*. 91:796-803.

Bunkenborg, J., G.E. Garcia, M.I. Paz, J.S. Andersen, and H. Molina. 2010. The minotaur proteome: avoiding cross-species identifications deriving from bovine serum in cell culture models. *Proteomics*. 10:3040-3044.

Campelo, F., and M.M. Kozlov. 2014. Sensing membrane stresses by protein insertions. *PLoS computational biology*. 10:e1003556.

Cartwright, B.R., D.D. Binns, C.L. Hilton, S. Han, Q. Gao, and J.M. Goodman. 2015. Seipin performs dissectible functions in promoting lipid droplet biogenesis and regulating droplet morphology. *Mol Biol Cell*. 26:726-739.

Carvalho, P., V. Goder, and T.A. Rapoport. 2006. Distinct ubiquitin-ligase complexes define convergent pathways for the degradation of ER proteins. *Cell*. 126:361-373.

Chen, W., B. Chang, P. Saha, S.M. Hartig, L. Li, V.T. Reddy, Y. Yang, V. Yechoor, M.A. Mancini, and L. Chan. 2012. Berardinelli-seip congenital lipodystrophy 2/seipin is a cell-autonomous regulator of lipolysis essential for adipocyte differentiation. *Mol Cell Biol*. 32:1099-1111.

Chernomordik, L.V., and M.M. Kozlov. 2005. Membrane hemifusion: crossing a chasm in two leaps. *Cell*. 123:375-382.

Connerth, M., K. Grillitsch, H. Kofeler, and G. Daum. 2009. Analysis of lipid particles from yeast. *Methods Mol Biol*. 579:359-374.

Cui, X., Y. Wang, Y. Tang, Y. Liu, L. Zhao, J. Deng, G. Xu, X. Peng, S. Ju, G. Liu, and H. Yang. 2011. Seipin ablation in mice results in severe generalized lipodystrophy. *Hum Mol Genet*. 20:3022-3030.

Currie, E., X. Guo, R. Christiano, C. Chitraju, N. Kory, K. Harrison, J. Haas, T.C. Walther, and R.V. Farese, Jr. 2014. High confidence proteomic analysis of yeast LDs identifies additional droplet proteins and reveals connections to dolichol synthesis and sterol acetylation. *J Lipid Res*. 55:1465-1477.

Drin, G., and B. Antonny. 2010. Amphipathic helices and membrane curvature. *FEBS Lett*. 584:1840-1847.

Drin, G., J.F. Casella, R. Gautier, T. Boehmer, T.U. Schwartz, and B. Antonny. 2007. A general amphipathic alpha-helical motif for sensing membrane curvature. *Nat Struct Mol Biol*. 14:138-146.

Fei, W., H. Li, G. Shui, T.S. Kapterian, C. Bielby, X. Du, A.J. Brown, P. Li, M.R. Wenk, P. Liu, and H. Yang. 2011a. Molecular characterization of seipin and its mutants: implications for seipin in triacylglycerol synthesis. *J Lipid Res*. 52:2136-2147.

Fei, W., G. Shui, B. Gaeta, X. Du, L. Kuerschner, P. Li, A.J. Brown, M.R. Wenk, R.G. Parton, and H. Yang. 2008. Fld1p, a functional homologue of human seipin, regulates the size of lipid droplets in yeast. *J Cell Biol*. 180:473-482.

Fei, W., G. Shui, Y. Zhang, N. Krahmer, C. Ferguson, T.S. Kapterian, R.C. Lin, I.W. Dawes, A.J. Brown, P. Li, X. Huang, R.G. Parton, M.R. Wenk, T.C. Walther, and H. Yang. 2011b. A role for phosphatidic Acid in the formation of "supersized" lipid droplets. *PLoS Genet*. 7:e1002201.

Folch, J., M. Lees, and G.H. Sloane Stanley. 1957. A simple method for the isolation and purification of total lipides from animal tissues. *J Biol Chem*. 226:497-509.

Fujimoto, T., and R.G. Parton. 2011. Not just fat: the structure and function of the lipid droplet. *Cold Spring Harb Perspect Biol*. 3.

Gaspar, M.L., M.A. Aregullin, S.A. Jesch, and S.A. Henry. 2006. Inositol induces a profound alteration in the pattern and rate of synthesis and turnover of membrane lipids in Saccharomyces cerevisiae. *J Biol Chem*. 281:22773-22785.

Gautier, R., D. Douguet, B. Antonny, and G. Drin. 2008. HELIQUEST: a web server to screen sequences with specific alpha-helical properties. *Bioinformatics*. 24:2101-2102.

Gentleman, R.C., V.J. Carey, D.M. Bates, B. Bolstad, M. Dettling, S. Dudoit, B. Ellis, L. Gautier, Y. Ge, J. Gentry, K. Hornik, T. Hothorn, W. Huber, S. Iacus, R. Irizarry, F. Leisch, C. Li, M. Maechler, A.J. Rossini, G. Sawitzki, C. Smith, G. Smyth, L. Tierney, J.Y. Yang, and J. Zhang. 2004. Bioconductor: open software development for computational biology and bioinformatics. *Genome biology*. 5:R80.

Grillitsch, K., M. Connerth, H. Kofeler, T.N. Arrey, B. Rietschel, B. Wagner, M. Karas, and G. Daum. 2011. Lipid particles/droplets of the yeast Saccharomyces cerevisiae revisited: lipidome meets proteome. *Biochim Biophys Acta*. 1811:1165-1176.

Guo, Y., T.C. Walther, M. Rao, N. Stuurman, G. Goshima, K. Terayama, J.S. Wong, R.D. Vale, P. Walter, and R.V. Farese. 2008. Functional genomic screen reveals genes involved in lipid-droplet formation and utilization. *Nature*. 453:657-661.

Guthrie, C., and G. Fink. 1991. Guide to yeast genetics and molecular biology. Academic Press.

Hancock, L.C., R.P. Behta, and J.M. Lopes. 2006. Genomic analysis of the Opi-phenotype. *Genetics*. 173:621-634.

Henry, S.A., S.D. Kohlwein, and G.M. Carman. 2012. Metabolism and regulation of glycerolipids in the yeast Saccharomyces cerevisiae. *Genetics*. 190:317-349.

Hofbauer, H.F., F.H. Schopf, H. Schleifer, O.L. Knittelfelder, B. Pieber, G.N. Rechberger, H. Wolinski, M.L. Gaspar, C.O. Kappe, J. Stadlmann, K. Mechtler, A. Zenz, K. Lohner, O. Tehlivets, S.A. Henry, and S.D. Kohlwein. 2014. Regulation of gene expression through a transcriptional repressor that senses acyl-chain length in membrane phospholipids. *Dev Cell*. 29:729-739.

Horchani, H., M. de Saint-Jean, H. Barelli, and B. Antonny. 2014. Interaction of the Spo20 membrane-sensor motif with phosphatidic acid and other anionic lipids, and influence of the membrane environment. *PLoS One*. 9:e113484.

Jacquier, N., V. Choudhary, M. Mari, A. Toulmay, F. Reggiori, and R. Schneiter. 2011. Lipid droplets are functionally connected to the endoplasmic reticulum in Saccharomyces cerevisiae. *J Cell Sci*. 124:2424-2437.

Janke, C., M.M. Magiera, N. Rathfelder, C. Taxis, S. Reber, H. Maekawa, A. Moreno-Borchart, G. Doenges, E. Schwob, E. Schiebel, and M. Knop. 2004. A versatile toolbox for PCR-based tagging of yeast genes: new fluorescent proteins, more markers and promoter substitution cassettes. *Yeast*. 21:947-962.

Krahmer, N., R.V. Farese, Jr., and T.C. Walther. 2013. Balancing the fat: lipid droplets and human disease. *EMBO molecular medicine*. 5:905-915.

Krahmer, N., Y. Guo, F. Wilfling, M. Hilger, S. Lingrell, K. Heger, H.W. Newman, M. Schmidt-Supprian, D.E. Vance, M. Mann, R.V. Farese, Jr., and T.C. Walther. 2011. Phosphatidylcholine synthesis for lipid droplet expansion is mediated by localized activation of CTP:phosphocholine cytidylyltransferase. *Cell Metab*. 14:504-515.

Leber, R., E. Zinser, G. Zellnig, F. Paltauf, and G. Daum. 1994. Characterization of lipid particles of the yeast, Saccharomyces cerevisiae. *Yeast*. 10:1421-1428.

Loewen, C.J., M.L. Gaspar, S.A. Jesch, C. Delon, N.T. Ktistakis, S.A. Henry, and T.P. Levine. 2004. Phospholipid metabolism regulated by a transcription factor sensing phosphatidic acid. *Science*. 304:1644-1647.

Loewen, C.J., A. Roy, and T.P. Levine. 2003. A conserved ER targeting motif in three families of lipid binding proteins and in Opi1p binds VAP. *EMBO J*. 22:2025-2035.

Longtine, M.S., A. McKenzie, 3rd, D.J. Demarini, N.G. Shah, A. Wach, A. Brachat, P. Philippsen, and J.R. Pringle. 1998. Additional modules for versatile and economical PCR-based gene deletion and modification in Saccharomyces cerevisiae. *Yeast*. 14:953-961.

Louvion, J.F., B. Havaux-Copf, and D. Picard. 1993. Fusion of GAL4-VP16 to a steroid-binding domain provides a tool for gratuitous induction of galactose-responsive genes in yeast. *Gene*. 131:129-134.

MacKinnon, M.A., A.J. Curwin, G.J. Gaspard, A.B. Suraci, J.P. Fernandez-Murray, and C.R. McMaster. 2009. The Kap60-Kap95 karyopherin complex directly regulates phosphatidylcholine synthesis. *J Biol Chem*. 284:7376-7384.

Magre, J., M. Delepine, E. Khallouf, T. Gedde-Dahl, Jr., L. Van Maldergem, E. Sobel, J. Papp, M. Meier, A. Megarbane, A. Bachy, A. Verloes, F.H. d'Abronzo, E. Seemanova, R. Assan, N. Baudic, C. Bourut, P. Czernichow, F. Huet, F. Grigorescu, M. de Kerdanet, D. Lacombe, P. Labrune, M. Lanza, H. Loret, F. Matsuda, J. Navarro, A. Nivelon-Chevalier, M. Polak, J.J. Robert, P. Tric, N. Tubiana-Rufi, C. Vigouroux, J. Weissenbach, S. Savasta, J.A. Maassen, O. Trygstad, P. Bogalho, P. Freitas, J.L. Medina, F. Bonnicci, B.I. Joffe, G. Loyson, V.R. Panz, F.J. Raal, S. O'Rahilly, T. Stephenson, C.R. Kahn, M. Lathrop, and J. Capeau. 2001. Identification of the gene altered in Berardinelli-Seip congenital lipodystrophy on chromosome 11q13. *Nat Genet*. 28:365-370.

Nakanishi, H., P. de los Santos, and A.M. Neiman. 2004. Positive and negative regulation of a SNARE protein by control of intracellular localization. *Mol Biol Cell*. 15:1802-1815.

Pol, A., S.P. Gross, and R.G. Parton. 2014. Review: biogenesis of the multifunctional lipid droplet: lipids, proteins, and sites. *J Cell Biol*. 204:635-646.

Prieur, X., L. Dollet, M. Takahashi, M. Nemani, B. Pillot, C. Le May, C. Mounier, H. Takigawa-Imamura, D. Zelenika, F. Matsuda, B. Feve, J. Capeau, M. Lathrop, P. Costet, B. Cariou, and J. Magre. 2013. Thiazolidinediones partially reverse the metabolic disturbances observed in Bscl2/seipin-deficient mice. *Diabetologia*. 56:1813-1825.

Rappsilber, J., M. Mann, and Y. Ishihama. 2007. Protocol for micro-purification, enrichment, pre-fractionation and storage of peptides for proteomics using StageTips. *Nat Protoc*. 2:1896-1906.

Sandager, L., M.H. Gustavsson, U. Stahl, A. Dahlqvist, E. Wiberg, A. Banas, M. Lenman, H. Ronne, and S. Stymne. 2002. Storage lipid synthesis is non-essential in yeast. *J Biol Chem*. 277:6478-6482.

Shen, H., P.N. Heacock, C.J. Clancey, and W. Dowhan. 1996. The CDS1 gene encoding CDP-diacylglycerol synthase in Saccharomyces cerevisiae is essential for cell growth. *J Biol Chem*. 271:789-795.

Shibata, Y., C. Voss, J.M. Rist, J. Hu, T.A. Rapoport, W.A. Prinz, and G.K. Voeltz. 2008. The reticulon and DP1/Yop1p proteins form immobile oligomers in the tubular endoplasmic reticulum. *J Biol Chem*. 283:18892-18904.

Smyth, G.K. 2004. Linear models and empirical bayes methods for assessing differential expression in microarray experiments. *Statistical applications in genetics and molecular biology*. 3:Article3.

Sorger, D., K. Athenstaedt, C. Hrastnik, and G. Daum. 2004. A yeast strain lacking lipid particles bears a defect in ergosterol formation. *J Biol Chem*. 279:31190-31196.

Szymanski, K.M., D. Binns, R. Bartz, N.V. Grishin, W.P. Li, A.K. Agarwal, A. Garg, R.G. Anderson, and J.M. Goodman. 2007. The lipodystrophy protein seipin is found at endoplasmic reticulum lipid droplet junctions and is important for droplet morphology. *Proc Natl Acad Sci U S A*. 104:20890-20895.

Thiam, A.R., B. Antonny, J. Wang, J. Delacotte, F. Wilfling, T.C. Walther, R. Beck, J.E. Rothman, and F. Pincet. 2013a. COPI buds 60-nm lipid droplets from reconstituted water-phospholipid-triacylglyceride interfaces, suggesting a tension clamp function. *Proc Natl Acad Sci U S A*. 110:13244-13249.

Thiam, A.R., R.V. Farese, Jr., and T.C. Walther. 2013b. The biophysics and cell biology of lipid droplets. *Nat Rev Mol Cell Biol*. 14:775-786.

Tian, Y., J. Bi, G. Shui, Z. Liu, Y. Xiang, Y. Liu, M.R. Wenk, H. Yang, and X. Huang. 2011. Tissue-autonomous function of Drosophila seipin in preventing ectopic lipid droplet formation. *PLoS Genet*. 7:e1001364.

Vamparys, L., R. Gautier, S. Vanni, W.F. Bennett, D.P. Tieleman, B. Antonny, C. Etchebest, and P.F. Fuchs. 2013. Conical lipids in flat bilayers induce packing defects similar to that induced by positive curvature. *Biophysical journal*. 104:585-593.

Vanni, S., L. Vamparys, R. Gautier, G. Drin, C. Etchebest, P.F. Fuchs, and B. Antonny. 2013. Amphipathic lipid packing sensor motifs: probing bilayer defects with hydrophobic residues. *Biophysical journal*. 104:575-584.

Wang, C.W., Y.H. Miao, and Y.S. Chang. 2014. Control of lipid droplet size in budding yeast requires the collaboration between Fld1 and Ldb16. *J Cell Sci*. 127:1214-1228.

Wilfling, F., A.R. Thiam, M.J. Olarte, J. Wang, R. Beck, T.J. Gould, E.S. Allgeyer, F. Pincet, J. Bewersdorf, R.V. Farese, Jr., and T.C. Walther. 2014. Arf1/COPI machinery acts directly on lipid droplets and enables their connection to the ER for protein targeting. *eLife*. 3:e01607.

Wilfling, F., H. Wang, J.T. Haas, N. Krahmer, T.J. Gould, A. Uchida, J.X. Cheng, M. Graham, R. Christiano, F. Frohlich, X. Liu, K.K. Buhman, R.A. Coleman, J. Bewersdorf, R.V. Farese, Jr., and T.C. Walther. 2013. Triacylglycerol synthesis enzymes mediate lipid droplet growth by relocalizing from the ER to lipid droplets. *Dev Cell*. 24:384-399.

Wolinski, H., D. Kolb, S. Hermann, R.I. Koning, and S.D. Kohlwein. 2011. A role for seipin in lipid droplet dynamics and inheritance in yeast. *J Cell Sci*. 124:3894-3904.

Yang, H., A. Galea, V. Sytnyk, and M. Crossley. 2012. Controlling the size of lipid droplets: lipid and protein factors. *Curr Opin Cell Biol*. 24:509-516.

Zeniou-Meyer, M., N. Zabari, U. Ashery, S. Chasserot-Golaz, A.M. Haeberle, V. Demais, Y. Bailly, I. Gottfried, H. Nakanishi, A.M. Neiman, G. Du, M.A. Frohman, M.F. Bader, and N. Vitale. 2007. Phospholipase D1 production of phosphatidic acid at the plasma membrane promotes exocytosis of large dense-core granules at a late stage. *J Biol Chem*. 282:21746-21757.

Supplementary Experimental Procedures

Plasmid construction

The *KES1* ORF (including 3'UTR) was amplified by PCR from genomic DNA using primers 1688 and 1689. The obtained PCR fragment was digested using XhoI and BamHI and ligated to FLAG-GFP from pPC874 plasmid originating pPC1131. pPC1224, an equivalent plasmid encoding for Flag-GFP-Kes1 $^{\Delta 2\text{-}29}$ lacking Kes1 amphipathic helix was obtained by PCR mutagenesis using primer 1731.

The PCT1 ORF (including 3'UTR) was amplified by PCR from genomic DNA using primers 1690 and 1691. The obtained PCR fragment was digested using XhoI and BamHI and ligated to FLAG-GFP from pPC874 plasmid originating pPC1130. pPC1226, an equivalent plasmid encoding for Flag-GFP-Pct1$^{\Delta 261\text{-}282}$ lacking Pct1 amphipathic helix was obtained by PCR mutagenesis using primer 1733.

The *GVP36* ORF (including 3'UTR) was amplified by PCR from genomic DNA using primers 1686 and 1687. The obtained PCR fragment was digested using XhoI and BamHI and ligated to FLAG-GFP from pPC874 plasmid originating pPC1129.

To generate pPC1184, encoding Gvp36-GFP, a PCR fragment encoding genomic Gvp36-GFP was generated using genomic DNA from yPC5554 as template and primers 1817 and 185 was amplified, digested with XhoI-XbaI cloned in pRS416. The predicted amphipatic helix (aa 2-35) was deleted by mutagenesis on this plasmid using primer 1818 to obtain the plasmid pPC1183.

The DNA fragment encoding for ADH1p-GAL4-ER-VP16 was isolated by EcoRI (blunted using Klenow) and NotI digestion from the plasmid described in (Louvion et al., 1993) coR1 (Blunted using Klenow) and ligated into SmaI/NotI digested pRS415 giving rise to pPC924.

The Q2 fragment from Opi1 containing residues 103-189 from Opi1 was amplified from genomic DNA using primers 1339 and 1340, digested with XhoI/HindIII and cloned into the backbone of pPC670 in frame with FLAG-GFP originating pPC974.

Supplemental file S1. Yeast Strains Used in this Study

Strain	Genotype
BY4741	*Mat a ura3Δ0 his3Δ1 leu2Δ0 met15Δ0*
BY4742	*Mat α ura3Δ0 his3Δ1 leu2Δ0 lys2Δ0*
yPC3975	*Mat a ura3Δ0 his3Δ1 leu2Δ0 met15Δ0 fld1::KAN*
yPC4002	*Mat a ura3Δ0 his3Δ1 leu2Δ0 met15Δ0 fld1::HYGB*
yPC4246	*Mat a ura3Δ0 his3Δ1 leu2Δ0 met15Δ0 ldb16::KAN*
yPC4307	*Mat a ura3Δ0 his3Δ1 leu2Δ0 met15Δ0* OSW5-GFP-KAN
yPC4397	*Mat a ura3Δ0 his3Δ1 leu2Δ0 met15Δ0* OSW5-GFP-KAN *ldb16::HYGB*
yPC5777	*Mat a ura3Δ0 his3Δ1 leu2Δ0 met15Δ0* PET10-GFP-HIS3
yPC5837	*Mat ? ura3Δ0 his3Δ1 leu2Δ0* PET10-GFP-HIS3 *ldb16::HYGB*
yPC5778	*Mat a ura3Δ0 his3Δ1 leu2Δ0 met15Δ0* TGL1-GFP-HIS3
yPC5840	*Mat ? ura3Δ0 his3Δ1 leu2Δ0* TGL1-GFP-HIS3 *ldb16::HYGB*
yPC5776	*Mat a ura3Δ0 his3Δ1 leu2Δ0 met15Δ0* YEH1-GFP-HIS3
yPC6438	*Mat a ura3Δ0 his3Δ1 leu2Δ0 met15Δ0* YEH1-GFP-HIS3 *ldb16::HYGB*
yPC5266	*Mat a ura3Δ0 his3Δ1 leu2Δ0 met15Δ0* OPI1-GFP-HIS3
yPC5583	*Mat ? ura3Δ0 his3Δ1 leu2Δ0* OPI1-GFP-HIS3 *ldb16::HYGB*
yPC5558	*Mat a ura3Δ0 his3Δ1 leu2Δ0 met15Δ0* PCT1-GFP-HIS3
yPC5577	*Mat ? ura3Δ0 his3Δ1 leu2Δ0* PCT1-GFP-HIS3 *ldb16::HYGB*
yPC7303	*Mat a ura3Δ0 his3Δ1 leu2Δ0 met15Δ0* PCT1-GFP-HIS3 *opi3::KAN*
yPC5559	*Mat a ura3Δ0 his3Δ1 leu2Δ0 met15Δ0* KES1-GFP-HIS3
yPC7811	*Mat a ura3Δ0 his3Δ1 leu2Δ0 met15Δ0* KES1-GFP-HIS3 *ldb16::HYGB*
yPC5581	*Mat a ura3Δ0 his3Δ1 leu2Δ0 met15Δ0* KES1-GFP-HIS3 *fld1::NAT*
yPC5554	*Mat a ura3Δ0 his3Δ1 leu2Δ0 met15Δ0* GVP36-GFP-HIS3
yPC5563	*Mat a ura3Δ0 his3Δ1 leu2Δ0 met15Δ0* GVP36-GFP-HIS3 *ldb16::HYGB*
yPC7300	*Mat a ura3Δ0 his3Δ1 leu2Δ0 met15Δ0* GVP36-GFP-HIS3 *opi3::KAN*
yPC5923	*Mat a ura3Δ0 his3Δ1 leu2Δ0 met15Δ0* VPS13-GFP-HIS3
yPC5985	*Mat a ura3Δ0 his3Δ1 leu2Δ0 met15Δ0* VPS13-GFP-HIS3 *ldb16::HYGB*
yPC6450	*Mat a ura3Δ0 his3Δ1 leu2Δ0 met15Δ0* OPI1-mCHERRY-URA2 HMG1-GFP-HIS3
yPC6453	*Mat ? ura3Δ0 his3Δ1 leu2Δ0* OPI1-mCHERRY-URA2 HMG1-GFP-HIS3 *ldb16::HYGB*
yPC7989	*Mat a ura3Δ0 his3Δ1 leu2Δ0 met15Δ0* PCT1-mCHERRY-URA3 HMG1-GFP-HIS3
yPC7425	*Mat a ura3Δ0 his3Δ1 leu2Δ0 met15Δ0* PCT1-mCHERRY-URA3 HMG1-GFP-HIS3 *ldb16::HYGB*
yPC7453	*Mat a ura3Δ0 his3Δ1 leu2Δ0 met15Δ0* KES1-mCHERRY-URA3 HMG1-GFP-HIS3
yPC7455	*Mat ? ura3Δ0 his3Δ1 leu2Δ0* KES1-mCHERRY-URA3 HMG1-GFP-HIS3 *ldb16::HYGB*
yPC8124	*Mat ? ura3Δ0 his3Δ1 leu2Δ0* PCT1-mCHERRY-URA3 KES1-GFP-HIS3
yPC8125	*Mat ? ura3Δ0 his3Δ1 leu2Δ0* PCT1-mCHERRY-URA3 KES1-GFP-HIS3 *fld1::NAT*

yPC8129	*Mat ? ura3Δ0 his3Δ1 leu2Δ0* PCT1-mCHERRY-URA3 KES1-GFP-HIS3 *ldb16::HYGB*
yPC5266	*Mat a ura3Δ0 his3Δ1 leu2Δ0 met15Δ0* OPI1-GFP-HIS3
yPC5585	*Mat a ura3Δ0 his3Δ1 leu2Δ0 met15Δ0* OPI1-GFP-HIS3 *fld1::NAT*
yPC5583	*Mat a ura3Δ0 his3Δ1 leu2Δ0 met15Δ0* OPI1-GFP-HIS3 *ldb16::HYGB*
yPC5950	*Mat ? ura3Δ0 his3Δ1 leu2Δ0* OPI1-GFP-HIS3 *scs2::KAN*
yPC5949	*Mat ? ura3Δ0 his3Δ1 leu2Δ0* OPI1-GFP-HIS3 *scs2::KAN fld1::NAT*
yPC5952	*Mat ? ura3Δ0 his3Δ1 leu2Δ0* OPI1-GFP-HIS3 *scs2::KAN ldb16::HYGB*
yPC6260	*Mat a leu2-3,122 ura3-52 his3D200 trp-D900 lys2-8-1 suc2D9* <PHO5p-GFP-Opi1^{FFAT}>
yPC6264	*Mat a leu2-3,122 ura3-52 his3D200 trp-D900 lys2-8-1 suc2D9 fld1::NAT* <PHO5p-GFP-Opi1^{FFAT}>
yPC6340	*Mat a leu2-3,122 ura3-52 his3D200 trp-D900 lys2-8-1 suc2D9 ldb16::HYGB* <PHO5p-GFP-Opi1^{FFAT}>
yPC6037	*Mat a ura3Δ0 his3Δ1 leu2Δ0 met15Δ0* <TEFp-GFP-Spo20$^{51-91}$,2micron,URA>
yPC6038	*Mat a ura3Δ0 his3Δ1 leu2Δ0 met15Δ0 fld1::HYGB* <TEFp-GFP-Spo20$^{51-91}$,2micron,URA>
yPC6058	*Mat a ura3Δ0 his3Δ1 leu2Δ0 met15Δ0 ldb16::KANR* <TEFp-GFP-Spo20$^{51-91}$,2micron,URA>
yPC6039	*Mat a ura3Δ0 his3Δ1 leu2Δ0 met15Δ0 opi3::KANR* <TEFp-GFP-Spo20$^{51-91}$,2micron,URA>
yPC7647	*Mat a ura3Δ0 his3Δ1 leu2Δ0 met15Δ0* < Flag-GFP-KES1, CEN, URA>
yPC7648	*Mat a ura3Δ0 his3Δ1 leu2Δ0 met15Δ0 ldb16::KAN* < Flag-GFP-KES1, CEN, URA>
yPC7669	*Mat a ura3Δ0 his3Δ1 leu2Δ0 met15Δ0 fld1::HYGB* < Flag-GFP-KES1, CEN, URA>
yPC7888	*Mat a ura3Δ0 his3Δ1 leu2Δ0 met15Δ0* < Flag-GFP-KES1 $^{\Delta 2-29}$, CEN, URA>
yPC7882	*Mat a ura3Δ0 his3Δ1 leu2Δ0 met15Δ0 ldb16::KAN* < Flag-GFP-KES1 $^{\Delta 2-29}$, CEN, URA>
yPC7885	*Mat a ura3Δ0 his3Δ1 leu2Δ0 met15Δ0 fld1::HYGB* < Flag-GFP-KES1 $^{\Delta 2-29}$, CEN, URA>
yPC7645	*Mat a ura3Δ0 his3Δ1 leu2Δ0 met15Δ0* < Flag-GFP-PCT1, CEN, URA>
yPC7646	*Mat a ura3Δ0 his3Δ1 leu2Δ0 met15Δ0 ldb16::KAN* < Flag-GFP-PCT1, CEN, URA>
yPC7668	*Mat a ura3Δ0 his3Δ1 leu2Δ0 met15Δ0 fld1::HYGB* < Flag-GFP-PCT1, CEN, URA>
yPC7881	*Mat a ura3Δ0 his3Δ1 leu2Δ0 met15Δ0* < Flag-GFP-PCT1 $^{\Delta 261-282}$, CEN, URA>
yPC7884	*Mat a ura3Δ0 his3Δ1 leu2Δ0 met15Δ0 ldb16::KAN* < Flag-GFP-PCT11 $^{\Delta 261-282}$, CEN, URA>
yPC788?	*Mat a ura3Δ0 his3Δ1 leu2Δ0 met15Δ0 fld1::HYGB* < Flag-GFP-PCT11 $^{\Delta 261-282}$, CEN, URA>
yPC8237	*Mat a ura3Δ0 his3Δ1 leu2Δ0 met15Δ0* < GVP36-GFP, CEN, URA>
yPC8241	*Mat a ura3Δ0 his3Δ1 leu2Δ0 met15Δ0 ldb16::KAN* < GVP36-GFP, CEN, URA>
yPC8239	*Mat a ura3Δ0 his3Δ1 leu2Δ0 met15Δ0 fld1::HYGB* < GVP36-GFP, CEN, URA>
yPC8238	*Mat a ura3Δ0 his3Δ1 leu2Δ0 met15Δ0* < GVP36 $^{\Delta 2-35}$-GFP, CEN, URA>
yPC8242	*Mat a ura3Δ0 his3Δ1 leu2Δ0 met15Δ0 ldb16::KAN* < GVP36 $^{\Delta 2-35}$-GFP, CEN, URA>
yPC8240	*Mat a ura3Δ0 his3Δ1 leu2Δ0 met15Δ0 fld1::HYGB* < GVP36 $^{\Delta 2-35}$-GFP, CEN, URA>
yPC7791	*Mat a ura3Δ0 his3Δ1 leu2Δ0 are1::KAN are2::HYGB dga1::NAT lro1::KAN* < Flag-GFP-PCT1, CEN, URA>
yPC7794	*Mat a ura3Δ0 his3Δ1 leu2Δ0 are1::KAN are2::HYGB dga1::NAT lro1::KAN ldb16::HIS* < Flag-GFP-PCT1, CEN, URA>

yPC8538	*Mat a ura3Δ0 his3Δ1 leu2Δ0 are1::KAN are2::HYGB dga1::NAT lro1::KAN fld1::HIS* < Flag-GFP-PCT1, CEN, URA>
yPC7267	*Mat a ura3Δ0 his3Δ1 leu2Δ0 are1::KAN are2::HYGB dga1::NAT lro1::KAN* <TEFp-GFP-Spo20$^{51-91}$, 2micron, URA>
yPC7268	*Mat a ura3Δ0 his3Δ1 leu2Δ0 are1::KAN are2::HYGB dga1::NAT lro1::KAN ldb16::HIS* <TEFp-GFP-Spo20$^{51-91}$, 2micron, URA>
yPC8540	*Mat a ura3Δ0 his3Δ1 leu2Δ0 are1::KAN are2::HYGB dga1::NAT lro1::KAN fld1::HIS* <TEFp-GFP-Spo20$^{51-91}$, 2micron, URA>
yPC8307	*Mat ? ura3Δ0 his3Δ1 leu2Δ0 are1::KANR are2::HYGB lro1::HIS KANR-GALp-DGA1* < Flag-GFP-KES1, CEN, URA> <ADH1p-GAL4-ER-VP16,CEN,LEU >
yPC8306	*Mat ? ura3Δ0 his3Δ1 leu2Δ0 are1::KANR are2::HYGB lro1::HIS KANR-GALp-DGA1 ldb16::NAT* < Flag-GFP-KES1, CEN, URA> <ADH1p-GAL4-ER-VP16,CEN,LEU >
yPC8305	*Mat ? ura3Δ0 his3Δ1 leu2Δ0 are1::KANR are2::HYGB lro1::HIS KANR-GALp-DGA1* < Flag-GFP-PCT1, CEN, URA> <ADH1p-GAL4-ER-VP16,CEN,LEU >
yPC8304	*Mat ? ura3Δ0 his3Δ1 leu2Δ0 are1::KANR are2::HYGB lro1::HIS KANR-GALp-DGA1 ldb16::NAT* < Flag-GFP-PCT1, CEN, URA> <ADH1p-GAL4-ER-VP16,CEN,LEU >
yPC8070	*Mat ? ura3Δ0 his3Δ1 leu2Δ0* KAN-GPD-CDS1 KES1-GFP-HIS3
yPC8073	*Mat ? ura3Δ0 his3Δ1 leu2Δ0* KAN-GPD-CDS1 KES1-GFP-HIS3 *fld1::NAT*
yPC8071	*Mat ? ura3Δ0 his3Δ1 leu2Δ0* KAN-GPD-CDS1 KES1-GFP-HIS3 *ldb16::HYGB*
yPC4092	*Mat a ura3Δ0 his3Δ1 leu2Δ0 met15Δ0 cho2::KAN*
yPC5617	*Mat ? ura3Δ0 his3Δ1 leu2Δ0 cho2::KAN ldb16::HYGB*
yPC4067	*Mat a ura3Δ0 his3Δ1 leu2Δ0 met15Δ0 opi3::KAN*
yPC5752	*Mat a ura3Δ0 his3Δ1 leu2Δ0 opi3::KAN ldb16::HYGB*
yPC7452	*Mat a ura3Δ0 his3Δ1 leu2Δ0 met15Δ0* GVP36-mCherry-URA3 HMG1-GFP-HIS3
yPC7456	*Mat ? ura3Δ0 his3Δ1 leu2Δ0* GVP36-mCherry-URA3 HMG1-GFP-HIS3 *ldb16::HYGB*
yPC7454	*Mat a ura3Δ0 his3Δ1 leu2Δ0 met15Δ0* VPS13-mCherry-URA3 HMG1-GFP-HIS3
yPC7458	*Mat ? ura3Δ0 his3Δ1 leu2Δ0* VPS13-mCherry-URA3 HMG1-GFP-HIS3 *ldb16::HYGB*
yPC7064	*Mat a ura3Δ0 his3Δ1 leu2Δ0 met15Δ0* Opi1-3HA-HIS3
yPC7065	*Mat a ura3Δ0 his3Δ1 leu2Δ0 met15Δ0* Opi1-3HA-HIS3 *fld1::HYGB*
yPC7066	*Mat a ura3Δ0 his3Δ1 leu2Δ0 met15Δ0* Opi1-3HA-HIS3 *ldb16::KAN*
yPC6258	*Mat a leu2-3,122 ura3-52 his3D200 trp-D900 lys2-8-1 suc2D9* <PHO5p-GFP-Scs2>
yPC6262	*Mat a leu2-3,122 ura3-52 his3D200 trp-D900 lys2-8-1 suc2D9 fld1::NAT* <PHO5p-GFP-Scs2>
yPC6338	*Mat a leu2-3,122 ura3-52 his3D200 trp-D900 lys2-8-1 suc2D9 ldb16::HYGB* <PHO5p-GFP-Scs2>
yPC6446	*Mat a ura3Δ0 his3Δ1 leu2Δ0 met15Δ0* <FLAG-GFP-OPI1 ^{Q2}, CEN, URA>
yPC6447	*Mat a ura3Δ0 his3Δ1 leu2Δ0 met15Δ0 ldb16::KAN* <FLAG-GFP-OPI1 ^{Q2}, CEN, URA>

yPC7792	*Mat a ura3Δ0 his3Δ1 leu2Δ0 are1::KAN are2::HYGB dga1::NAT lro1::KAN* < Flag-GFP-KES1, CEN, URA>
yPC7795	*Mat a ura3Δ0 his3Δ1 leu2Δ0 are1::KAN are2::HYGB dga1::NAT lro1::KAN ldb16::HIS* < Flag-GFP-KES1, CEN, URA>
yPC8539	*Mat a ura3Δ0 his3Δ1 leu2Δ0 are1::KAN are2::HYGB dga1::NAT lro1::KAN fld1::HIS?* < Flag-GFP-KES1, CEN, URA>
yPC7828	*Mat a ura3Δ0 his3Δ1 leu2Δ0 met15Δ0* KAN-GPD-CDS1 <Flag-GFP-PCT1, CEN, URA>
yPC7832	*Mat a ura3Δ0 his3Δ1 leu2Δ0 met15Δ0* KAN-GPD-CDS1 *ldb16::HYGB* <Flag-GFP-PCT1, CEN, URA>
yPC7834	*Mat a ura3Δ0 his3Δ1 leu2Δ0 met15Δ0* KAN-GPD-CDS1 *fld1::NAT* <Flag-GFP-PCT1, CEN, URA>
yPC5144	*Mat α ura3Δ0 his3Δ1 leu2Δ0 lys2Δ0* ELO3-mCherry-URA
yPC5199	*Mat ? ura3Δ0 his3Δ1 leu2Δ0* ELO3-mCherry-URA *fld1::NAT*
yPC5201	*Mat ? ura3Δ0 his3Δ1 leu2Δ0* ELO3-mCherry-URA *ldb16::HYGB*
yPC1573	*Mat a ura3Δ0 his3Δ1 leu2Δ0 met15Δ0* SEC63-GFP-HIS5
yPC8122	*Mat a ura3Δ0 his3Δ1 leu2Δ0 met15Δ0* SEC63-GFP-HIS5 *fld1::NAT*
yPC8121	*Mat a ura3Δ0 his3Δ1 leu2Δ0 met15Δ0* SEC63-GFP-HIS5 *ldb16::NAT*

Supplemental file S2. Plasmids Used in this Study

Name	Insert/Gene	Primers used	Vector	Source
pPC941	PHO5p-GFP-Opi1^{FFAT}, URA3		pRS406	Loewen et al., 2003
pPC933	TEFp-GFP-Spo20$^{51-91}$,2µ,URA3		pRS426	Nakanishi et al., 2004
pPC1131	Flag-GFP-KES1, CEN, URA3	1688+1689	pRS316	This study
pPC1224	Flag-GFP-KES1 $^{\Delta 2-29}$, CEN, URA3	1731	pRS316	This study
bPC1130	Flag-GFP-PCT1, CEN, URA3	1690+1691	pRS316	This study
pPC1226	Flag-GFP-PCT1 $^{\Delta 261-282}$, CEN, URA3	1733	pRS316	This study
pPC1129	Flag-GFP-GVP36, CEN, URA3	1686+1687	pRS316	This study
pPC1184	GVP36-GFP, CEN, URA3		pRS316	This study
pPC1183	GVP36 $^{\Delta 2-35}$-GFP, CEN, URA3	1818	pRS416	This study
pPC924	ADH1p-GAL4-ER-VP16,CEN,LEU		pRS415	This study (based on Louvion et al., 1993)
pPC938	PHO5p-GFP-Scs2		pRS406	Loewen et al., 2003
pPC974	FLAG-GFP-OPI1 ^{Q2}, CEN, URA3	1339+1340	pRS316	This study

Supplemental file S3. Primers Used in this Study

Number	Name	Sequence
1688	Kes1FXhoI	CATGGATGAACTATACAAACTCgagATGTCTCAATACGCAAGCTC
1689	Kes1RBamHI	CTATAGGGCGAATTGGCTAGTGGATCcGAGCGATCTGTCTATCAATAATTA
1731	Kes1Δ(2-29)	GATGAACTATACAAACTCgagATGCCTCCATTCATTTTATCTCCAATC
1690	Pct1FXhoI	GATGAACTATACAAACTCgagATGGCAAACCCAACAACAGGGAAG
1691	Pct1RBamHI	GCGAATTGGCTAGTGGATCCTAATCAACTTTCTCTCCTTCAAATC
1733	Pct1Δ(261-282)	GACAGGAGCTGAACGTTTCTCACATCAATGAATTCAGGTC
1686	Gvp36FXhoI	GAACTATACAAACTCgagATGTCGTTTAATGCCTTCGCCAG
1687	Gvp36RBamHI	GCGAATTGGCTAGTGGATCCGTATTGCGGTTGAGTAGCGTC
1818	Gvp36Δ(2-35)	CAAATCATAGTCATCAATGCAAAGAATGGTCCAGGAAC
185	Yos9R5	CTATTGTACTCGAGCGAGGCAAGCTAAACAGATC
1339	Opi1Q2FXhoI	GAACTATACAAACTCgagGATGAGTTCTTCACCAACAAG
1340	Opi1Q2RHindIII	CACATACACGCTAAGCTTTTACTCGTCCTCGCCAGCTCCAG

IV. DISCUSSION

Cellular lipids are distributed unevenly within and between membrane bilayers. The resulting lipid composition is fundamental for recognition and targeting of proteins and establishment of organelle identity. The ER, which constitutes the major lipid source and it is central to lipid homeostasis, plays a pivotal role in this process. Indeed, lipid and protein sorting from the ER to the other organelles are tightly coordinated. Lipid droplets, the main energy storage organelles, are directly derived from the ER and share with it an intimate connection which is fundamental for lipid buffering processes. All the enzymes synthesizing the core and surface lipids of LDs are located at the ER, and most of the proteins targeted to LDs surface also pass through the ER before being targeted to LDs. Thus, LDs are assumed to derive from the ER's cytosolic leaflet and to spend most of their life in contact with it (Bartz et al., 2007a; Penno et al., 2013; Tauchi-Sato et al., 2002). Although it is not clear how the coordinate packaging of the neutral lipid core and the surface phospholipid monolayer is regulated during LDs biogenesis, it seems clear that the conserved ER protein seipin, by localizing at the ER-LDs contact sites may have a key role in this process.

The focus of my thesis was understanding the role of the Seipin/Fld1p complex in the LDs biogenesis and lipid homeostasis in yeast.

Excessive energy and fat storage leads to obesity and related diseases as diabetes, atherosclerosis and cancer. More recent are the indications that also deficiencies in forming and maintaining LDs are detrimental. One of the most severe diseases directly related to LD functions is the Berardinelli-Seip congenital lipodistrophy type 2. This form is associated with loss of function recessive mutations at the locus *BSCL2* which encodes seipin, a protein of unknown function with conserved structure in animals, plants and fungi (Magre et al., 2001). The yeast seipin homologue Fld1 was identified in two independent screenings in *S. cerevisiae*. The protein was shown to localise at the ER-LDs junction and to be involved in LDs morphology (Fei et al., 2008; Szymanski et al., 2007). Interestingly, yeast cells lacking *FLD1* showed either a strong decrease in the number of LDs concomitant with an increase in size, or aberrant LD assembly in grape-like clusters able to fuse depending on growth conditions (Fei et al., 2008). The relevance of this resides in the fact that number and size of LDs reflect the balance of the neutral lipids and phospholipids in the cells derived either by changes in the levels of synthesis or in mobilization, so that abnormalities at LDs levels reflects metabolic dysfunctions.

In my thesis I used a combination of biochemistry and microscopy to unravel the role of seipin in cellular lipid homeostasis. By looking for yeast seipin binding partners we discovered that Fld1 forms a complex with other proteins of unknown function, Ldb16 and Ymr147w-Ymr148w. Previous studies failed to identify any binding partners for Fld1 (Binns et al., 2010), but we show by using mass-spec analysis and reciprocal IPs that these proteins form a complex that we named the seipin complex. This could start answering the unsolved question of how Fld1, which is mostly extended in the ER lumen, regulates the morphology of cytoplasmic LDs. We propose that Fld1 and Ldb16 constitute the core of this complex whilst Ymr147w-Ymr148w could perform a different function. This hypothesis relies on the following evidences.
(1) We found that Ldb16p and Fld1p bind to each other independently of the presence of Ymr147w-Ymr148w. On the contrary, incorporation of Ymr147w-Ymr148w in the complex is compromised by Fld1 deletion or by expression of its pathogenic analogous mutations. (2) While deletion of *FLD1* or *LDB16* gives the same LDs phenotype (either supersized or small and clustered depending on growth conditions), LDs in *ymr147wΔ* or *ymr148wΔ* strains were indistinguishable from those in *wt* cells. (3) The subcellular localization was not the same for all the binding partners of the complex. Indeed, while Ldb16 is also distributed at *foci* at ER-LDs contact sites as previously shown for Fld1 (Fei et al., 2008; Szymanski et al., 2007), Ymr147w-Ymr148w has a dual distribution, either at LDs surface or in *foci* partially co-localizing with Ldb16-GFP.

What is the role of Ymr147w-Ymr148w in the seipin complex? It was not possible in the time frame of this thesis to give a precise answer to this question, but I believe we gathered some interesting preliminary insights.
First of all, we found that despite being annotated as two independent ORFs, Ymr147w-Ymr148w are instead a single protein whose length is the result of alternative splicing. These findings were supported by previous deep sequencing data (Miura et al., 2006) in which an event of alternative splicing was identified for these two consecutive ORFs. We found that the transmembrane protein Ymr148w can be expressed as a short form its own promoter. Alternatively, it exists as a longer form comprehensive of most of the Ymr147w ORF plus Ymr148w ORF, after splicing of the intronic sequence that is connecting the two ORFs. Ymr147w was never detected on its own unless YMR148w ORF was deleted. Moreover, when a strong promoter was placed in front of Ymr147w, the only form present was the longer one (here referred as Ymr147w-Ymr148w), suggesting that the transcriptional regulation of the two forms is lost in these conditions.

Secondly, by expressing N-terminal GFP-tagged version of Ymr147w-Ymr148w under the control of constitutive promoters of different strengths, we observed a great proliferation and clustering of LDs. Moreover, the fusion-protein was distributed at LDs surface but only in a subpopulation of LDs. We also found that the LDs marker Erg6-Cherry was partially redistributed to the ER in these conditions, and often excluded from LDs labelled by GFP-Ymr147w. It is possible that GFP-Ymr147w overexpression saturates the LDs surface causing Erg6 to relocate back at the ER. Interestingly, the same proliferation of LDs was not observed upon overexpression of Ymr148w alone (data not shown). This suggests that the differential expression of the two isoforms might have a role in controlling LD numbers.
How this process is regulated, and what is the role of this protein isoforms in the seipin complex will require further efforts and is currently under investigation in the lab. As we couldn't identify a KO LDs phenotype, their role seems not as directly involved in the biogenesis of LDs, as proposed for Fld1. An appealing possibility is that Ymr147-148w might work as a sensor in the complex, for growth state or for nutrients, to regulate LDs numbers.

We then focused on the characterization of the core components of the Seipin complex. We noticed that Ldb16 is destabilized in absence of its binding partner Fld1 and that its degradation is dependent on the ER ubiquitin ligase Doa10. These results suggest that Fld1 and Ldb16 interact in the complex with a certain stoichiometry. This observation was also confirmed by Wang and colleagues (Wang et al., 2014), that extended the analysis by showing that Ldb16 was also stabilized by deletion of Doa10 co-factors or by impairment of downstream ERAD components (*i.e. npl4-1, ufd1-2* and proteasome inhibitors). However, rescuing the levels of Ldb16 by Doa10 deletion or by Ldb16 overexpression was not complementing the LDs phenotype in *fld1Δ* cells. Moreover, the fact that Fld1 stability is not affected by Ldb16 depletion, but its binding with itself is diminished (Wang et al., 2014), suggests that the two proteins might have a further level of regulation that is not dependent on their expression levels but on their physical interaction. Indeed, in absence of the binding partner the LDs phenotype is altered even when the proteins are maintained at *wt* levels.

To assess the minimal requirements for Ldb16 functionality, we generated progressive deletions from the C-terminal side of the protein. We found that the TMs are necessary for normal LDs morphology as well as for maintaining the interaction with its binding

partner Fld1. During the completion of this work, Wang et al. also reached similar conclusions: Fld1 and Ldb16 interact through their TM domain and deletions not affecting the TM domain have no effect on LDs morphology. However, in contrast with what we observed, they reported that overexpression of full-length Ldb16, rather than Ldb16(1-133), causes defective LDs. A reason for this inconsistency could be that they expressed the protein using a plasmid in a *wt* background. This could result in higher expression levels than the integrated GPD-Lbd16 we used in our experiments leading to a different phenotype.

Interestingly, we found that all the analysed Ldb16 truncations were more stable than the full length protein, particularly in the absence of Fld1. This suggests that the C-terminal part is involved in the regulation of Ldb16 stability. Another possibility is that it is required for sensing the cell growth state possibly through its interaction with Ymr147-148w. In this context the deregulation due to the C-terminal deletion could explain why the overexpression of Ldb16(1-133) leads to a defect in LDs morphology that is not affected by the presence of inositol in the media. Interestingly, it was recently reported that an Fld1 mutant deleted of its 14 N-terminal amino acids displayed SLDs but also insensitivity to inositol (Cartwright et al., 2015). It is conceivable that these mutants retain a partial function of the complex but lose their regulation. Consistently, when Fld1 is overexpressed in the GPD-Ldb16(1-133) background the LDs phenotype is rescued, suggesting that this equilibrates the stoichiometry between the two binding partners, and compensates for the partial loss of function phenotype due to overexpression of the deregulated protein.

Although Ldb16 homologs are present in fungi, we and others could not find Ldb16 homologs in higher eukaryotes (Wang et al., 2014). However, Wang et al. show that overexpression of *wt* human seipin remarkably complements the LDs phenotype in cells deleted of Fld1, Ldb16 or both. Interestingly, the human seipin C-terminal extension, which is absent in Fld1, is not required for this complementation. This suggests that during evolution the function of the two yeast proteins converged on the transmembrane portion of Seipin.

Fld1 and Ldb16 deletion mutants and mutants defective in the PEMT pathway display the same SLDs phenotype in minimal media lacking phospholipid precursors (Fei et al., 2011c). They also have an Opi$^-$ phenotype (*i.e.* inositol excretion in the media due to de-repression of INO1 gene, which is responsible for *de novo* synthesis of inositol) (Hancock et al., 2006). However, whilst choline or inositol supplementation rescues both SLD and

Opi$^-$ phenotype in PEMT-pathway mutants (Henry et al., 2014; Henry and Patton-Vogt, 1998), it did not have the same effect on Fld1/Ldb16 mutants. Indeed, inositol addition was not rescuing INO1 upregulation (Hancock et al., 2006) but it was shifting *fld1Δ* or *ldb16Δ* LD morphology from supersized to clustered. This, together with the fact that we could not detect major alterations in lipid composition in these mutants, led us to conclude that the mechanism generating SLD in *fld1Δ* or *ldb16Δ* cells is distinct from defects in the PEMT pathway.

A possible explanation for the observed Opi$^-$ phenotype derives from our evidence that Opi1 is mislocalized in the *fld1Δ* or *ldb16Δ* mutants, forming *foci* at the nuclear envelope that are often in proximity of LDs clusters. Opi1 represses INO1 expression through binding to Ino2-Ino4 activators in the nucleus. When INO1 activity is required, Opi1 is retained at the nuclear envelope through interaction with Scs2 and PA (Henry et al., 2012; Loewen et al., 2004; Young et al., 2010). We believe that Opi1 ability to be released from its ER-bound condition upon inositol addition and PA consumption, and to repress INO1, is impaired in seipin complex mutants. However, INO1 constitutive upregulation is not the cause of the SLDs phenotype as *opi1Δ* cells display normal LDs.

On the other hand, it has been proposed that the distribution of ER-localized phosphatidic acid is altered in *fld1Δ* cells, causing the SLD phenotype (Fei et al., 2011c). We also investigated this possibility but we could not detect more than small differences in the PA cellular levels. However, it remains possible that the technique used was not sensitive enough to measure the low amount of this phospholipid. We also used the PA biosensor GFP-Spo20$^{51-91}$ to test whether the cellular pools of PA were altered in these mutants. We observed that the localization was changed from being evenly distributed at the plasma membrane to form *foci* at the nuclear envelope often in contact with LDs. However, this defect was further increased by addition of inositol or by overexpression of Cds1, conditions that consume PA. In line with this, Horchani and colleagues recently showed that Spo20$^{51-91}$ *in vitro* has a general preference for anionic phospholipids and not necessarily for PA (Horchani et al., 2014). Although we could not exclude the increase of PA previously reported in absence of seipin (Cui et al., 2011; Fei et al., 2011c), based on our results we propose that the amphipatic helix of the GFP-Spo20$^{51-91}$ probe recognizes other features besides PA at the nuclear ER, as localized lipid imbalances. Likely, this is also the case for Opi1 retention at the NE.

Through LDs isolation and mass spectrometry we identified a number of other proteins enriched at LDs surface and with an altered distribution in seipin mutants. The only

obvious common characteristic of these proteins was the presence of an amphipatic helix (see also Chapter 3.3 for discussion). This suggested that the clustered structures containing membranes bilayers and LDs that we observed by light and electromicroscopy recruit proteins that are normally distributed elsewhere. This supports the idea that these aggregated structures assume characteristics that are distinct both from the ER membrane and from the lipid droplets. We therefore believe that clustered LDs formed in absence of the seipin complex have a compromised membrane identity. To understand whether these clustered structures and the concomitant abnormal protein recruitment are cause or effect of the impaired LD formation, we followed the distribution of two of these proteins during the process of LDs biogenesis in presence or absence of inositol. From this we concluded that (1) seipin mutants have a defect in the LDs biogenesis which is alleviated in absence of inositol. This suggests that in absence of the seipin complex there is an impairment in the organization of this process at the ER membrane. (2) Protein recruitment defects are a consequence of this impairment, as they are not present in absence of LDs.

In conclusion, here we show that Fld1 forms a complex with the uncharacterized ER membrane protein Ldb16. This seipin complex localizes to the ER-LD contact sites which is essential for correct LD assembly. In absence of the seipin complex, LD assembly results in localized differences in phospholipid composition and packing detected by the amphipatic helices of different proteins, and ultimately in aberrant LDs. These data support a model by which the complex facilitates LD assembly by acting as a diffusion barrier at the site of LDs biogenesis (See chapter 3.3 for further discussion). This is reflected in maintenance of the phospholipids balance at the NE by allowing the normal formation of specific domains for LDs growth. In its absence the NE composition might be affected and destabilized causing loss of segregation between compartments and mistargeting of lipid binding proteins due to deregulated LDs biogenesis/turnover. In these conditions a single droplet (or an aggregate of small LDs) might grow at sites where the barrier is missing and its morphology is then depends on the ER phospholipid availability.

The possibility that the complex activity affects the acyl chain pattern of phospholipids/TAG (Fei, 2008 #122) altering the LDs properties is also currently under investigation in the lab. These changes could potentially affect thickness, intrinsic curvature, and fluidity of membranes and therefore dynamic processes such as membrane fusion and fission.

In the end, we provided novel insights into the role of the yeast seipin complex. This will likely open up new lines of research for further uncovering the detailed molecular mechanisms underlying in LDs biogenesis. Now the challenge remains to test whether results obtained in yeast could be upheld in mammalian cell lines to unveil the molecular function of this important disease-causing protein.

REFERENCES

Anand, P., Cermelli, S., Li, Z., Kassan, A., Bosch, M., Sigua, R., Huang, L., Ouellette, A.J., Pol, A., Welte, M.A.*, et al.* (2012). A novel role for lipid droplets in the organismal antibacterial response. eLife *1*, e00003.

Andrianov, V., Borisjuk, N., Pogrebnyak, N., Brinker, A., Dixon, J., Spitsin, S., Flynn, J., Matyszczuk, P., Andryszak, K., Laurelli, M.*, et al.* (2010). Tobacco as a production platform for biofuel: overexpression of Arabidopsis DGAT and LEC2 genes increases accumulation and shifts the composition of lipids in green biomass. Plant biotechnology journal *8*, 277-287.

Athenstaedt, K., and Daum, G. (2003). YMR313c/TGL3 encodes a novel triacylglycerol lipase located in lipid particles of Saccharomyces cerevisiae. The Journal of biological chemistry *278*, 23317-23323.

Athenstaedt, K., and Daum, G. (2005). Tgl4p and Tgl5p, two triacylglycerol lipases of the yeast Saccharomyces cerevisiae are localized to lipid particles. The Journal of biological chemistry *280*, 37301-37309.

Athenstaedt, K., Zweytick, D., Jandrositz, A., Kohlwein, S.D., and Daum, G. (1999). Identification and characterization of major lipid particle proteins of the yeast Saccharomyces cerevisiae. Journal of bacteriology *181*, 6441-6448.

Atkinson, K.D., Jensen, B., Kolat, A.I., Storm, E.M., Henry, S.A., and Fogel, S. (1980). Yeast mutants auxotrophic for choline or ethanolamine. J Bacteriol *141*, 558-564.

Bartz, R., Li, W.H., Venables, B., Zehmer, J.K., Roth, M.R., Welti, R., Anderson, R.G., Liu, P., and Chapman, K.D. (2007a). Lipidomics reveals that adiposomes store ether lipids and mediate phospholipid traffic. Journal of lipid research *48*, 837-847.

Bartz, R., Zehmer, J.K., Zhu, M., Chen, Y., Serrero, G., Zhao, Y., and Liu, P. (2007b). Dynamic activity of lipid droplets: protein phosphorylation and GTP-mediated protein translocation. Journal of proteome research *6*, 3256-3265.

Beller, M., Thiel, K., Thul, P.J., and Jackle, H. (2010). Lipid droplets: a dynamic organelle moves into focus. FEBS letters *584*, 2176-2182.

Benjamini, Y., and Hochberg, Y. (1995). Controlling the false discovery rate: a practical and powerful approach to multiple testing. J R Stat Soc Ser B, 289–300.

Bhatla, S.C., Kaushik, V., and Yadav, M.K. (2010). Use of oil bodies and oleosins in recombinant protein production and other biotechnological applications. Biotechnology advances *28*, 293-300.

Binns, D., Januszewski, T., Chen, Y., Hill, J., Markin, V.S., Zhao, Y., Gilpin, C., Chapman, K.D., Anderson, R.G., and Goodman, J.M. (2006). An intimate collaboration between peroxisomes and lipid bodies. The Journal of cell biology *173*, 719-731.

Binns, D., Lee, S., Hilton, C.L., Jiang, Q.X., and Goodman, J.M. (2010). Seipin is a discrete homooligomer. Biochemistry *49*, 10747-10755.

Blaner, W.S., O'Byrne, S.M., Wongsiriroj, N., Kluwe, J., D'Ambrosio, D.M., Jiang, H., Schwabe, R.F., Hillman, E.M., Piantedosi, R., and Libien, J. (2009). Hepatic stellate cell lipid droplets: a specialized lipid droplet for retinoid storage. Biochimica et biophysica acta *1791*, 467-473.

Boutet, E., El Mourabit, H., Prot, M., Nemani, M., Khallouf, E., Colard, O., Maurice, M., Durand-Schneider, A.M., Chretien, Y., Gres, S.*, et al.* (2009). Seipin deficiency alters fatty acid Delta9 desaturation and lipid droplet formation in Berardinelli-Seip congenital lipodystrophy. Biochimie *91*, 796-803.

Buers, I., Hofnagel, O., Ruebel, A., Severs, N.J., and Robenek, H. (2011). Lipid droplet associated proteins: an emerging role in atherogenesis. Histology and histopathology *26*, 631-642.

Bunkenborg, J., Garcia, G.E., Paz, M.I., Andersen, J.S., and Molina, H. (2010). The minotaur proteome: avoiding cross-species identifications deriving from bovine serum in cell culture models. Proteomics *10*, 3040-3044.

Campelo, F., and Kozlov, M.M. (2014). Sensing membrane stresses by protein insertions. PLoS computational biology *10*, e1003556.

Cartwright, B.R., Binns, D.D., Hilton, C.L., Han, S., Gao, Q., and Goodman, J.M. (2015). Seipin performs dissectible functions in promoting lipid droplet biogenesis and regulating droplet morphology. Molecular biology of the cell *26*, 726-739.

Carvalho, P., Goder, V., and Rapoport, T.A. (2006). Distinct ubiquitin-ligase complexes define convergent pathways for the degradation of ER proteins. Cell *126*, 361-373.

Cermelli, S., Guo, Y., Gross, S.P., and Welte, M.A. (2006). The lipid-droplet proteome reveals that droplets are a protein-storage depot. Current biology : CB *16*, 1783-1795.

Cole, N.B., Murphy, D.D., Grider, T., Rueter, S., Brasaemle, D., and Nussbaum, R.L. (2002). Lipid droplet binding and oligomerization properties of the Parkinson's disease protein alpha-synuclein. The Journal of biological chemistry *277*, 6344-6352.

Connerth, M., Grillitsch, K., Kofeler, H., and Daum, G. (2009). Analysis of lipid particles from yeast. Methods Mol Biol *579*, 359-374.

Cui, X., Wang, Y., Tang, Y., Liu, Y., Zhao, L., Deng, J., Xu, G., Peng, X., Ju, S., Liu, G., *et al.* (2011). Seipin ablation in mice results in severe generalized lipodystrophy. Human molecular genetics *20*, 3022-3030.

Currie, E., Guo, X., Christiano, R., Chitraju, C., Kory, N., Harrison, K., Haas, J., Walther, T.C., and Farese, R.V., Jr. (2014). High confidence proteomic analysis of yeast LDs identifies additional droplet proteins and reveals connections to dolichol synthesis and sterol acetylation. Journal of lipid research *55*, 1465-1477.

Czabany, T., Wagner, A., Zweytick, D., Lohner, K., Leitner, E., Ingolic, E., and Daum, G. (2008). Structural and biochemical properties of lipid particles from the yeast Saccharomyces cerevisiae. The Journal of biological chemistry *283*, 17065-17074.

Chapman, K.D., Dyer, J.M., and Mullen, R.T. (2012). Biogenesis and functions of lipid droplets in plants: Thematic Review Series: Lipid Droplet Synthesis and Metabolism: from Yeast to Man. Journal of lipid research *53*, 215-226.

Chen, W., Chang, B., Saha, P., Hartig, S.M., Li, L., Reddy, V.T., Yang, Y., Yechoor, V., Mancini, M.A., and Chan, L. (2012). Berardinelli-seip congenital lipodystrophy 2/seipin is a cell-autonomous regulator of lipolysis essential for adipocyte differentiation. Molecular and cellular biology *32*, 1099-1111.

Chen, W., Yechoor, V.K., Chang, B.H., Li, M.V., March, K.L., and Chan, L. (2009). The human lipodystrophy gene product Berardinelli-Seip congenital lipodystrophy 2/seipin plays a key role in adipocyte differentiation. Endocrinology *150*, 4552-4561.

Chernomordik, L.V., and Kozlov, M.M. (2005). Membrane hemifusion: crossing a chasm in two leaps. Cell *123*, 375-382.

Divi, U.K., and Krishna, P. (2009). Brassinosteroid: a biotechnological target for enhancing crop yield and stress tolerance. New biotechnology *26*, 131-136.

Drin, G., and Antonny, B. (2010). Amphipathic helices and membrane curvature. FEBS Lett *584*, 1840-1847.

Drin, G., Casella, J.F., Gautier, R., Boehmer, T., Schwartz, T.U., and Antonny, B. (2007). A general amphipathic alpha-helical motif for sensing membrane curvature. Nat Struct Mol Biol *14*, 138-146.

Durrett, T.P., Benning, C., and Ohlrogge, J. (2008). Plant triacylglycerols as feedstocks for the production of biofuels. The Plant journal : for cell and molecular biology *54*, 593-607.

Fei, W., Du, X., and Yang, H. (2011a). Seipin, adipogenesis and lipid droplets. Trends in endocrinology and metabolism: TEM *22*, 204-210.

Fei, W., Li, H., Shui, G., Kapterian, T.S., Bielby, C., Du, X., Brown, A.J., Li, P., Wenk, M.R., Liu, P.*, et al.* (2011b). Molecular characterization of seipin and its mutants: implications for seipin in triacylglycerol synthesis. Journal of lipid research *52*, 2136-2147.

Fei, W., Shui, G., Gaeta, B., Du, X., Kuerschner, L., Li, P., Brown, A.J., Wenk, M.R., Parton, R.G., and Yang, H. (2008). Fld1p, a functional homologue of human seipin, regulates the size of lipid droplets in yeast. The Journal of cell biology *180*, 473-482.

Fei, W., Shui, G., Zhang, Y., Krahmer, N., Ferguson, C., Kapterian, T.S., Lin, R.C., Dawes, I.W., Brown, A.J., Li, P.*, et al.* (2011c). A role for phosphatidic acid in the formation of "supersized" lipid droplets. PLoS genetics *7*, e1002201.

Fei, W., Zhong, L., Ta, M.T., Shui, G., Wenk, M.R., and Yang, H. (2011d). The size and phospholipid composition of lipid droplets can influence their proteome. Biochemical and biophysical research communications *415*, 455-462.

Folch, J., Lees, M., and Sloane Stanley, G.H. (1957). A simple method for the isolation and purification of total lipides from animal tissues. J Biol Chem *226*, 497-509.

Frandsen, G.I., Mundy, J., and Tzen, J.T. (2001). Oil bodies and their associated proteins, oleosin and caleosin. Physiologia plantarum *112*, 301-307.

Fujimoto, T., and Parton, R.G. (2011). Not just fat: the structure and function of the lipid droplet. Cold Spring Harbor perspectives in biology *3*.

Garg, A., and Agarwal, A.K. (2009). Lipodystrophies: disorders of adipose tissue biology. Biochimica et biophysica acta *1791*, 507-513.

Gaspar, M.L., Aregullin, M.A., Jesch, S.A., and Henry, S.A. (2006). Inositol induces a profound alteration in the pattern and rate of synthesis and turnover of membrane lipids in Saccharomyces cerevisiae. J Biol Chem *281*, 22773-22785.

Gautier, R., Douguet, D., Antonny, B., and Drin, G. (2008). HELIQUEST: a web server to screen sequences with specific alpha-helical properties. Bioinformatics *24*, 2101-2102.

Gentleman, R.C., Carey, V.J., Bates, D.M., Bolstad, B., Dettling, M., Dudoit, S., Ellis, B., Gautier, L., Ge, Y., Gentry, J.*, et al.* (2004). Bioconductor: open software development for computational biology and bioinformatics. Genome biology *5*, R80.

Gong, J., Sun, Z., Wu, L., Xu, W., Schieber, N., Xu, D., Shui, G., Yang, H., Parton, R.G., and Li, P. (2011). Fsp27 promotes lipid droplet growth by lipid exchange and transfer at lipid droplet contact sites. The Journal of cell biology *195*, 953-963.

Greenberg, A.S., Egan, J.J., Wek, S.A., Garty, N.B., Blanchette-Mackie, E.J., and Londos, C. (1991). Perilipin, a major hormonally regulated adipocyte-specific phosphoprotein associated with the periphery of lipid storage droplets. The Journal of biological chemistry *266*, 11341-11346.

Grillitsch, K., Connerth, M., Kofeler, H., Arrey, T.N., Rietschel, B., Wagner, B., Karas, M., and Daum, G. (2011). Lipid particles/droplets of the yeast Saccharomyces cerevisiae revisited: lipidome meets proteome. Biochimica et biophysica acta *1811*, 1165-1176.

Gronke, S., Beller, M., Fellert, S., Ramakrishnan, H., Jackle, H., and Kuhnlein, R.P. (2003). Control of fat storage by a Drosophila PAT domain protein. Current biology : CB *13*, 603-606.

Gubern, A., Barcelo-Torns, M., Casas, J., Barneda, D., Masgrau, R., Picatoste, F., Balsinde, J., Balboa, M.A., and Claro, E. (2009). Lipid droplet biogenesis induced by stress involves triacylglycerol synthesis that depends on group VIA phospholipase A2. The Journal of biological chemistry *284*, 5697-5708.

Guo, Y., Walther, T.C., Rao, M., Stuurman, N., Goshima, G., Terayama, K., Wong, J.S., Vale, R.D., Walter, P., and Farese, R.V. (2008). Functional genomic screen reveals genes involved in lipid-droplet formation and utilization. Nature *453*, 657-661.

Guthrie, C., and Fink, G. (1991). Guide to yeast genetics and molecular biology, Vol 194 (Academic Press).

Hancock, L.C., Behta, R.P., and Lopes, J.M. (2006). Genomic analysis of the Opi- phenotype. Genetics *173*, 621-634.

Henry, S.A., Gaspar, M.L., and Jesch, S.A. (2014). The response to inositol: regulation of glycerolipid metabolism and stress response signaling in yeast. Chemistry and physics of lipids *180*, 23-43.

Henry, S.A., Kohlwein, S.D., and Carman, G.M. (2012). Metabolism and regulation of glycerolipids in the yeast Saccharomyces cerevisiae. Genetics *190*, 317-349.

Henry, S.A., and Patton-Vogt, J.L. (1998). Genetic regulation of phospholipid metabolism: yeast as a model eukaryote. Progress in nucleic acid research and molecular biology *61*, 133-179.

Hickenbottom, S.J., Kimmel, A.R., Londos, C., and Hurley, J.H. (2004). Structure of a lipid droplet protein; the PAT family member TIP47. Structure *12*, 1199-1207.

Hofbauer, H.F., Schopf, F.H., Schleifer, H., Knittelfelder, O.L., Pieber, B., Rechberger, G.N., Wolinski, H., Gaspar, M.L., Kappe, C.O., Stadlmann, J*., et al.* (2014). Regulation of gene expression through a transcriptional repressor that senses acyl-chain length in membrane phospholipids. Dev Cell *29*, 729-739.

Horchani, H., de Saint-Jean, M., Barelli, H., and Antonny, B. (2014). Interaction of the Spo20 membrane-sensor motif with phosphatidic acid and other anionic lipids, and influence of the membrane environment. PloS one *9*, e113484.

Ingelmo-Torres, M., Gonzalez-Moreno, E., Kassan, A., Hanzal-Bayer, M., Tebar, F., Herms, A., Grewal, T., Hancock, J.F., Enrich, C., Bosch, M.*, et al.* (2009). Hydrophobic and basic domains target proteins to lipid droplets. Traffic *10*, 1785-1801.

Jacquier, N., Choudhary, V., Mari, M., Toulmay, A., Reggiori, F., and Schneiter, R. (2011). Lipid droplets are functionally connected to the endoplasmic reticulum in Saccharomyces cerevisiae. Journal of cell science *124*, 2424-2437.

Janke, C., Magiera, M.M., Rathfelder, N., Taxis, C., Reber, S., Maekawa, H., Moreno-Borchart, A., Doenges, G., Schwob, E., Schiebel, E.*, et al.* (2004). A versatile toolbox for PCR-based tagging of yeast genes: new fluorescent proteins, more markers and promoter substitution cassettes. Yeast *21*, 947-962.

Jolivet, P., Roux, E., D'Andrea, S., Davanture, M., Negroni, L., Zivy, M., and Chardot, T. (2004). Protein composition of oil bodies in Arabidopsis thaliana ecotype WS. Plant physiology and biochemistry : PPB / Societe francaise de physiologie vegetale *42*, 501-509.

Jones, H.E., Harwood, J.L., Bowen, I.D., and Griffiths, G. (1992). Lipid composition of subcellular membranes from larvae and prepupae of Drosophila melanogaster. Lipids *27*, 984-987.

Kimmel, A.R., Brasaemle, D.L., McAndrews-Hill, M., Sztalryd, C., and Londos, C. (2010). Adoption of PERILIPIN as a unifying nomenclature for the mammalian PAT-family of intracellular lipid storage droplet proteins. Journal of lipid research *51*, 468-471.

Koffel, R., Tiwari, R., Falquet, L., and Schneiter, R. (2005). The Saccharomyces cerevisiae YLL012/YEH1, YLR020/YEH2, and TGL1 genes encode a novel family of membrane-anchored lipases that are required for steryl ester hydrolysis. Molecular and cellular biology *25*, 1655-1668.

Kopelman, P.G. (2000). Obesity as a medical problem. Nature *404*, 635-643.

Krahmer, N., Farese, R.V., Jr., and Walther, T.C. (2013a). Balancing the fat: lipid droplets and human disease. EMBO molecular medicine *5*, 905-915.

Krahmer, N., Guo, Y., Wilfling, F., Hilger, M., Lingrell, S., Heger, K., Newman, H.W., Schmidt-Supprian, M., Vance, D.E., Mann, M.*, et al.* (2011). Phosphatidylcholine

synthesis for lipid droplet expansion is mediated by localized activation of CTP:phosphocholine cytidylyltransferase. Cell metabolism *14*, 504-515.

Krahmer, N., Hilger, M., Kory, N., Wilfling, F., Stoehr, G., Mann, M., Farese, R.V., Jr., and Walther, T.C. (2013b). Protein correlation profiles identify lipid droplet proteins with high confidence. Molecular & cellular proteomics : MCP *12*, 1115-1126.

Leber, R., Zinser, E., Zellnig, G., Paltauf, F., and Daum, G. (1994). Characterization of lipid particles of the yeast, Saccharomyces cerevisiae. Yeast *10*, 1421-1428.

Lin, L.J., Tai, S.S., Peng, C.C., and Tzen, J.T. (2002). Steroleosin, a sterol-binding dehydrogenase in seed oil bodies. Plant physiology *128*, 1200-1211.

Liu, P., Bartz, R., Zehmer, J.K., Ying, Y.S., Zhu, M., Serrero, G., and Anderson, R.G. (2007). Rab-regulated interaction of early endosomes with lipid droplets. Biochimica et biophysica acta *1773*, 784-793.

Loewen, C.J., Gaspar, M.L., Jesch, S.A., Delon, C., Ktistakis, N.T., Henry, S.A., and Levine, T.P. (2004). Phospholipid metabolism regulated by a transcription factor sensing phosphatidic acid. Science *304*, 1644-1647.

Loewen, C.J., Roy, A., and Levine, T.P. (2003). A conserved ER targeting motif in three families of lipid binding proteins and in Opi1p binds VAP. EMBO J *22*, 2025-2035.

Londos, C., Brasaemle, D.L., Schultz, C.J., Segrest, J.P., and Kimmel, A.R. (1999). Perilipins, ADRP, and other proteins that associate with intracellular neutral lipid droplets in animal cells. Seminars in cell & developmental biology *10*, 51-58.

Longtine, M.S., McKenzie, A., 3rd, Demarini, D.J., Shah, N.G., Wach, A., Brachat, A., Philippsen, P., and Pringle, J.R. (1998). Additional modules for versatile and economical PCR-based gene deletion and modification in Saccharomyces cerevisiae. Yeast *14*, 953-961.

Louvion, J.F., Havaux-Copf, B., and Picard, D. (1993). Fusion of GAL4-VP16 to a steroid-binding domain provides a tool for gratuitous induction of galactose-responsive genes in yeast. Gene *131*, 129-134.

Lundin, C., Nordstrom, R., Wagner, K., Windpassinger, C., Andersson, H., von Heijne, G., and Nilsson, I. (2006). Membrane topology of the human seipin protein. FEBS letters *580*, 2281-2284.

MacKinnon, M.A., Curwin, A.J., Gaspard, G.J., Suraci, A.B., Fernandez-Murray, J.P., and McMaster, C.R. (2009). The Kap60-Kap95 karyopherin complex directly regulates phosphatidylcholine synthesis. J Biol Chem *284*, 7376-7384.

Mackinnon, W.B., May, G.L., and Mountford, C.E. (1992). Esterified cholesterol and triglyceride are present in plasma membranes of Chinese hamster ovary cells. European journal of biochemistry / FEBS *205*, 827-839.

Magre, J., Delepine, M., Khallouf, E., Gedde-Dahl, T., Jr., Van Maldergem, L., Sobel, E., Papp, J., Meier, M., Megarbane, A., Bachy, A.*, et al.* (2001). Identification of the gene altered in Berardinelli-Seip congenital lipodystrophy on chromosome 11q13. Nature genetics *28*, 365-370.

Mattoo, A.K., Shukla, V., Fatima, T., Handa, A.K., and Yachha, S.K. (2010). Genetic engineering to enhance crop-based phytonutrients (nutraceuticals) to alleviate diet-related diseases. Advances in experimental medicine and biology *698*, 122-143.

Meyers, N.L., Wang, L., and Small, D.M. (2012). Apolipoprotein C-I binds more strongly to phospholipid/triolein/water than triolein/water interfaces: a possible model for inhibiting cholesterol ester transfer protein activity and triacylglycerol-rich lipoprotein uptake. Biochemistry *51*, 1238-1248.

Miura, F., Kawaguchi, N., Sese, J., Toyoda, A., Hattori, M., Morishita, S., and Ito, T. (2006). A large-scale full-length cDNA analysis to explore the budding yeast transcriptome. Proceedings of the National Academy of Sciences of the United States of America *103*, 17846-17851.

Mumberg, D., Muller, R., and Funk, M. (1995). Yeast vectors for the controlled expression of heterologous proteins in different genetic backgrounds. Gene *156*, 119-122.

Murphy, D.J., and Vance, J. (1999). Mechanisms of lipid-body formation. Trends in biochemical sciences *24*, 109-115.

Murphy, S., Martin, S., and Parton, R.G. (2009). Lipid droplet-organelle interactions; sharing the fats. Biochimica et biophysica acta *1791*, 441-447.

Naested, H., Frandsen, G.I., Jauh, G.Y., Hernandez-Pinzon, I., Nielsen, H.B., Murphy, D.J., Rogers, J.C., and Mundy, J. (2000). Caleosins: Ca2+-binding proteins associated with lipid bodies. Plant molecular biology *44*, 463-476.

Nakamura, N., Banno, Y., and Tamiya-Koizumi, K. (2005). Arf1-dependent PLD1 is localized to oleic acid-induced lipid droplets in NIH3T3 cells. Biochemical and biophysical research communications *335*, 117-123.

Nakanishi, H., de los Santos, P., and Neiman, A.M. (2004). Positive and negative regulation of a SNARE protein by control of intracellular localization. Mol Biol Cell *15*, 1802-1815.

Oelkers, P., Cromley, D., Padamsee, M., Billheimer, J.T., and Sturley, S.L. (2002). The DGA1 gene determines a second triglyceride synthetic pathway in yeast. The Journal of biological chemistry *277*, 8877-8881.

Ohsaki, Y., Cheng, J., Fujita, A., Tokumoto, T., and Fujimoto, T. (2006). Cytoplasmic lipid droplets are sites of convergence of proteasomal and autophagic degradation of apolipoprotein B. Molecular biology of the cell *17*, 2674-2683.

Patel, R.T., Soulages, J.L., Hariharasundaram, B., and Arrese, E.L. (2005). Activation of the lipid droplet controls the rate of lipolysis of triglycerides in the insect fat body. The Journal of biological chemistry *280*, 22624-22631.

Payne, V.A., Grimsey, N., Tuthill, A., Virtue, S., Gray, S.L., Dalla Nora, E., Semple, R.K., O'Rahilly, S., and Rochford, J.J. (2008). The human lipodystrophy gene BSCL2/seipin may be essential for normal adipocyte differentiation. Diabetes *57*, 2055-2060.

Penno, A., Hackenbroich, G., and Thiele, C. (2013). Phospholipids and lipid droplets. Biochimica et biophysica acta *1831*, 589-594.

Ploegh, H.L. (2007). A lipid-based model for the creation of an escape hatch from the endoplasmic reticulum. Nature *448*, 435-438.

Pol, A., Gross, S.P., and Parton, R.G. (2014). Review: biogenesis of the multifunctional lipid droplet: lipids, proteins, and sites. The Journal of cell biology *204*, 635-646.

Pol, A., Luetterforst, R., Lindsay, M., Heino, S., Ikonen, E., and Parton, R.G. (2001). A caveolin dominant negative mutant associates with lipid bodies and induces intracellular cholesterol imbalance. The Journal of cell biology *152*, 1057-1070.

Prieur, X., Dollet, L., Takahashi, M., Nemani, M., Pillot, B., Le May, C., Mounier, C., Takigawa-Imamura, H., Zelenika, D., Matsuda, F.*, et al.* (2013). Thiazolidinediones partially reverse the metabolic disturbances observed in Bscl2/seipin-deficient mice. Diabetologia *56*, 1813-1825.

Rambold, A.S., Cohen, S., and Lippincott-Schwartz, J. (2015). Fatty Acid trafficking in starved cells: regulation by lipid droplet lipolysis, autophagy, and mitochondrial fusion dynamics. Developmental cell *32*, 678-692.

Rappsilber, J., Mann, M., and Ishihama, Y. (2007). Protocol for micro-purification, enrichment, pre-fractionation and storage of peptides for proteomics using StageTips. Nat Protoc *2*, 1896-1906.

Rigaut, G., Shevchenko, A., Rutz, B., Wilm, M., Mann, M., and Seraphin, B. (1999). A generic protein purification method for protein complex characterization and proteome exploration. Nature biotechnology *17*, 1030-1032.

Robenek, H., Hofnagel, O., Buers, I., Robenek, M.J., Troyer, D., and Severs, N.J. (2006). Adipophilin-enriched domains in the ER membrane are sites of lipid droplet biogenesis. Journal of cell science *119*, 4215-4224.

Sandager, L., Gustavsson, M.H., Stahl, U., Dahlqvist, A., Wiberg, E., Banas, A., Lenman, M., Ronne, H., and Stymne, S. (2002). Storage lipid synthesis is non-essential in yeast. The Journal of biological chemistry *277*, 6478-6482.

Shen, H., Heacock, P.N., Clancey, C.J., and Dowhan, W. (1996). The CDS1 gene encoding CDP-diacylglycerol synthase in Saccharomyces cerevisiae is essential for cell growth. J Biol Chem *271*, 789-795.

Shibata, Y., Voss, C., Rist, J.M., Hu, J., Rapoport, T.A., Prinz, W.A., and Voeltz, G.K. (2008). The reticulon and DP1/Yop1p proteins form immobile oligomers in the tubular endoplasmic reticulum. J Biol Chem *283*, 18892-18904.

Singh, R., Kaushik, S., Wang, Y., Xiang, Y., Novak, I., Komatsu, M., Tanaka, K., Cuervo, A.M., and Czaja, M.J. (2009). Autophagy regulates lipid metabolism. Nature *458*, 1131-1135.

Smyth, G.K. (2004). Linear models and empirical bayes methods for assessing differential expression in microarray experiments. Statistical applications in genetics and molecular biology *3*, Article3.

Soni, K.G., Mardones, G.A., Sougrat, R., Smirnova, E., Jackson, C.L., and Bonifacino, J.S. (2009). Coatomer-dependent protein delivery to lipid droplets. Journal of cell science *122*, 1834-1841.

Sorger, D., Athenstaedt, K., Hrastnik, C., and Daum, G. (2004). A yeast strain lacking lipid particles bears a defect in ergosterol formation. J Biol Chem *279*, 31190-31196.

Stone, S.J., Levin, M.C., and Farese, R.V., Jr. (2006). Membrane topology and identification of key functional amino acid residues of murine acyl-CoA:diacylglycerol acyltransferase-2. The Journal of biological chemistry *281*, 40273-40282.

Sturley, S.L., and Hussain, M.M. (2012). Lipid droplet formation on opposing sides of the endoplasmic reticulum. Journal of lipid research *53*, 1800-1810.

Sun, Z., Gong, J., Wu, H., Xu, W., Wu, L., Xu, D., Gao, J., Wu, J.W., Yang, H., Yang, M., *et al.* (2013). Perilipin1 promotes unilocular lipid droplet formation through the activation of Fsp27 in adipocytes. Nature communications *4*, 1594.

Szymanski, K.M., Binns, D., Bartz, R., Grishin, N.V., Li, W.P., Agarwal, A.K., Garg, A., Anderson, R.G., and Goodman, J.M. (2007). The lipodystrophy protein seipin is found at endoplasmic reticulum lipid droplet junctions and is important for droplet morphology. Proceedings of the National Academy of Sciences of the United States of America *104*, 20890-20895.

Tauchi-Sato, K., Ozeki, S., Houjou, T., Taguchi, R., and Fujimoto, T. (2002). The surface of lipid droplets is a phospholipid monolayer with a unique Fatty Acid composition. The Journal of biological chemistry *277*, 44507-44512.

Thiam, A.R., Antonny, B., Wang, J., Delacotte, J., Wilfling, F., Walther, T.C., Beck, R., Rothman, J.E., and Pincet, F. (2013a). COPI buds 60-nm lipid droplets from reconstituted water-phospholipid-triacylglyceride interfaces, suggesting a tension clamp

function. Proceedings of the National Academy of Sciences of the United States of America *110*, 13244-13249.

Thiam, A.R., Farese, R.V., Jr., and Walther, T.C. (2013b). The biophysics and cell biology of lipid droplets. Nature reviews Molecular cell biology *14*, 775-786.

Tian, Y., Bi, J., Shui, G., Liu, Z., Xiang, Y., Liu, Y., Wenk, M.R., Yang, H., and Huang, X. (2011). Tissue-autonomous function of Drosophila seipin in preventing ectopic lipid droplet formation. PLoS genetics *7*, e1001364.

Vamparys, L., Gautier, R., Vanni, S., Bennett, W.F., Tieleman, D.P., Antonny, B., Etchebest, C., and Fuchs, P.F. (2013). Conical lipids in flat bilayers induce packing defects similar to that induced by positive curvature. Biophysical journal *104*, 585-593.

van Zutphen, T., Todde, V., de Boer, R., Kreim, M., Hofbauer, H.F., Wolinski, H., Veenhuis, M., van der Klei, I.J., and Kohlwein, S.D. (2014). Lipid droplet autophagy in the yeast Saccharomyces cerevisiae. Molecular biology of the cell *25*, 290-301.

Vanni, S., Vamparys, L., Gautier, R., Drin, G., Etchebest, C., Fuchs, P.F., and Antonny, B. (2013). Amphipathic lipid packing sensor motifs: probing bilayer defects with hydrophobic residues. Biophysical journal *104*, 575-584.

Walther, T.C., and Farese, R.V., Jr. (2009). The life of lipid droplets. Biochimica et biophysica acta *1791*, 459-466.

Walther, T.C., and Farese, R.V., Jr. (2012). Lipid droplets and cellular lipid metabolism. Annual review of biochemistry *81*, 687-714.

Wang, C.W., Miao, Y.H., and Chang, Y.S. (2014). Control of lipid droplet size in budding yeast requires the collaboration between Fld1 and Ldb16. Journal of cell science *127*, 1214-1228.

Wilfling, F., Haas, J.T., Walther, T.C., and Farese, R.V., Jr. (2014a). Lipid droplet biogenesis. Current opinion in cell biology *29*, 39-45.

Wilfling, F., Thiam, A.R., Olarte, M.J., Wang, J., Beck, R., Gould, T.J., Allgeyer, E.S., Pincet, F., Bewersdorf, J., Farese, R.V., Jr*., et al.* (2014b). Arf1/COPI machinery acts directly on lipid droplets and enables their connection to the ER for protein targeting. eLife *3*, e01607.

Wilfling, F., Wang, H., Haas, J.T., Krahmer, N., Gould, T.J., Uchida, A., Cheng, J.X., Graham, M., Christiano, R., Frohlich, F.*, et al.* (2013). Triacylglycerol synthesis enzymes mediate lipid droplet growth by relocalizing from the ER to lipid droplets. Developmental cell *24*, 384-399.

Windpassinger, C., Auer-Grumbach, M., Irobi, J., Patel, H., Petek, E., Horl, G., Malli, R., Reed, J.A., Dierick, I., Verpoorten, N.*, et al.* (2004). Heterozygous missense mutations in BSCL2 are associated with distal hereditary motor neuropathy and Silver syndrome. Nature genetics *36*, 271-276.

Wolins, N.E., Brasaemle, D.L., and Bickel, P.E. (2006). A proposed model of fat packaging by exchangeable lipid droplet proteins. FEBS letters *580*, 5484-5491.

Wolins, N.E., Skinner, J.R., Schoenfish, M.J., Tzekov, A., Bensch, K.G., and Bickel, P.E. (2003). Adipocyte protein S3-12 coats nascent lipid droplets. The Journal of biological chemistry *278*, 37713-37721.

Wolinski, H., Kolb, D., Hermann, S., Koning, R.I., and Kohlwein, S.D. (2011). A role for seipin in lipid droplet dynamics and inheritance in yeast. J Cell Sci *124*, 3894-3904.

Xu, N., Zhang, S.O., Cole, R.A., McKinney, S.A., Guo, F., Haas, J.T., Bobba, S., Farese, R.V., Jr., and Mak, H.Y. (2012). The FATP1-DGAT2 complex facilitates lipid droplet expansion at the ER-lipid droplet interface. The Journal of cell biology *198*, 895-911.

Yang, H., Galea, A., Sytnyk, V., and Crossley, M. (2012a). Controlling the size of lipid droplets: lipid and protein factors. Current opinion in cell biology *24*, 509-516.

Yang, L., Ding, Y., Chen, Y., Zhang, S., Huo, C., Wang, Y., Yu, J., Zhang, P., Na, H., Zhang, H.*, et al.* (2012b). The proteomics of lipid droplets: structure, dynamics, and functions of the organelle conserved from bacteria to humans. Journal of lipid research *53*, 1245-1253.

Young, B.P., Shin, J.J., Orij, R., Chao, J.T., Li, S.C., Guan, X.L., Khong, A., Jan, E., Wenk, M.R., Prinz, W.A.*, et al.* (2010). Phosphatidic acid is a pH biosensor that links membrane biogenesis to metabolism. Science *329*, 1085-1088.

Zanghellini, J., Wodlei, F., and von Grunberg, H.H. (2010). Phospholipid demixing and the birth of a lipid droplet. Journal of theoretical biology *264*, 952-961.

Zehmer, J.K., Bartz, R., Bisel, B., Liu, P., Seemann, J., and Anderson, R.G. (2009). Targeting sequences of UBXD8 and AAM-B reveal that the ER has a direct role in the emergence and regression of lipid droplets. Journal of cell science *122*, 3694-3702.

Zehmer, J.K., Bartz, R., Liu, P., and Anderson, R.G. (2008). Identification of a novel N-terminal hydrophobic sequence that targets proteins to lipid droplets. Journal of cell science *121*, 1852-1860.

Zeniou-Meyer, M., Zabari, N., Ashery, U., Chasserot-Golaz, S., Haeberle, A.M., Demais, V., Bailly, Y., Gottfried, I., Nakanishi, H., Neiman, A.M.*, et al.* (2007). Phospholipase D1 production of phosphatidic acid at the plasma membrane promotes exocytosis of large dense-core granules at a late stage. J Biol Chem *282*, 21746-21757.

Zimmermann, R., Lass, A., Haemmerle, G., and Zechner, R. (2009). Fate of fat: the role of adipose triglyceride lipase in lipolysis. Biochimica et biophysica acta *1791*, 494-500.

Zweytick, D., Athenstaedt, K., and Daum, G. (2000). Intracellular lipid particles of eukaryotic cells. Biochimica et biophysica acta *1469*, 101-120.